# A STUDY OF MUTUAL COUPLING EFFECTS IN FINITE MICROSTRIP ARRAYS

**DSS CONTRACT 06ST.36100-5-0090**

**FINAL REPORT**

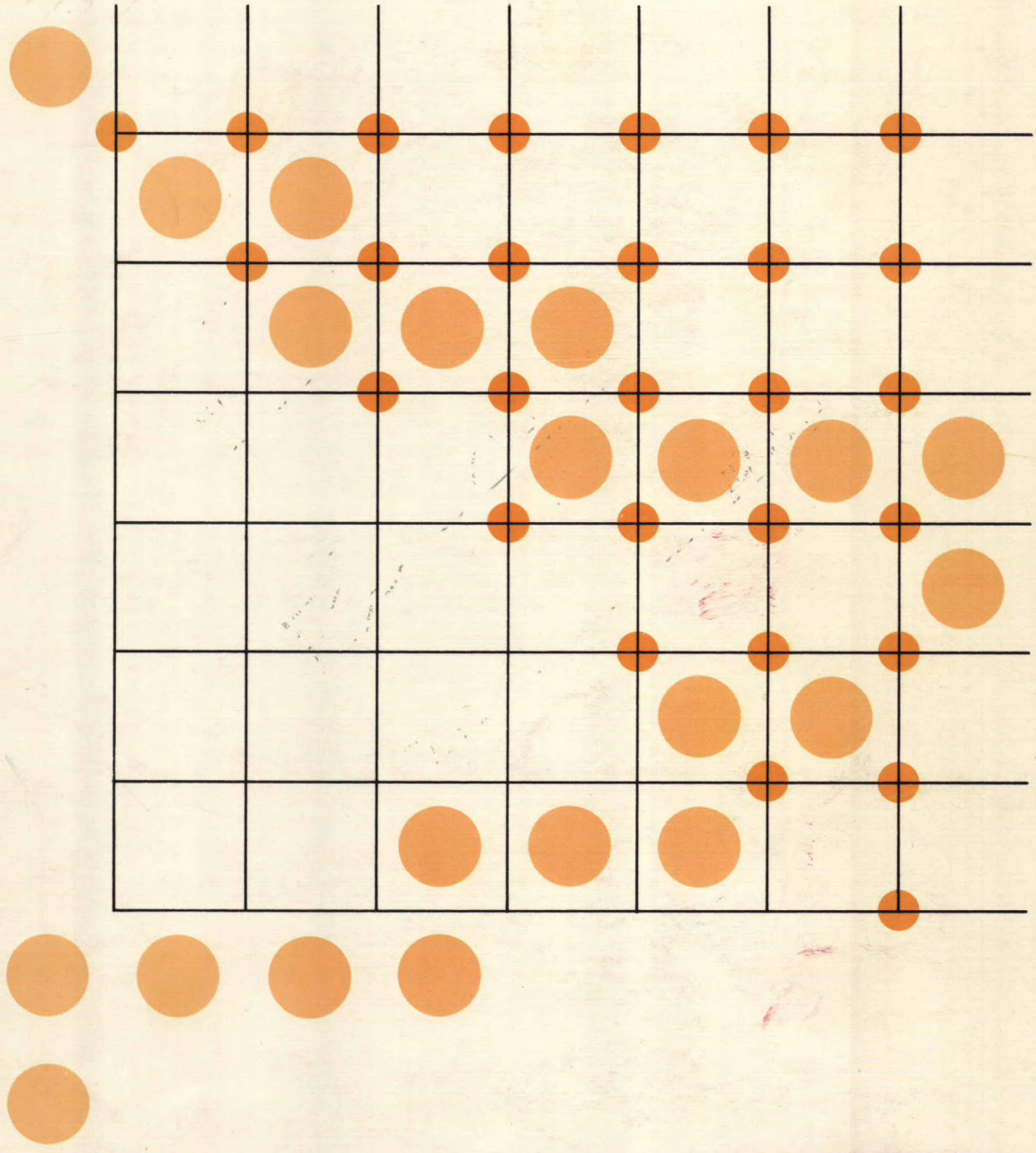



Department of Electrical Engineering
The University of Manitoba
Winnipeg, Manitoba, Canada
R3T 2N2

# A STUDY OF MUTUAL COUPLING EFFECTS IN FINITE MICROSTRIP ARRAYS

DSS CONTRACT 06ST.36100-5-0090

**Final Report**

Prepared for

Communication Research Centre

Department of Communications

Shirley Bay

P.O. Box 11490, Station H

Ottawa, Ontario

K2H 8S2

by

L. Shafai

O. Aboul-Atta

A. Bhattacharyya

D.L. Lai

Department of Electrical Engineering

University of Manitoba

Winnipeg, Manitoba, R3T 2N2



March 1986

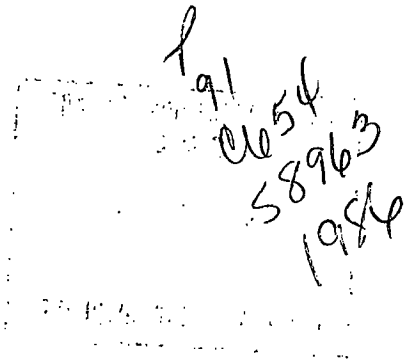

TABLE OF CONTENTS

## LIST OF FIGURES

## SUMMARY

In this report the mathematical formulation of mutual coupling between elements of a microstrip array is provided. The generated models are used to investigate both the impedance and the array radiation patterns. The computed array patterns indicate that, generally, the mutual coupling reduces the array gain, but has a small effect on the sidelobe levels. The problem was also studied numerically for coupling between two patch arrays and reported in the program report. It indicated that the mutual coupling increases with beam scan and becomes considerable when the array beam approaches the array plane.

A case of two-dimensional array is also studied. A 19-element array using circular patch elements having a hexagonal grid is considered. It is fabricated using a substrated height of h = 1/16 inch and a permittivity of $\varepsilon_r = 2.65$. The array beam is scanned to the direction of $\phi_o = 7.5°$, $\theta_o = 55°$, using coaxial lines of appropriate length to feed the array elements. The array beam is then measured experimentally. The array radiation pattern is also computed with and without the mutual coupling. Comparing the results it is found that the array gain is reduced considerably due to the mutual coupling. The computed result with the inclusion of mutual coupling is, otherwise, in good agreement with the experiment.

Recommendation for future work

The work in this phase of study was involved with the development of mathematical models, computation of mutual coupling effect on the

array patterns and a comparison of the results with experiment. Several areas, however, need careful examinations, which should be studied during the second phase of project.

1) the effect of mutual coupling on the input impedance has not been examined experimentally. This should be studied with sample arrays and compared with experimental data.

2) So far, the effect of coupling is conidered for the dominant mode. In certain applications higher order modes may be used and their coupling should also be investigated.

3) So far, the experimental comparison is made for the main polarization. The coupling effect on the cross-polarization can provide additional information and because of its small magnitude may become too sensitive to scanning and inter-element coupling.

4) The radiation patterns of isolated patches are normally obtained approximately, using the fringing field concept. This method fails to provide accurate radiation patterns near the horizontal plane. Further improvement in the pattern prediction is desirable to enable better co-polar and cross-polar pattern calculations.

## 1. INTRODUCTION

In any array environment of finite elements in planar configuration, the elements in close proximity to each other behave differently than when they are isolated. The problem is particularly difficult in small arrays since the elements are in asymmetrical positions and the mutual coupling differs for each elements. Qualitatively, the literature survey indicates that the mutual coupling between the array elements can have a substantial effect on the total performance of the antenna as compared with the standard simplified prediction that sums up the relative phase location of every element weighted by its own excitation only. This simplified array factor, when it multiplies the far field of a single isolated patch, generates the array radiation pattern without incorporating the mutual interaction. In order to introduce the coupling effect into the array theory, these weighting factors for all elements are treated as an excitation coefficient column vector that is linearly related to the actual excitation vector by a transformation matrix (N x N) where N is the number of the patches in the array. This transformation matrix can be dimensionless, an admittance in mhos, or an impedance in ohms, as the dependent and independent variables in the array are defined. The diagonal elements in this transformation matrix behave exactly as the simple array theory mentioned above while the off-diagonal elements of the matrix accounts for the mutual interaction between the patches. Since the transformation matrix is deducible from laboratory measurements [11], [23] or by analytical means [20], the current work is devoted to the analytical approach to build a complete and valid model for practical use in an-

tenna analysis or synthesis routine of microstrip planar arrays. It is obvious that any analytical study of the interaction effect must conform to the method of analysis used for the single resonant patch of the array in order to introduce the coupling correctly. The rectangular patch and the circular patch are the most commonly analyzed and measured and accordingly the two cases are selected for the current analysis. The more rigorous treatments of these resonant patches are considered cumbersome and time consuming for regular engineering applications. On the other hand it has been shown [1], for the rectangular patch, that the TEM transmission line model provides a numerically efficient substitute specially as the model has been improved and modified [2] so as to be free from earlier limitations. The rectangular resonant patch in the transmission line model has been viewed in the literature [1], [2], [20], [23] as equivalent to two radiating apertures both linked together internally by the transmission line and its excitation while mutually coupled to themselves (as well as to all other apertures in the array) via the free space radiation interaction mechanism of parallel magnetic current strips. The analysis is simplified further by neglecting the interaction through the surface waves, which limits the validity of the anlysis to patches having substrates of small permittivity and thickness. The experimental verification of this validity has been provided [23] for permittivities up to 2.5 and substrate thickness up to $0.15\lambda_o$. The electromagnetic field under the patch can be uniquely identified in terms of the excitation current and its location as well as an impedance (or admittance) boundary condition at the apertures. Note that the common methods of excitation are the coaxial cable from behind the ground plane positioned somewhere under

the patch or microstrip line attached to the perimeter of the patch on the top of the substrate. The impedance (or admittance) boundary condition is identified directlyby its stationary integral expression [9] relating the interaction between two separate apertures with magnetic currents of the same spacial distribution. Much of the previous work [20], [21] dealt with two rectangular patches (E-plane coupled, H-plane coupled, or a general translated orientation without relative rotation) where extensive comparison with the experimental observations was made in order to confirm the validity of this model. Hence an attempt is made to generalize the theory and derive analytically the matrix relation between the aperture electric field (or the radiating edge voltage) and the excitation column vector (input currents) for a rectangular patch planar array based on the TEM-Transmission line model.

The other case selected for the analysis is the circular disc patch planar microstrip array. The literature survey [1]-[6] confirms that the cavity model for the circular patch is the simplest and most compact. This model dictates that the electromagnetic field in the substrate is dominantly transverse magnetic with respect to the cylindrical radial direction. Its decomposition into TM modes gives a complete set capable of representing any arbitrary TM-field at the perimeter of the disc where the mutual interaction between different apertures can be introduced. The patch viewed from the top, when separated from the ground plane by the substrate creates a cavity with cylindrical wall of circumferential magnetic current ribbon, formed by dropping perpendiculars from the patch perimeter to the ground plane. Hence the terminology "Cavity Model" is used and the magnetic current ribbon is visualized to radiate from its outer surface while the inside surface

is choked by the cavity. The cavity also serves as the means of transferring the energy needed, by the single radiating aperture, from the current source. As mentioned above, the field inside the cavity can be uniquely identified form the current source, its location, and the impedance boundary condition at the perimeter relating the circumferential magnetic field to the axial electric field of the aperture. In the planar microstrip array situation with mutual interaction included, one invokes a linear relation between the aperture magnetic field of one element and all existing aperture electric fields of elements in the array. This step brings the free space radiation interaction between magnetic current ribbons into effect and the corresponding variational expression for matrix elements are defined without the choking effect of the cavity. Then the Green's function solution of an excited cavity with impedance boundary condition completes the model by relating the diagonal element of the radiation interaction matrix to the cavity characteristics and its excitation. Although this cavity model is also applicable to the rectangular patch case, no attempt is made to pursue it since the trend in the literature has accepted, for the dominant mode of the rectangular patch applications, the TEM-transmission line model as the simplest and the most suited analysis for efficient evaluation of the patch's characteristics.

The analysis to follow starts with the circular patch case as it is the more compact of the two and analytically more tractable because the array has only one aperture per element and the electromagnetic field under the patch behaves according to the dielectric characteristic of the substrate $\varepsilon_r$. In the case of the rectangular patch array the analysis deals with two apertures per element and the TEM-mode used

in the transmission line model guides the energy in the air and partially in the dielectric. Hence the analysis must rely on an estimated effective permittivity that is experimentally verifiable. The complete analysis is formulated in this report with the principal electromagnetic field quantities (E,H) and only in the last stage of the model computation a transfer to the more common electric parameter (currents, voltages, impedances, and so on) are executed.

## 2. THE CIRCULAR PATCH MODEL

A circular disc patch operating in one of its resonant modes is the most prevalent microstrip antenna configurations. It offers performance, in its $TM_{11}$-mode, similar to that of the rectangular geometry and might have in some applications certain advantages over other shapes. Of the various methods available for the analysis of the disc patch antenna [1]-[6], the Green's function method or its equivalent radial transmission line modelling provides a reasonably good agreement between calculated and measured input impedances and predicts adequately the radiation characteristics.

The two parallel metalic circular discs separated by a small distance apart has been used as a means for guiding the electromagnetic energy flow radially outward in the cylindrical sense as in radial transmission line theory [7]. When the separation between the plates is much less than a half wave length, the transverse magnetic modes with circumferential variation and no variation along the axial direction controls this mechanism of the power transfer. The metalic disc patch over the ground plane separated by a thin substrate of relative permittivity $\varepsilon_r$ and thickness $h$ provides the same mentioned environ-

ment and the electromagnetic field in the substrate under the patch may be expressed in its circumferential modal expansion as follows:

$$E_z = \sum_n C_n Z_n(k\rho) \cos [n(\phi-\phi_o)]$$

$$H_\phi = -\frac{j}{\eta} \sum_n C_n Z'_n(k\rho) \cos [n(\phi-\phi_o)]$$

$$H_\rho = -\frac{j}{\eta} \sum_n \frac{C_n}{k\rho} Z_n(k\rho) \sin [n(\phi-\phi_o)]$$

where

$$Z_n(k\rho) = \begin{cases} J_n(k\rho) + A_n Y_n(k\rho) & , \rho \neq 0 \\ J_n(k\rho) & , (\rho = 0)\ \varepsilon V \end{cases}$$

The two main field components $E_z$ and $H_\phi$ in this model can be treated in some normalized sense as voltages and currents on a radial transmission line. For example, $(-E_z h)$ can be taken to be a total voltage between the ground plane and the patch (upper plate as positive) while $(2\pi\rho H_\phi)$ represents the total radial outward current in the upper plate (the patch). Other conventions like $(I = -2\pi\rho H_\phi, V = E_z h)$ is also acceptable and in the following analysis the work concentrates on the proportionality between the two quantities $(-\eta_o H_\phi)$ and $(E_z)$ which is a dimensionless ratio and leaves the final definition of impedances and admittances until the point of comparison with other published results and the extraction of the equivalent electric circuit parameters when the

array is treated as an N-port network. The analysis proceeds step by step in a self-contained fashion without any outside supplement until the need arises for the empirical extension formula to account for the fringing field effect at the aperture. First we extend the model of the cavity to include a current excitation source where the geometry of a single cell, say the i-th patch, is shown in figure (1) with a current $I_i$ pointed out of the figure (the z-direction) at the location $(\rho_i, \phi_i)$ and an angular spread $(2\delta)$. Without loss of generality, the effective radial thickness of the source is assumed infinitesimal which makes the cavity react to a surface current source $\bar{K}_e^i$ that is decomposable into a circumferential spectrum at $\rho = \rho_i$.

$$\bar{K}_e^{\,i} = \hat{z}\,\frac{I}{2\pi\rho_i}\,\delta(\rho-\rho_i)\left\{U\,[\,\phi-(\phi_i-\delta)\,]-U\,[\,\phi-(\phi_i+\delta)\,]\right\}$$

$$= \hat{z}\,\frac{I}{2\pi\rho_i}\,\delta(\rho-\rho_i)\left[\sum_0^{\infty}\left(\frac{2}{1+\delta_{no}}\right)\left(\frac{\sin n\delta}{n\delta}\right)\cos\left[\,n(\phi-\phi_i)\,\right]\right] \qquad (1)$$

But the two dimensional wave equation with no z-variation

$$(\nabla^2 + k^2)\,E_z^i = jk\eta J_z^i$$

indicates that the electric field $(E_z^i)$, under the i-th patch, have the same $\phi$-dependance as its own excitation current especially when outside influences such as coupling and scattering are ignored. Therefore, the electromagnetic field under the patch can be written in the following form for $\rho_i < \rho < b$,

$$E_z{}^i = \sum_0^\infty E_i{}^n \left( \frac{J_n(k\rho) + A_n{}^i\, Y_n(k\rho)}{J_n(kb) + A_n{}^i\, Y_n(kb)} \right) \cos\left[ n(\phi - \phi_i) \right] \tag{2}$$

$$H_\phi{}^i = -\frac{j}{\eta} \sum_0^\infty E_i{}^n \left( \frac{J'_n(k\rho) + A_n{}^i\, Y'_n(k\rho)}{J_n(kb) + A_n{}^i\, Y_n(kb)} \right) \cos\left[ n(\phi - \phi_i) \right] \tag{3}$$

and for $0 < \rho < \rho_o$

$$E_z{}^i = \sum E_i{}^n \left( \frac{J_n(k\rho_i) + A_n{}^i\, Y_n(k\rho_i)}{J_n(kb) + A_n{}^i\, Y_n(kb)} \right) \frac{J_n(k\rho)}{J_n(k\rho_i)} \cos\left[ n(\phi - \phi_i) \right] \tag{4}$$

$$H_\phi{}^i = -\frac{j}{\eta} \sum E_i{}^n \left( \frac{J_n(k\rho_i) + A_n{}^i\, Y_n(k\rho_i)}{J_n(kb) + A_n{}^i\, Y_n(kb)} \right) \frac{J'_n(k\rho)}{J_n(k\rho_i)} \cos\left[ n(\phi - \phi_i) \right] \tag{5}$$

In the above four equations (2)-(5) the continuity of the electric field from $\rho_i^-$ to $\rho_i^+$ (the source radial location) is introduced and the constant term $E_i^n$ becomes a representatives of the maximum amplitude of the modal electric field distribution in the aperture. The magnetic field as written is only consistant with the Maxwell's equation (proportional to the derivative of $E_z$) and its discontinuity at $\rho = \rho_i$ can be invoked to conform to the existance of the source current according to,

$$H_\phi(\rho=\rho_i^+) - H_\phi(\rho-\rho_i^-) = K_e$$

This defines the maximum amplitude $E_i^n$ of the modal electric field at the aperture as a function of the excitation current and the constant $A_n^i$ as follows:

$$E_i^n = jk\eta\, I \left(\frac{1}{2[1+\delta_{no}]}\right)\left(\frac{\sin n\delta}{n\delta}\right) J_n(k\rho_i)\left[\frac{J_n(kb)}{A_n^i} + Y_n(kb)\right] \tag{6}$$

Equations (2) and (3) at the aperture defines the parameter $A_n^i$ in terms of the field's ratio $p_i^n = (-\eta_o H_\phi^i / E_z^i)|_{\rho=b}$. That is,

$$A_n^i = -\left(\frac{p_i^n\, J_n(kb) - j\frac{\eta_o}{\eta} J'_n(kb)}{p_i^n\, Y_n(kb) - j\frac{\eta_o}{\eta} Y'_n(kb)}\right) \tag{7}$$

$$E_i^n = -\frac{\eta_o I_i}{\pi b}\;\frac{\frac{\sin n\delta}{n\delta}}{1+\delta_{no}}\left(\frac{\frac{J_n(k\rho_i)}{J_n(kb)}}{p_i^n - j\frac{\eta_o}{\eta}\frac{J'_n(kb)}{J_n(kb)}}\right) \tag{8}$$

Which means, the two dimensional wave equation gives the field in two regions, for $\rho_i < \rho < b$

$$E_z^i = \frac{j\eta k I_i}{2}\sum \frac{\frac{\sin n\delta}{n\delta}}{1+\delta_{no}} J_n(k\rho_i)\left[Y_n(k\rho) + \frac{1}{A_n^i} J_n(k\rho)\right]\cos[n(\phi-\phi_i)] \tag{2}'$$

$$H_\phi^i = \frac{kI_i}{2}\sum \frac{\frac{\sin n\delta}{n\delta}}{1+\delta_{no}} J_n(k\rho_i)\left[Y'_n(k\rho) + \frac{1}{A_n^i} J'_n(k\rho)\right]\cos[n(\phi-\phi_i)] \tag{3}'$$

and for $0 \le \rho \le \rho_i$

$$E_z^{\,i} = \frac{j\eta k I_i}{2} \sum \frac{\frac{\sin n\delta}{n\delta}}{1+\delta_{no}} J_n(k\rho) \left[ Y_n(k\rho_i) + \frac{1}{A_n^{\,i}} J_n(k\rho_i) \right] \cos\left[n(\phi-\phi_i)\right] \quad (4)'$$

$$H_\phi^{\,i} = \frac{k I_i}{2} \sum \frac{\frac{\sin n\delta}{n\delta}}{1+\delta_{no}} J'_n(k\rho) \left[ Y_n(k\rho_i) + \frac{1}{A_n^{\,i}} J_n(k\rho_i) \right] \cos\left[n(\phi-\phi_i)\right] \quad (5)'$$

consistant with Maxwell's equations, the continuity of the electric field at $\rho = \rho_i$, and the dicontinuity of the magnetic field is in accordance with the excitation current as given in Fig. (1). The only unknown left in the equations is the modal constant $A_n^i$, which is selected in the present work from the boundary condition at $\rho = b$. This is given by equation (7) in terms of a normalized (dimensionless) admittance parameter $p_i^n$ defined above. Therefore, the circumferential spectrum of the main field components at the aperture are represented by the two relations

$$(E_z^{\,i})_{aperture} = -\frac{\eta_o I_i}{\pi b} \sum_n \left( \frac{\frac{\sin n\delta}{n\delta}}{1+\delta_{no}} \right) \left( \frac{\frac{J_n(k\rho_i)}{J_n(kb)}}{p_i^{\,n} - j\frac{\eta_o}{\eta} \frac{J'_n(kb)}{J_n(kb)}} \right) \cos\left[n(\phi-\phi_i)\right] \quad (9)$$

$$(H_\phi^{\,i})_{aperture} = \frac{I_i}{\pi b} \sum_n \left( \frac{\frac{\sin n\delta}{n\delta}}{1+\delta_{no}} \right) \left( \frac{p_i^{\,n} \frac{J_n(k\rho_i)}{J_n(kb)}}{p_i^{\,n} - j\frac{\eta_o}{\eta} \frac{J'_n(kb)}{J_n(kb)}} \right) \cos\left[n(\phi-\phi_i)\right] \quad (10)$$

From equation (2)' the input impedance can be defined according to,

$$Z_{in} = \frac{-j\eta kh}{2} \sum \frac{\left(\frac{\sin n\delta}{n\delta}\right)}{1+\delta_{no}} J_n(k\rho_i)\left[ Y_n(k\rho_i) + \frac{1}{A_n{}^i} J_n(k\rho_i) \right] \tag{11}$$

and equation (9) indicates that, for the special case of a microstrip line feed connected to the edge, the input impedance becomes

$$Z_e = \frac{\eta_o h}{\pi b} \sum \frac{\frac{\sin n\delta}{n\delta}}{1+\delta_{no}} \left( \frac{1}{p_i{}^n - j\frac{\eta_o}{\eta}\frac{J'_n(kb)}{J_n(kb)}} \right) \tag{12}$$

Up to this step in the analysis, all information on the cavity characteristics and its current excitation have been introduced. The given equations become uniquely defined whenever the parameters $p_n^i$ are established which can be evaluated from the total array configuration, as seen in Fig. (2), and according to the free space radiation interaction mechanism. Before this step is explained, certain simplification can be identified. In order to achieve radiation coherence from the planar array, the individual currents must be injected into the patches in a similar fashion (i.e. $\phi_i$ is the same for all i's) and without loss to the generality of the analysis $\phi_i$ can be taken as zero. This assumption, as Fig. (2) shows, establishes the xz-plane as the E-plane of the array while the yz-plane is taken here as the H-plane of the array. The radiation is emitted from a magnetic current ribbon of radius b and a height h, in place of the aperture, backed by a perfectly conducting metalic pill box in place of the cavity. At any arbitrary aperture in the array, say the i-th, the aperture field when decomposed in its circumferential spectrum reads

$$H_\phi{}^i = \sum H_i{}^n \cos(n\phi) \quad , \quad E_z{}^i = \sum E_i{}^n \cos(n\phi)$$

To achieve the mutual coupling and its link to the above cavity formulation, a linear proportionality between the magnetic aperture field of one element and the aperture electric fields of all existing cells in the array must be assumed. This is accomplished by invoking on the above aperture spectrum the following proportionality

$$H_i{}^n = -\frac{1}{\eta_o} \sum_1^N p_{ij}{}^n \, E_j{}^n \tag{13}$$

That is,

$$p_i{}^n \, E_i{}^n = \sum_1^N p_{ij}{}^n \, E_j{}^n \tag{14}$$

Equation (13) is for an arbitrary element and can be generalized for the total array by considering those maximum amplitudes of the aperture field distribution as column vectors $H^{(n)}$, $E^{(n)}$ connected together by the matrix relation,

$$\mathbf{H}^{(n)} = -\frac{1}{\eta_o} \mathbf{p}^{(n)} \mathbf{E}^{(n)} \tag{15}$$

which is known as the short circuit admittance formulation of the coupling because of the definition of the $p^{(n)}$ matrix,

$$\mathbf{p}_{ij}{}^{(n)} = -\eta_o \left[ \frac{H_i{}^n}{E_j{}^n} \right] \quad , \; E_k{}^n = 0 \;\; when \;\; k \neq j$$

$$= -\eta_o \left[ \frac{(H_\phi{}^i)_{w.av.}}{E_j} \right] \quad , \; E_k{}^n = 0 \;\; when \;\; k \neq j \tag{16}$$

As seen from the purely mathematical definition of equation (16), the magnetic field $H_i^n$ on the i-th aperture is generated from the existance of an assumed electric field $E_j^n$ on the j-th aperture only, while all others are shorted. That means, the weighted average circumferential magnetic field $(H_\phi^i)_{wav}$ is generated by a magnetic current ribbon of a known strength ($\bar{K}_m^j = \hat{\phi}\, E_j^n \cos n\phi$) under the influence of the existing shorts. The word "weighted average" is clear in this case from the orthogonality of the spectrum,

$$(H_\phi{}^i)_{w.\,av.} = H_i{}^n = \frac{\int H_\phi{}^i \cos(n\phi)\, d\phi}{\int \cos^2(n\phi)\, d\phi}$$

This definition is extended to the interaction between identical apertures of arbitrary shapes, but similar distribution w(s) on the surface to yield the following general expression

$$(\hat{l}_i \cdot \bar{H}^i)_{w.\,av.} = \frac{\int\int ds_i\, W(s_i)\, (\hat{l}_i \cdot \bar{H}^i)}{\int\int ds_i\, W^2(s_i)}$$

where $\hat{\ell}_i$ is a tangential unit vector to the circumference ($\hat{z} \times \hat{n}_i = \hat{\ell}_i$). The unification of this approach to patches (apertures) of different shapes is accomplished by assuming a standardized electric field in the z-direction at the aperture of a real distribution function w(s) that corresponds to the mode in question ($E_z^j = E^j W(s_j)\hat{z}$). Let the outward normal $n_j$ to the aperture points into the radiation space and is a function of the patch's perimeter. This electric field yields a magnetic surface current ($\bar{K}_m^j = E^j W(\hat{s}_j)\hat{\ell}_j$) where the unit vector $\hat{\ell}_j$ conforms to the right hand rule of the cross product $\hat{\ell}_j = \hat{z} \times \hat{n}_j$.

Accordingly, the definition of the short circuit admittance parameter $p^{(n)}$ becomes,

$$\mathbf{p}_{ij}{}^{(n)} = -\eta_o \left[ \frac{(\hat{l}_i \cdot \bar{H})_{w.\,av.}}{E_j{}^n} \right] \quad , \; E_k{}^n = 0 \;\text{ for }\; k \neq j$$

As the magnetic field is generated by the magnetic current $\bar{K}_m^j$, its mathematical expression becomes

$$\mathbf{H} = \int\int ds_j \; \mathbf{G}^a \cdot \mathbf{K}_m{}^j \quad , \; \mathbf{G}^a = (\mathbf{I} + \frac{\nabla\nabla}{k_o{}^2}) \left( \frac{k_o}{j2\pi\eta_o} \; \frac{e^{-jk_oR}}{R} \right)$$

Note that the second order tensor $G^a$ is twice the free space Green's dyadic because of the image needed for the "Equivalence Theorem" [8]. Then,

$$\hat{l}_i \cdot \mathbf{H} = E_j \int\int ds_j \; W(s_j) \left[ \hat{l}_i \cdot \mathbf{G}^a \cdot \hat{l}_j \right]$$

$$(\hat{l}_i \cdot \mathbf{H})_{w.\,av.} = E_j \; \frac{\int\int ds_i \; W(s_i) \int\int \; ds_j \; W(s_j) \; [\hat{l}_i \cdot \mathbf{G}^a \cdot \hat{l}_j]}{\int\int \; ds_i \; W^2(s_i)}$$

Therefore,

(17)

$$\mathbf{p}_{ij}{}^{(n)} = - \frac{\int\int\int\int ds_i \; ds_j \; W(s_i) \; W(s_j) \; f \; (\hat{l}_i \, | \hat{l}_j)}{\int\int ds_i \; W^2(s_i)} \qquad (17)$$

$$f(\hat{l}_i \mid \hat{l}_j) = \frac{e^{-jk_o R}}{j2\pi k_o R^3}\left[2(1+jkR)(\hat{l}_i \cdot \hat{l}_j) + \left\{k_o^2 R^2 - 3[1+jk_o R]\right\}(\hat{R}\times\hat{l}_i)\cdot(\hat{R}\times\hat{l}_j)\right] \quad (18)$$

and R represents the distance between the source and observation points. The above generalized expression for $p_{ij}^{(n)}$, equations (17) and (18), coincides within a normalization factor with the stationary expression for the short circuit admittance derived from the variational principle and is given in the literature [8], [9]. To demonstrate the actual use of this generalized interaction formula, the current case of the circular disc patch array is brought back for evaluation. Since every patch in the array can be defined by its centre coordinates $(x_i, y_i)$, radius b, thickness h, $\hat{\ell}_i = \hat{\phi}_i$, and $\hat{n}_i = \hat{\rho}_i$, then the definition of an element of area $ds_i = bdzd\phi_i$ and the distribution function $W(s_i) = \cos(n\phi_i)$ becomes obvious. To investigate the interaction between this patch with any other arbitrary element of the array, say the j-th, the details of the geometry is explained in Fig. (3). The separation between the two patches and their relative orientation becomes,

$$D_m = \sqrt{(x_j - x_i)^2 + (y_j - y_i)^2} \quad , \quad \Phi_m = TAN^{-1}\left[\frac{Y_j - Y_i}{X_j - X_i}\right]$$

Let the two area elements be at two arbitrary locations defined by the variables $\phi_i$ and $\phi_j$ respectively, as shown by the horizontal projection plane of Fig. (3). The arbitrary location $\phi_j$ defines the triangle ($D_m$bL) completely, since the angle between $D_m$ and b becomes $(\pi+\phi_m-\phi_j)$ and yields the expression for L,

$$L = \sqrt{D_m^2 + b^2 + 2b\, D_m \cos(\phi_j - \phi_m)}$$

The other arbitrary surface element at $\phi_i$ defines the triangle (Lbρ) and the solution for ρ becomes

$$\rho = \sqrt{L^2 + b^2 - 2b\,L\cos\theta} \quad , \quad \theta = (\phi_i - \phi_m) - SIN^{-1}\left[\frac{b}{L}\sin(\phi_j - \phi_m)\right]$$

$$\beta = \theta + SIN^{-1}\left[\frac{b}{\rho}\sin\theta\right] \quad , \quad R = \sqrt{(z_j - z_i)^2 + \rho^2}$$

$$\hat{l}_i \cdot \hat{l}_j = \cos(\phi_j - \phi_i) \quad , \quad \hat{R} = \frac{\rho}{R}\,\hat{\rho} + \frac{z_j - z_i}{R}\,\hat{z}$$

$$(\hat{R}\times\hat{l}_i)\cdot(\hat{R}\times\hat{l}_j) = \frac{l^2}{R^2}\cos(\beta)\cos(\beta + \phi_j - \phi_i) + \frac{(z_j - z_i)^2}{R^2}\cos(\phi_j - \phi_i)$$

Therefore,

$$p_{ij}^{(n)} = -\frac{(\frac{b}{n})}{(1+\delta_{no})\,\pi}\int\int\int\int dz_i\,d\phi_i\;dz_j\,d\phi_j\;\cos(n\phi_i)\cos(n\phi_j)\,f_c(\hat{l}_i\,|\,\hat{l}_j)$$

$$f_c(\hat{l}_i\,|\,\hat{l}_j) = \frac{e^{-jk_oR}}{j2\pi k_oR^3}\left[\left\{\left\{2-3\frac{(z_j-z_i)^2}{R^2}\right\}(1+jk_oR) + k_o^2\,(z_j-z_i)^2\right\}\cos(\phi_j-\phi_i)\right.$$

$$\left. + \left\{k_o^2\rho^2 - 3\,\frac{\rho^2}{R^2}\,(1+jk_oR)\right\}\cos\beta\,\cos(\beta+\phi_j-\phi_i)\right] \qquad (19)$$

When the minimum separtion ($D_m$-2b) is much greater than h, the approximation of nill z-variation in $f_c(\ell_i\,|\,\ell_j)$ and $R \simeq \rho$ is acceptable. This reduces the above double area integration to a more manageable double contour integration,

$$p_{ij}^{(n)} = \frac{j(\frac{h}{b})}{2\pi^2(1+\delta_{no})}\int\int d\phi_i\;d\phi_j\;\cos(n\phi_i)\cos(n\phi_j)\,(\frac{b}{\rho})^2\,\frac{e^{-jk_o\rho}}{k_o\rho}\,\cdot$$

$$\left[2(1+jk_o\rho)\cos(\phi_j-\phi_i) + \left\{k_o^2\rho^2 - 3[1+jk_o\rho]\right\}\cos\beta\,\cos(\beta+\phi_j-\phi_i)\right] \qquad (20)$$

Equation (20) can be executed numerically for lack of a closed form solution. Although equations (19) and (20) hold also for the self

interaction of the diagonal elements in the matrix, where $s_i = s_j$, the evaluation is sensitive to handle in the neighbourhood of the singularity R = 0. If the integral expression is split in real and imaginary parts, the real part is found to be behaving well and render itself to a numerical evaulation.

$$\mathrm{Re}\,[p_{ii}^{(n)}] = \frac{(\frac{b}{h})}{2\pi}\int\int dzdz \cdot \int d\alpha\, \frac{\cos(n\alpha)}{k_o R^3} \cdot$$

$$\left[\left\{2-(\frac{\rho}{2b})^2\right\}\left\{\sin(k_oR)-k_oR\cos(k_oR)\right\} - (\frac{\rho}{2b})^2 k_o^2 R^2 \sin(k_oR)\right.$$

$$\left. + \left\{k_o^2R^2\sin(k_oR)-3[\sin(k_oR)-k_oR\cos(k_oR)]\right\}\left\{1-(\frac{\rho}{2b})^2\right\}\frac{(z\cdot-z)^2}{R^2}\right]$$

where, $$R = \sqrt{\rho^2 + (z\cdot - z)^2} \quad , \quad \rho = 2\,b\,\sin(\frac{\alpha}{2})$$

The approximation of the above for thin aperture becomes,

$$\mathrm{Re}\,[p_{ii}^{(n)}] = \frac{(\frac{h}{b})}{2\pi}\int d\alpha\,\cos(n\alpha)\,(\frac{b}{\rho})^2\,\frac{1}{k_o\rho}\left[(1+\cos^2\frac{\alpha}{2})\left\{\sin(k_o\rho)\right.\right.$$

$$\left.\left. - k_o\rho\,\cos(k_o\rho)\right\} - k_o^2\rho^2\,\sin(k_o\rho)\,\sin^2(\frac{\alpha}{2})\right] \qquad (21)$$

The radius ($\rho$ = 2b sin ($\frac{\alpha}{2}$)) upon substitution in Taylor-expansions of the trigonometic function yields an integrand polynomial in ($k_o$ b) within trigonometric coefficients in $\alpha$ that can be integrated exactly and the outcome is as follows:

$$\mathrm{Re}\,[p_{ii}^{(0)}] = (\frac{h}{b})\left[\frac{(k_ob)^4}{6} - \frac{(k_ob)^6}{30} + \frac{(k_ob)^8}{336} - \frac{(k_ob)^{10}}{6480} + - - - -\right]$$

$$\mathrm{Re}\,[p_{ii}^{(1)}] = (\frac{h}{b})\left[\frac{(k_ob)^2}{3} - \frac{2}{15}(k_ob)^4 + \frac{11}{420}(k_ob)^6 - \frac{11}{5436}(k_ob)^8\right.$$

$$\left. + \frac{37}{285120}(k_ob)^{10} + - - -\right]$$

$$\mathrm{Re}\,[p_{ii}^{(2)}] = (\frac{h}{b})\left[\frac{(k_ob)^4}{20} - \frac{(k_ob)^6}{84} + \frac{29}{22680}(k_ob)^8 - \frac{19}{249480}(k_ob)^{10} + - -\right]$$

In fact, we found from an intirely different technique that a general formula can be generated according to:

$$\mathrm{Re}\,[p_{ii}^{(n)}] = \left(\frac{h}{b}\right)\left[\frac{k_o b}{4}\int_0^{2k_o b}\left\{J_{2(n-1)}(x) + J_{2(n+1)}(x)\right\}dx - \frac{n^2}{2k_o b}\int_0^{2k_o b} J_{2n}(x)\,dx\right]$$

$$= \left(\frac{h}{b}\right)\sum_0^{\infty}\frac{(-1)^m\,(k_o)^{2(m+n)}}{m!\,(m+2n)!}\left[n + \frac{m(m-1)}{2(m+n)-1} - \frac{n^2}{2(m+n)+1}\right] \qquad (22)$$

Since it has been shown in reference [2] that a numerical evaluation of equation (21) gives good agreement with Shen's results [10], based on the far field calculation, then the confidence in formulation (22) for accuracy is established. Although the rest of the admittance can still be handled analytically from the imaginary part of equation (19) with a special care, the trend in the literature is to fit the reactive part so as to agree with the measured value of the modal resonance. To account for this step we assume

$$IM\,[p_{ii}^{(n)}] = \frac{\eta_o}{\eta}\left[\frac{J_n'(kb) - \dfrac{J_n'(kb_e)}{Y_n'(kb_e)}\,Y_n'(kb)}{J_n(kb) - \dfrac{J_n'(kb_e)}{Y_n'(kb_e)}\,Y_n(kb)}\right] \qquad (23)$$

where $b_e$ is a parameter yet to be determined. Note that the reactive part as assumed is in fact the normalized input susceptance at ($\rho$ = b) for a radial transmission line opened at $\rho = b_e$. To see how $b_e$ is to be estimated we go back to equation (9) and write down the relation between the modal electric field amplitude at the aperture and the excitation input current as follows,

$$\left(p_i^n - j\,\frac{\eta_o}{\eta}\,\frac{J_n'(kb)}{J_n(kb)}\right)E_i^n = -\frac{\eta_o}{\pi b(1+\delta_{no})}\left(\frac{\sin n\delta}{n\delta}\right)\frac{J_n(k\rho_i)}{J_n(kb)}\,I_i\ ,$$

and substitute relation (14) to obtain

$$\left( p_{ii}^{\,n} - j \frac{\eta_o}{\eta} \frac{J'_n(kb)}{J_n(kb)} \right) E_i^{\,n} + \sum_{j \neq i} p_{ij}^{(n)} E_j^{\,n} =$$

$$- \frac{\eta_o}{\pi b (1 + \delta_{no})} \left( \frac{\sin n\delta}{n\delta} \right) \frac{J_n(k\rho_i)}{J_n(kb)} I_i \quad , \tag{24}$$

Since the above equation is valid for i = 1, 2, ..., N, then the complete general relation of the array in matrix form becomes

$$\mathbf{P}^{(n)} \mathbf{E}^{(n)} = - \frac{\eta_o}{\pi b (1 + \delta_{no})} \left( \frac{\sin n\delta}{n\delta} \right) \mathbf{S}^{(n)} \mathbf{I}_z \tag{25}$$

where

$$(\mathbf{S}^{(n)})_{ij} = \delta_{ij} \frac{J_n(k\rho_i)}{J_n(kb)} \quad ; \; \delta_{ij} \; is \; 1 \text{ for } i = j \text{ and } 0 \; otherwise$$

$$(\mathbf{P}^{(n)})_{ij} = (p^{(n)})_{ij} - j \frac{\eta_o}{\eta} \frac{J'_n(kb)}{J_n(kb)} \delta_{ij}$$

Note that the $P^{(n)}$ matrix differs from the radiation admittance matrix $p^{(n)}$ only in the diagonal element. The new diagonal element is the same for all i's and by using (22) and (23) it can be written as

$$(\mathbf{P}^{(n)})_{ii} = \left[ \left( \left( \frac{h}{b} \right) \sum_0^{\infty} \frac{(-1)^m (k_o b)^{2(m+n)}}{m!\,(m+2n)!} \left[ n + \frac{m(m-1)}{2(m+n)-1} - \frac{n^2}{2(m+n)+1} \right] \right) \right.$$

$$\left. - j \frac{\eta_o}{\eta} \frac{2}{\pi kb} \left( \frac{\dfrac{J'_n(kb_e)}{J_n(kb)}}{Y'_n(kb_e) J_n(kb) - J'_n(kb_e) Y_n(kb)} \right) \right] \tag{26}$$

The imaginary part of the above expression represents both the assumed fringe field effect and the loading of the cavity, and does indicate resonance at $J'_n(kb_e) = 0$ according to the m-th root $J'_n(K_{mn}) = 0$ of the Bessell's function. That is,

$$f_r = \frac{K_{mn}\, c}{2\pi b_e \sqrt{\varepsilon_r}} \quad , \quad c \text{ is the velocity of light in free space.}$$

It is found [5], [6], [11] that the effective radius $b_e$ given by,

$$b_e = b \sqrt{1 + \frac{1}{\varepsilon_r} \left(\frac{2h}{\pi b}\right) \left[\ln\left(\frac{\pi b}{2h}\right) + 1.7726\right]}$$

predicts the observed resonance very well for $(b/h) \gg 1$.

If we assume no angular spread for the source location or that we are interested only in the earlier resonant modes so that $(\sin(n\delta)/n\delta)$ is approximately one, equation (25) renders the edge characteristics of the array's patch in the standard voltage, current, impedance, admittance form as follows: -

$$\mathbf{V}_e^{(n)} = \mathbf{Z}_e^{(n)}\, \mathbf{I}_{in} = \mathbf{Y}_n^{-1}\, \mathbf{S}^{(n)}\, \mathbf{I}_{in} \tag{27}$$

$$(\mathbf{Y}_n)_{ij} = \frac{j}{2\pi\eta_o} \int\int d\phi\, d\phi' \cos(n\phi) \cos(n\phi')\, F_{ij}$$

$$(\mathbf{Y}_n)_{ii} = \frac{1+\delta_{no}}{120} \left[ \left( \sum \frac{(-1)^m (k_o)^{2(m+n)}}{m!\,(m+2n)!} \left[ n + \frac{m(m-1)}{2(m+n)-1} - \frac{n^2}{2(m+n)+1} \right] \right) \right.$$

$$\left. - j\, \frac{2}{\pi (k_o h)} \left( \frac{\frac{J_n'(kb_e)}{J_n(kb)}}{Y_n'(kb_e)\, J_n(kb) - J_n'(kb_e)\, Y_n(kb)} \right) \right]$$

$$F_{ij} = \left(\frac{b}{\rho}\right)^2 \frac{e^{-jr}}{r} \left[ 2(1+jr) \cos(\phi'-\phi) + (r^2 - 3[1+jr]) \cos\beta \cos(\beta+\phi'-\phi) \right]$$

$$r = k_o \rho$$

Equation (2) can now be used at ($\rho$ = b) and ($\rho = \rho_i$) in order to eliminate $A_n^i$ and relate the input electric field to that at the edge plus the input excitation current which produces the following expression for the modal input network parameters,

$$\mathbf{V}_{in}^{(n)} = \mathbf{Z}_{in}^{(n)}\,\mathbf{I} = \left\{ \mathbf{S}^{(n)}\,\mathbf{Y}_n^{-1}\,\mathbf{S}^{(n)} + \mathbf{Z}_s^{(n)}\,\mathbf{S}^{(n)} \right\} \mathbf{I} \tag{28}$$

$$\left[\mathbf{Z}_s^{(n)}\right]_{ij} = j\,\delta_{ij}\,\frac{\eta_o(k_o h)}{2(1+\delta_{no})}\left[ J_n(k\rho_i)\,Y_n(kb) - J_n(kb)\,Y_n(k\rho_i) \right] \tag{29}$$

Since the desired antenna characteristics such as high gain, beam scanning, or steering capability are possible when discrete patches are combined to form an array such as the one discussed or in different arrangement; a general program has to be written for planar array of arbitrary configuration. Array theory has been treated in many texts [8], [12], [13], [14], [15] with emphasis on the array factor ($T_T = T_x T_y$) eminating from relative spacial distribution of the patches ($R_j = R_o - \rho_j \cos\gamma_j$, and $\gamma_j = \cos\theta\cos\theta_j + \sin\theta\sin_j\cos(\phi-\phi_j)$) weighted by a coefficient proportional to contribution of the j-th element ability to radiate under the indluence of coupling to its neighbours. That is to say,

$$T_t^{(n)} = \sum_{k=1}^{N} \left[\mathbf{V}_e^{(n)}\right]_k e^{jk_o (X_k \sin\theta\cos\phi + Y_k \sin\theta\sin\phi)} \tag{30}$$

If we accept the theoretical far field radiation pattern for a magnetic current loop of radius b as the value to be modulated, then we can write the total far field of the array as follows: -

$$E_\theta^{(n)} = \left[ -(j)^n\,(bk_o)\,\frac{e^{-jk_oR_o}}{R_o} \right] J'_n(k_o b\,\sin\theta)\cos(n\phi)\,T_t^{(n)} \tag{31}$$

$$E_\phi^{(n)} = \left[ (j)^n\,(bk_o)\,\frac{e^{-jk_oR_o}}{R_o} \right] \frac{n\,\cos\theta\,J_n(kb\,\sin\theta)}{kb\,\sin\theta}\,\sin(n\phi)\,T_t^{(n)} \tag{32}$$

Relation (31), (32) and (27) completes the tool for studying the total radiation pattern as a function of independent excitation currents. By artificially equating the off diagonal matrix elements $(Y_n)_{ij}$ to zero we can also generate the hypothetical case of the array theory without coupling. Hence the quantitative analytical study of their difference becomes feasible.

## 3. THE RECTANGULAR PATCH MODEL

The simplest microstrip patch configuration is undoubtedly the rectangular microstrip element as shown in Fig. (4). This simplicity has led a large number of researchers [1], [2], [17], [18], [19] to make numerous attempts to predict and evaluate its radiation and circuit characteristics. The mutual coupling between two rectangular patches has been studied [20], [21] and measured using the TEM- transmission line model as the internal line of communicaton between the two radiating apertures and the current source. This is the simplest method used by the researchers to develop a step-by-step procedure for the antenna design and to augment other factors as the need arises [2] to improve the model to its final completion. If one wonders why then the choice is made in this report to start with the analysis of the circular disc patch instead. The main rational is that the disc is one aperture patch, where the orthogonality of the circumferential modes are evident and the radial propagation characteristics of the TM-modes under the patch is uniquely defined by the dielectric constant of the substrate and its thickness. In contrast, the case at hand deals with two apertures per each rectangular patch that are linked together and to the excitation source via a TEM-transmission line. Simultaneously

they are also coupled to all other radiating apertures, including each other, from the outside through the radiation interaction mechanism of parallel magnetic current strips. Also an estimate for the propagation characteristics of the transmission line must be established since the TEM-mode propagates the energy in a mix of free space and the dielectric media.

Since in most of the common applications the rectangular patch array excites the transmission line mode of uniform aperture field distribution, the current analysis conforms to this demand and can in future be extended to any other required modal distribution. Because we are dealing with two, left and right, radiating apertures per patch in the planar array seen in Fig. (5), we assume the injected excitation current to split the resonant length L to $L_i^-$ and $L_i^+$. The corresponding electric field at these apertures are $E_i^-$ and $E_i^+$, assumed in the positive z-direction. The quantities ($E_i^- h$) and ($E_i^+ h$) are the left and right edge voltages by convention in this case and Fig. (6) indicates the corresponding quantities needed to evaluate the interaction admittance by the generalized variational expression generated in the previous section.

Since only the uniform aperture mode is discussed, the superscript (n) is dropped and the aperture magnetic field is defined according to the radiation convention $\hat{n}_i^- = -\hat{x}$, $\hat{n}_i^+ = +\hat{x}$, $\hat{\ell}_i^- = \hat{z} \times \hat{n}_i^-$, $\hat{\ell}_i^+ = \hat{z} \times \hat{n}_i^+$. That is,

$$\bar{H}^-_{aperture} = -\mathbf{H}^-_i \hat{\mathbf{l}}^-_i \quad , \mathbf{H}^-_i = -\left(\hat{\mathbf{l}}^-_i \cdot \bar{\mathbf{H}}^-_{aperture}\right)_{w.\,av}$$

$$\bar{H}^+_{aperture} = -\mathbf{H}^+_i \hat{\mathbf{l}}^+_i \quad , \mathbf{H}^+_i = -\left(\hat{\mathbf{l}}^+_i \cdot \bar{\mathbf{H}}^+_{aperture}\right)_{w.\,av} .$$

Note that the weighted average is a simple average in this case since we are dealing with the uniform distribution mode W(s) = 1. The electromagnetic field under the patch can be written in a transverse electromagnetic configuration ($E_z^i$, $H_y^i$) for the i-th patch

$$E_z^{TL} = A_1^i \cos k x + B_1^i \sin kx \qquad \text{for } 0 \leq x \leq L_i^-$$

$$H_y^{TL} = \frac{jA_1^i}{\eta} \sin k x + \frac{B_1^i}{j\eta} \cos kx$$

and

$$E_z^{TL} = A_z^i \cos k(L-x) + B_z^i \sin k(L-x) \qquad \text{for } L_i^- \leq x \leq L_i$$

$$H_y^{TL} = \frac{A_2^i}{j\eta} \sin k(L-x) + j\frac{B_2^i}{\eta} \cos k(L-x)$$

The arbitrary constants can be identified from the aperture quantities, and the non-ideal TEM-transmission is compensated for by effective propagation constants $k_e$ and $\eta_e$. That is

$$E_z^{TL} = E_i^- \cos (k_e x) + j\eta_e H_i^- \sin (k_e x) \qquad \text{for } 0 \leq x \leq L_i^-$$

$$H_y^{TL} = j\frac{E_i^-}{\eta_e} \sin (k_e x) + H_i^- \cos (k_e x)$$

and

$$E_z^{TL} = E_i^+ \cos [k_e(L-x)] + j\,\eta_e H_i^+ \sin [k_e(L-x)] \qquad \text{for } L_i^- \leq x \leq L_i$$

$$H_y^{TL} = \frac{E_i^+}{j\,\eta_e} \sin\left[k_e k(L-x)\right] - H_i^+ \cos\left[k_e(L-x)\right]$$

where, $k_e = k_i\sqrt{\varepsilon}_e$ , $\eta_e = \eta_o/\sqrt{\varepsilon}_e$

$$\varepsilon_e = \frac{1}{2}\left[(\varepsilon_r+1) + (\varepsilon_r-1)\left(1+\frac{12h}{W}\right)^{-\frac{1}{2}}\right], \text{ see reference (1).}$$

The above two sets of equations must also satisfy the continuity of the electric field at $x = L_i^-$, and that the discontinuity of the magnetic field $\left[H_y^{TL}(x = L_i^- + \delta) - H_y^{TL}(x = L_i^- - \delta)\right]$ has to equal the average excitation current in the z-direction $(I_z^i/W)$ where W represents the width of the patch in the y-direction. That is,

$$\left(H_i^+ \sin(k_e L_i^+) - H_i^- \sin(k_e L_i^-)\right) - \frac{j}{\eta_e}\left(E_i^+ \cos(k_e L_i^+) - E_i^- \cos(k_e L_i^-)\right) = 0 \qquad (33)$$

$$\left(H_i^+ \cos(k_e L_i^+) + H_i^- \cos(k_e L_i^-)\right) + \frac{j}{\eta_e}\left(E_i^+ \sin(k_e L_i^+) + E_i^- \sin(k_e L_i^-)\right) = -\frac{I_z^i}{W} \qquad (34)$$

Although equations (33) and (34) are the two physical conditions of the model, and we could introduce the coupling at this stage, they proved to be cumbersome to handle before further simplification. If we multiply (34) by sin $(k_e L_i^-)$ and (33) by cos$(kL_i^-)$ then add both, a mathematically simpler equation is produced, and if (34) is multiplied by sin $(k_e L_i^+)$ and (33) by cos $(kL_i^+)$ then by subtraction the other simplified relation is also produced. Hence the physical pair (33), (34) is equivalent to the following mathematical pair,

$$H_i^+ - \frac{j}{\eta_e}\left\{ \cot(k_e L_i)\, E_i^+ - \csc(k_o L_i)\, E_i^- \right\} = -\frac{1}{W}\left(\frac{\sin kL_i^-}{\sin kL_i}\right) I_z^i \qquad (35)$$

$$H_i^- + \frac{j}{\eta_e}\left\{ \csc(k_e L_i)\, E_i^+ - \cot(k_o L_i)\, E_i^- \right\} = -\frac{1}{W}\left(\frac{\sin kL_i^+}{\sin kL_i}\right) I_z^i \qquad (36)$$

These two principal mathematical quations have successfully isolated the dependance of the aperture field on the excitation location to the right hand side, and allowed the loading effect of the rectangular cavity (as in the circular case) to appear explicitly by the two terms $(-j \frac{1}{\eta_e} \cot(k_e L_i))$ and $(j \frac{1}{\eta_e} \csc(k_e L_i))$.

To bring the radiation interaction into the picture we assume a linear proportionality between the aperture magnetic field and all existing aperture electric fields. Since we are dealing with two apertures per patch, an attempt can be made to relate the proportionality to the definition of the normalized radiation admittance used in the circular case, which by the variational expression given earlier by equation (17) provides.

$$H_i^+ = \frac{1}{\eta_o} \sum (p_{ij}^{++} E_j^+ + p_{ij}^{+-} E_j^-)$$

$$H_i^- = \frac{1}{\eta_o} \sum (p_{ij}^{-+} E_j^+ + p_{ij}^{--} E_j^-)$$

Once the array configuration becomes like Fig. (5) and no relative rotation between patches are recognized, then the simple reduction of the above four matrix elements to only two basic matrix elements, gives

$$p_{ij}^{--} = p_{ij}^{++} = p_{ij}$$

$$p_{ij}^{-+} = p_{ji}^{+-} = q_{ij}$$

$$H_i^+ = \frac{1}{\eta_o} \sum (p_{ij} E_j^+ + q_{ji} E_j^-)$$

$$H_i^- = \frac{1}{\eta_o} \sum (q_{ij} E_j^+ + p_{ij} E_j^-)$$

where $p_{ij}$ is the mutual normalized admittance between any two apertures, of the same polarity, in the i-th and the j-th patches. It obeys formula (17) and takes the explicit expression

$$p_{ij} = \frac{j(\frac{h}{w})}{2\pi} \int_{-\frac{w}{2}}^{\frac{w}{2}} \int_{-\frac{w}{2}}^{\frac{w}{2}} dy dy' \frac{e^{-jk_o\rho}}{k_o\rho^3} \left[ k_o^2 (x_j - x_i)^2 + (1 + jk\rho) \left[ 2 - 3\frac{(x_j - x_i)^2}{\rho^2} \right] \right] \quad (37)$$

$$\rho = \sqrt{(x_j - x_i)^2 + (y_j - y_j + y' - y)^2}$$

where $(x_i, y_i)$ is the coordinate of the i-th patch centre and $(y, y')$ are the dummy variables of integration in the longitudinal aperture direction.

Note that this matrix is symmetric ($p_{ij} = p_{ji}$). On the other hand, the $q_{ij}$ represents the mutual admittance matrix element between the negative aperture of the i-th cell $(x_i - \frac{L_i}{2}, y_i + y)$ and the positive aperture of the j-th patch $(x_j + \frac{L_i}{2}, y_j + y')$. The opposite polarity dictates that $\hat{\ell}_i \cdot \hat{\ell}_j = -1$.

$$q_{ij} = -\frac{j(\frac{h}{w})}{2\pi}\int_{-w/2}^{w/2}\int_{-\frac{w}{2}}^{w/2} dydy' \frac{e^{-jk_o\rho}}{k_o\rho^3}\left[k_o^2(x_j - x_i + L)^2\right.$$

$$\left. + (1+jk\rho)\left(2-3\frac{(x_j - x_i + L)^2}{\rho^2}\right)\right] \qquad (38)$$

$$\rho = \sqrt{(x_j - x_i + L)^2 + (y_j - y_j + y' - y)^2} \quad , \; L_i = L_j = L \quad , \; q_{ij} \neq q_{ji}$$

When the mutual interaction $p_{ij}^{+-}$ between the apertures $(x_i+\frac{L}{2},\ y_i+y)$ and $(x_j - \frac{L}{2},\ y_j+y')$ is constructed, the formulation becomes the same as equation (38) with the role of $(x_i, x_j)$ interchanged $(p_{ij}^{+-} = q_{ji})$. Hence, the substitution of the invoked linearity in equation (35), (36) for all i's (i = 1, 2, ..., N) produces the two matrix equations

$$\mathbf{P}\,\mathbf{E}^+ + \mathbf{Q}_i\,\mathbf{E}^- = -\frac{\eta_o}{w}\,\mathbf{S}^-\,\mathbf{I}_z \qquad (39)$$

$$\mathbf{Q}\,\mathbf{E}^+ + \mathbf{P}\,\mathbf{E}^- = -\frac{\eta_o}{w}\,\mathbf{S}^+\,\mathbf{I}_z \qquad (40)$$

where the P and Q matrices differ only from equations (37), (38) in the diagonal element where the cavity loading takes place,

$$(\mathbf{P})_{ii} = (p)_{ii} - j\,\frac{\eta_o}{\eta_e}\,cot(k_e L_i) \quad , \; (\mathbf{P})_{ij} = (p)_{ij} \qquad i \neq j$$

$$(\mathbf{Q})_{ii} = (q)_{ii} + j\,\frac{\eta_o}{\eta_e}\,\csc(k_e L_i) \quad , \; (\mathbf{Q})_{ij} = (q)_{ij} \qquad i \neq j$$

$$(\mathbf{S}^+)_{ij} = \delta_{ij}\left[\sin(k_e L_i^+)/\sin(k_e L_i)\right], \; (\mathbf{S}^-)_{ij} = \delta_{ij}\left[\sin(k_e L_i^-)/\sin(k_e L_i)\right]$$

Equations (39) and (40) are the two coupled equations between the aperture fields and the decoupling yields

$$(\mathbf{P} - \mathbf{Q}_t\ \mathbf{P}^{-1}\ \mathbf{Q}\ )\ \mathbf{E}^{+} = -\ \frac{\eta_o}{w}\ (\mathbf{S}^{-} - \mathbf{Q}_t\ \mathbf{P}^{-1}\ \mathbf{S}^{+})\ \mathbf{I}_z \qquad (41)$$

$$(\mathbf{P} - \mathbf{Q}\ \mathbf{P}^{-1}\ \mathbf{Q}_t\ )\ \mathbf{E}^{-} = -\ \frac{\eta_o}{w}\ (\mathbf{S}^{+} - \mathbf{Q}\ \mathbf{P}^{-1}\ \mathbf{S}^{-})\ \mathbf{I}_z \qquad (42)$$

These final matrix relations are the ones to be handled with the aid of a computer program in order to obtain the aperture electric field dependence on the excitation current with the inclusion of the mutual interaction. These equations can be converted to the standard electric circuit parameters (edge voltages, input currents, and admittance/impedance matrices) to look like,

$$\mathbf{V}_e^{+} = \mathbf{Z}_e^{+}\ \mathbf{I} = (\ \mathbf{Y}_s - \mathbf{Y}_{pn}\ \mathbf{Y}_s^{-1}\ \mathbf{Y}_{np}\ )^{-1}\ (\mathbf{S}^{-} - \mathbf{Y}_{pn}\ \mathbf{Y}_s^{-1}\ \mathbf{S}^{+}\ )\ \mathbf{I} \qquad (43)$$

$$\mathbf{V}_e^{-} = \mathbf{Z}_e^{-}\ \mathbf{I} = (\ \mathbf{Y}_s - \mathbf{Y}_{np}\ \mathbf{Y}_s^{-1}\ \mathbf{Y}_{pn}\ )^{-1}\ (\mathbf{S}^{+} - \mathbf{Y}_{np}\ \mathbf{Y}_s^{-1}\ \mathbf{S}^{-}\ )\ \mathbf{I} \qquad (44)$$

$$\mathbf{Y}_s = \frac{(\frac{w}{h})}{\eta_o}\ \mathbf{P}\ \ ,\ \mathbf{Y}_{np} = \frac{(\frac{w}{h})}{\eta_o}\ \mathbf{Q}\ \ ,\ \mathbf{Y}_{pn} = \mathbf{Y}_{np}^{t}$$

$$(\mathbf{P})_{ii} = \eta_o\ (\frac{h}{w}) \left[ \left( \frac{(\frac{w}{\lambda_o})^2}{15} \sum \frac{(-1)^m\ (k_o w)^{2m}}{(2m+3)\ !\ (2m+1)} \right) + j \left( \frac{1}{60}\ (\frac{w}{\lambda_o})\ (\frac{\Delta l}{h})\ \epsilon_e - \frac{w}{\eta_e h}\ cot\ (k_e L_i) \right) \right] \qquad (45)$$

$$\epsilon_e = \frac{1}{2}\ [\ (\epsilon_r + 1) + (\epsilon_r - 1)\ (1 + 12\frac{h}{w}\ )^{-\frac{1}{2}}\ ]$$

$$\frac{\Delta l}{h} = .412 \left[ \frac{(\epsilon_e + .3)\ (\frac{w}{h} + .264)}{(\epsilon_e - .258)\ (\frac{w}{h} + .8)} \right]$$

Note that the real part has been accomplished exactly while the imaginary part of the self-admittance of the aperture has been estimated with the extention formula supplied by reference (1). That is to say, the self-admittance of a radiating aperture becomes:

$$Y_a = G_a + j\,B_a = \left( \frac{(\frac{w}{\lambda_o})^2}{15} \sum \frac{(-1)^m\,(k_o w)^{2m}}{(2m+3)\,!\,(2m+1)} \right) + j \left( \frac{1}{60}\,(\frac{w}{\lambda_o})\,(\frac{\Delta l}{h})\,\epsilon_e \right) \qquad (46)$$

where the imaginary part is the same as reference [1], equation (2.30b) page 46, and real part gives the actual value of the radiation conductance that in the limit of $W << \lambda_o$ coincides with equation (2.50) of the reference mentioned. As a check on the mathematical model, we considered the special case of one patch without mutual coupling between the negative and positive edges $[Y_{np})_{11} = j\frac{W}{\eta_e} j\ \csc(k_e L)]$ and injected the input current at the left edge $[S^+ = 1,\ S^- = 0]$. The corresponding expression, using equation (44), for the input admittance becomes

$$Y_{in} = Y_a + \frac{w}{\eta_e\,h}\,\frac{y_a + j\,\frac{w}{\eta_e h}\tan(k_e L)}{\frac{w}{\eta_e\,h} + j\,Y_a\tan(k_e L)}$$

which is identical to reference [1], equation 2.55, once the characteristic admittance is recognized by $y_o = \frac{W}{\eta_e h}$. As a final check the case of two different patches, arbitrarily translated from each other, are injected both from the negative edge so that $S^+ = I$, and $S^- = 0$. The (2 x 2) matrices can be handled analytically and produces the final input admittance parameters,

$$Y_{11} = Y_{ST1} - \left\{ Y_{MT1}{}^2\,Y_{ST2} - 2\,Y_s{}^{12}\,Y_{np}{}^{12}\,Y_{MT1} + [Y_{np}{}^{12}]^2\,Y_{ST1} \right\} / N$$

$$Y_{11} = Y_{ST2} - \left\{ Y_{MT2}^{\,2}\, Y_{ST1} - 2\, Y_s^{\,12}\, Y_{np}^{\,21}\, Y_{MT2} + [Y_{np}^{\,21}]^2\, Y_{ST2} \right\} / N$$

$$Y_{12} = Y_{21} = Y_s^{\,12} - \left\{ Y_{MT1}\, Y_{ST2} + Y_{MT2}\, Y_{ST1} - Y_{MT1}\, Y_{MT2}\, Y_s^{\,12} - Y_s^{\,12}\, Y_{np}^{\,12}\, Y_{np}^{\,21} \right\} /N$$

$$Y_{ST1} = Y_a^{\,1} - j\, Y_o^{\,1} \cot(k_e L_1) \quad , \; Y_{MT1} = Y_{np}^{\,1} + jY_o^{\,1} \csc(k_e L_1)$$

$$Y_{ST2} = Y_a^{\,2} - j\, Y_o^{\,2} \cot(k_e L_2) \quad , \; Y_{MT2} = Y_{np}^{\,2} + jY_o^{\,2} \csc(k_e L_2)$$

$$N = Y_{ST1}\, Y_{ST2} - (Y_s^{\,12})^2$$

These results are identical to those of Van Lil and Van de Cappelle [20], and we conclude that the model as it stands is correct and ready for numerical programming of the general case.

It is desirable from the feed point of view to know the input impedance at any arbitrary location and not the special case of $L_i^- = 0$ discussed above. This step can be explained by going back to the transmission line equation, where the input electric field $E_{in}^i$ is the same as $E_i^{TL}$ at $x = L_i^-$. That is,

$$E_{in} = E_i^{\,+} \cos(k_e L_i^{\,+}) + j\, \eta_e\, H_i^{\,+} \sin(k_e L_i^{\,+}) \tag{47}$$

or from left of the source

$$E_{in} = E_i^{\,-} \cos(k_e L_i^{\,-}) + j\, \eta_e\, H_i^{\,-} \sin(k_e L_i^{\,-}) \tag{48}$$

use any of the two equations and substitute the corresponding aperture magnetic field ($H_i^+/H_i^-$) from equations (35/36) to obtain the following relation

$$E_{in}{}^{i} = \left(\frac{\sin(k_e L_i{}^-)}{\sin(k_e L_i)}\right) E_i{}^+ + \left(\frac{\sin(k_e L_i{}^+)}{\sin(k_e L_i)}\right) E_i{}^- - j\,\frac{\eta_e}{w}\sin k_e L_i \left(\frac{\sin(k_e L_i{}^-)}{\sin(k_e L_i)}\right)\left(\frac{\sin(k_e L_i{}^+)}{\sin(k_e L_i)}\right) I_z{}^{i}$$

which must hold for all i = 1, 2, ..., N in the array.

Therefore,

$$\mathbf{E}_{in} = \mathbf{S}^- \mathbf{E}^+ + \mathbf{S}^+ \mathbf{E}^- - j\,\frac{\eta_e}{w}\sin(k_e L)\,\mathbf{S}^+ \mathbf{S}^- \mathbf{I}_z \qquad (49)$$

Hence, the conversion to the circuit parameters gives

$$\mathbf{V}_{in} = \mathbf{Z}_{in}\,\mathbf{I}_{in} \qquad (50)$$

$$\mathbf{Z}_{in} = \mathbf{S}^- \mathbf{Z}_e{}^+ + \mathbf{S}^+ \mathbf{Z}_e{}^- + j\,\frac{\eta_e h}{w}\sin(k_e L)\,\mathbf{S}^- \mathbf{S}^+ \qquad (51)$$

where the edge impedance are defined by equations (43) and (44).

## 4. NUMERICAL CHECKS OF THE MODELS

Both models clearly exhibit complexity far beyond the capability of just a disc calculator even for the limiting case of only two patch array. The main obstacles are the numerical integration required for the variational form of the mutual interaction and the need to invert complex matrices in order to study the array performance. Therefore, an efficient computer program has been written to manipulate these given formulations toward the different characteristics of interest to the designer. Two prototype programs are written in FORTRAN for both the circular and rectangular planar arrays. While they are still in infancy, some of their results are shown here for comparison with the available data in the literature and to validate the acceptability of the model formulation as given in this report. The case of a single rectangular patch, resonant at 2.2 GHz, with the dimension (L = 4.14 cm, W = 6.858 cm, h = 0.159 cm) and a relative permittivity $\varepsilon_r = 2.62$, is injected from a microstrip line at $\bar{L} = 1.016$ cm is put to the program for the calculation of the input impedance. Since this is a duplicate of a case studied [2] in the literature, to see the effect of including the mutual interaction between the left and right apertures in the transmission line theory, we have the chance to validate our calcualtion. Figure (7) shows the modal input impedance of the $TEM_1$-mode in the neighbourhood of its resonance for the case above as compared with a circular disc patch ($TM_{11}$-mode) that resonates at the same frequency and is fed by a hypothetical strip line at $\phi = 0$. The results seems to be reasonable compared to the available data. Since we evaluate the self-conductance of a radiating aperture analyti-

cally, a test for the variation of the radiation admittance, for different operating modes of the circular disc patch, with frequency are shown in figures [8]-[12] and the result of the $TM_{11}$ mode agrees with the available data [2], [10]. Figures [13]-[18] investigate the variation of the mutual coupling with the separation, for various orientations (E-coupling, H-coupling, and the middle plane) of two circular patches in different modes of operation. Finally figures [19]-[22] show the effect of coupling on the array radiation pattern of a five element array with both E-plane and H-plane coupled configurations. The circular array operates in the $TM_{11}$-mode and the rectangular case is in the $TEM_1$-mode. The result is acceptable and the testing of the programs are completed. A complete listing of the two programs are documented at the end of the report with a short user manual. Most of the parameters used in the program itself are the one used in this report to facilitate any future augmentation and modification by the users.

## EXPERIMENTAL VERIFICATION

In the previous section mutual coupling effects in linear arrays was investigated. No experimental verification was provided. To examine the validity of the solutions it is, of course, desirable to compare the computed results with experimental data. In this section, we provide a sample case and compare the computed radiation patterns with measured ones.

For the array, a planar geometry is considered, which is shown in Fig. 23. It consists of 19-circular patches designed with a hexagonal grid. Each element is excited by a coaxial probe, at an appropriate point to match the line impedance. Since, the effect of mutual coupling increases with the beam scan, the array elements were phased to generate a main beam along the 35° elevation. The element phases were achieved by using cables of appropriate lengths. The radiation pattern without the effect of mutual coupling gives a main beam with a peak gain of about 12.5 dB, which is considerably higher than the measured gain of about 10 dB. Including the effects of mutual coupling reduces the gain to that of the measured one. Their agreement is quite satisfactory, except near the second sidelobe, where the measured results give a higher level.

These results indicate that, for the selected array the inclusion of the mutual coupling effect improves the prediction of the array pattern, essentially in all ranges of the $\theta$-angle, except near the zero elevation angle. This is of course expected, since the analytic model is based on the assumption of infinite ground plane and the measurement is for an array with a finite ground plane. This single comparison also validates the accuracy of the array modelling. Further comparison

should be carried out to investigate the accuracy of the cross-polar components and also the effects of higher order modes.

## REFERENCES

[1] Bahl, I.J. and Bhartia, P., Microstrip Antenna, Artech House., 1980.

[2] Bhattacharayya, A.K., "Generalized Transmission Line Model of Microstrip Patch Antennas and Some Applications", Ph.D. Thesis, Indian Institute of Technology, Kharagpur-721 302, India, Feb. 1985.

[3] Watkins, J., "Circular Resonant Structures in Microstrip", Electron. lett., Vol. 5, 1969.

[4] Long, S.A. Shen, L.C., and Morel, P.B., "Theory of the Circular Disc Printed Circuit Antenna", Proc. IEE, vol. 125, 1978.

[5] Derneryd, A.G., "Analysis of the Microstrip Disc Antenna Element", IEEE Trans. on Antenna and Propag., vol. AP-27, 1979.

[6] Shen, L.C., et. al., "Resonant Frequency of a Circular Disc, Printed-Circuit Antenna", IEEE Trans. on Antenna and Propag., vol. AP-25, 1977.

[7] Ramo, S., and Whinnery, J.R., "Field and Waves in Modern Radio", 2nd edition, John Wiley & Sons, NY, 1960.

[8] Collin, R.E. and Zucker, F.J., "Antenna Theory, Part 1", Inter-University Electronic Series, vol. 7, McGraw-Hill, 1969.

[9] Harrington, R.F., "Time Harmonic Electromagnetic Fields", McGraw-Hill, 1961.

[10] Shen, L.C., "Analysis of a Circular Disc Printed Circuit Antenna", Proc. IEE, vol. 126, 1979.

[11] Long, S.A. and Shen, L.C., "The Circular Disc, Printed Circuit Antenna", IEEE AP-S, Int. Symp. Digest, 1977.

[12] Ma, M.T., "Theory and Application of Antenna Arrays", Wiley-Interscience, NY, 1974.

[13] IEEE Trans. on Antenna and Propag., "Special Issue on Conformal Arrays", Jan. 1974.

[14] IEEE Proceeding "Special Issue on Electronic Scanning", Nov. 1968.

[15] IEEE Trans. on Antenna and Propag., "Special Issue on Adaptive Antennas", Sept. 1976.

[16] Proc. Workshop on Printed Circuit Antenna Technology, New Mexico State University, Las Cruses, Oct. 1979.

[17] Derneryd, A.G., "A Network Model of the Rectangular Microstrip Antenna", IEEE AP-S, Int. Symp. Digest, 1977.

[18] Derneryd, A.G., "A Theoretical Investigation of the Rectangular Microstrip Antenna Element", IEEE Trans. on Antenna and Propag., vol. AP-26, 1978.

[19] Derneryd, A.G., and Lind, A.G., "Extended Analyusis of Rectangular Microstrip Antennas", IEEE Trans. on Antenna and Propag., vol. AP-27, 1979.

[20] Van Lil, E.H., and Van de Cappelle, A.R., "Transmission Line Model for Mutual Coupling Between Microstrip Antennas", IEEE Trans. on Antenna and Propag., vol. AP-31, No. 1, 1983.

[21] Krowne, C.M., "Dielectric and Width Effect on H-plane and E-plane Coupling Between Rectangular Microstrip Antennas", IEEE Trans. on Antenna and Propag., vol. AP-31, No. 1, 1983.

[22] Carver, K.R. and Coffey, E.L., "Theoretical Investigation of Microstrip Antennas", Physics and Sci. Lab., New Mexico State University Tech. Rep. PT-00929, Jan. 1979.

[23] Jedlicka, R.P. and Carver, K.R., "Mutual Coupling Between Microstrip Antennas", Proceeding of the Workshop on Printed Circuit Antenna Technology, New Mexico State University, Las Cruces, New Mexico, 1979.

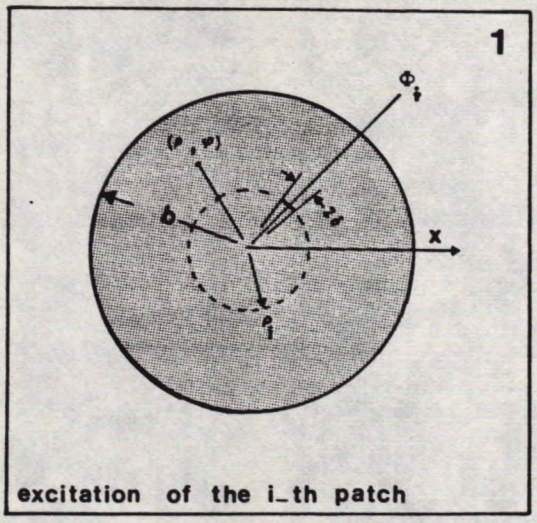


Fig. 1

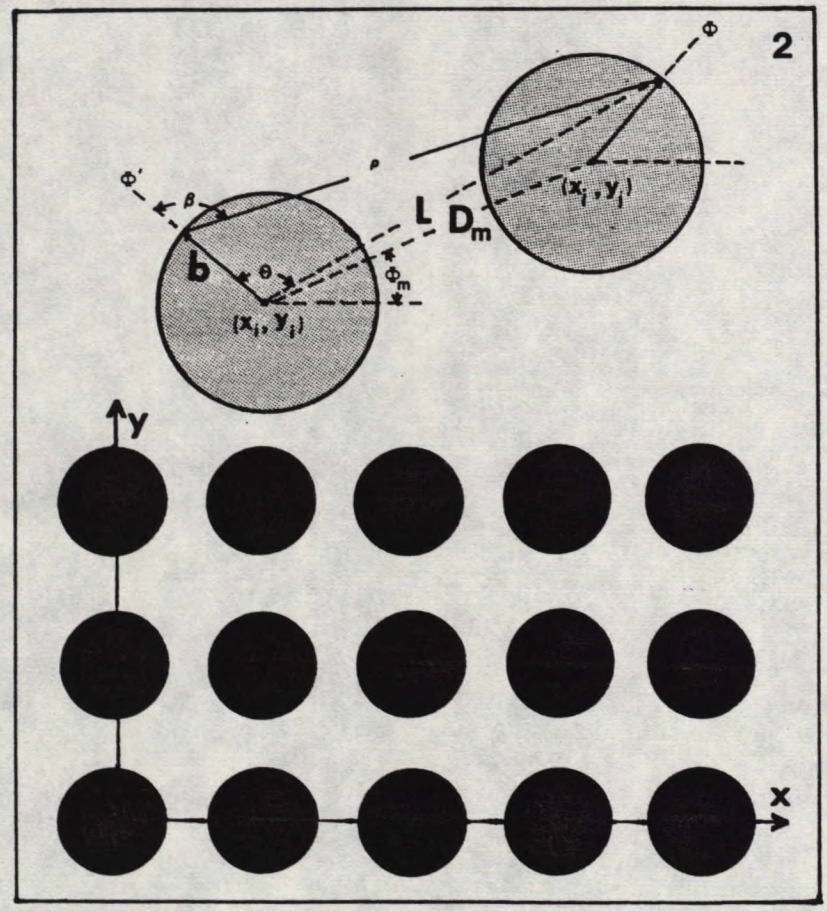


Fig. 2

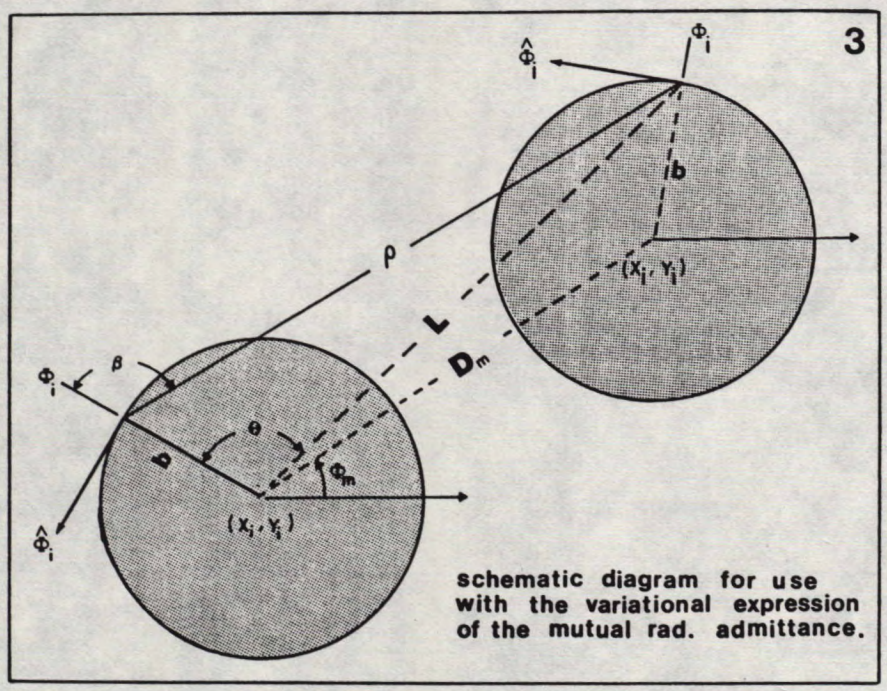
3
$\hat{\Phi}_i$
$\Phi_i$
b
ρ
$(X_i, Y_i)$
L
$D_m$
$\Phi_i$
β
θ
b
$\Phi_m$
$(X_j, Y_j)$
$\hat{\Phi}_j$
schematic diagram for use with the variational expression of the mutual rad. admittance.

Fig. 3

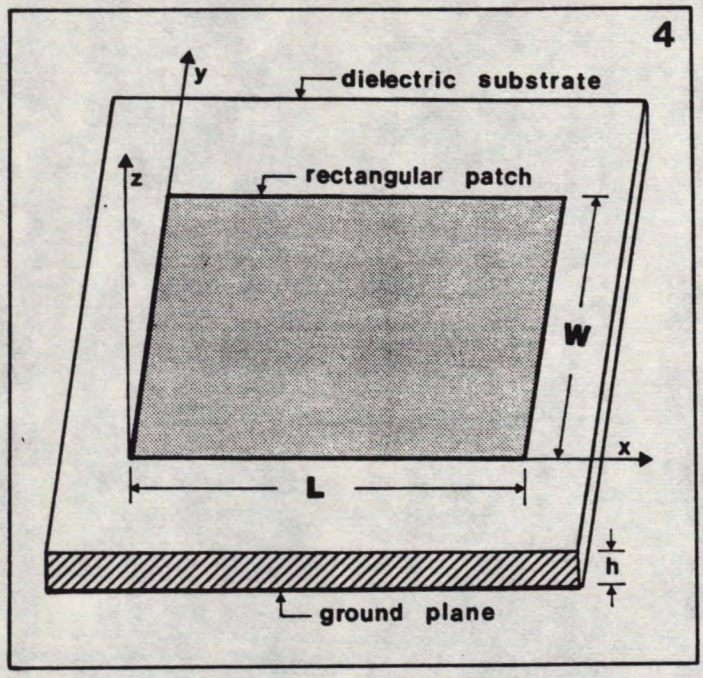
4
y
dielectric substrate
z
rectangular patch
W
x
L
h
ground plane

Fig. 4

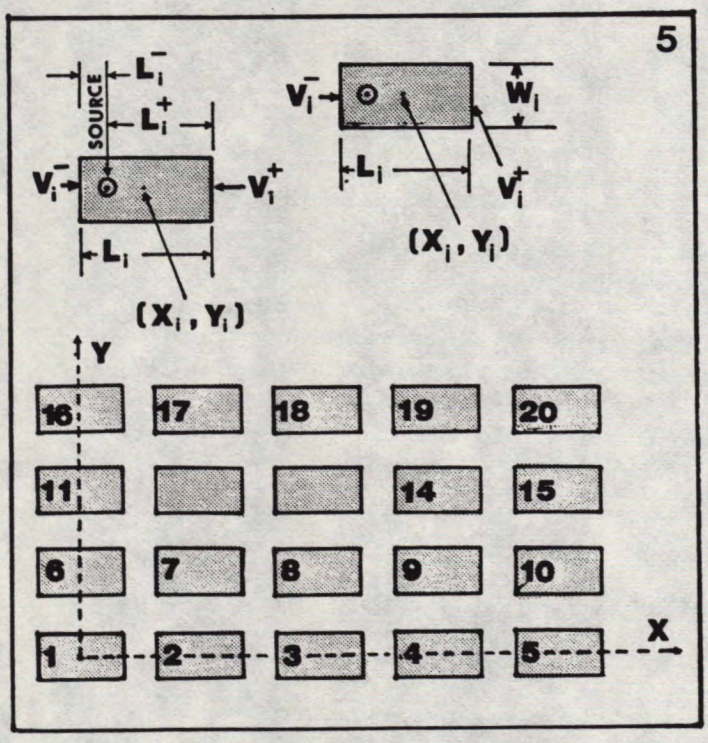
5
SOURCE
$L_i^-$
$L_i^+$
$V_i^-$
$V_i^+$
$L_i$
$(X_i, Y_i)$
$W_i$
Y
16
17
18
19
20
11
14
15
6
7
8
9
10
1
2
3
4
5
X

Fig. 5

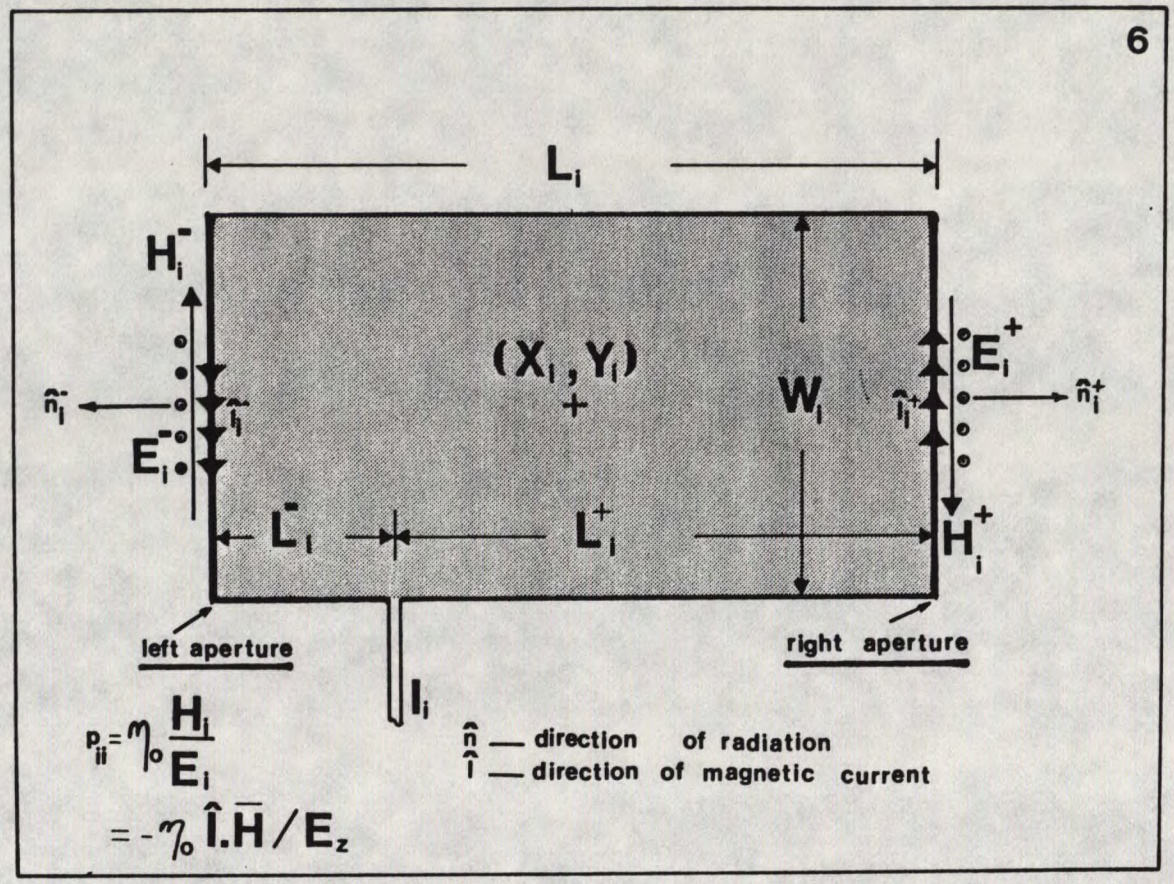


Fig. 6

**CELL'S PARAMETERS FOR RECTANGULAR MICROSTRIP PATCH PLANAR ARRAY**

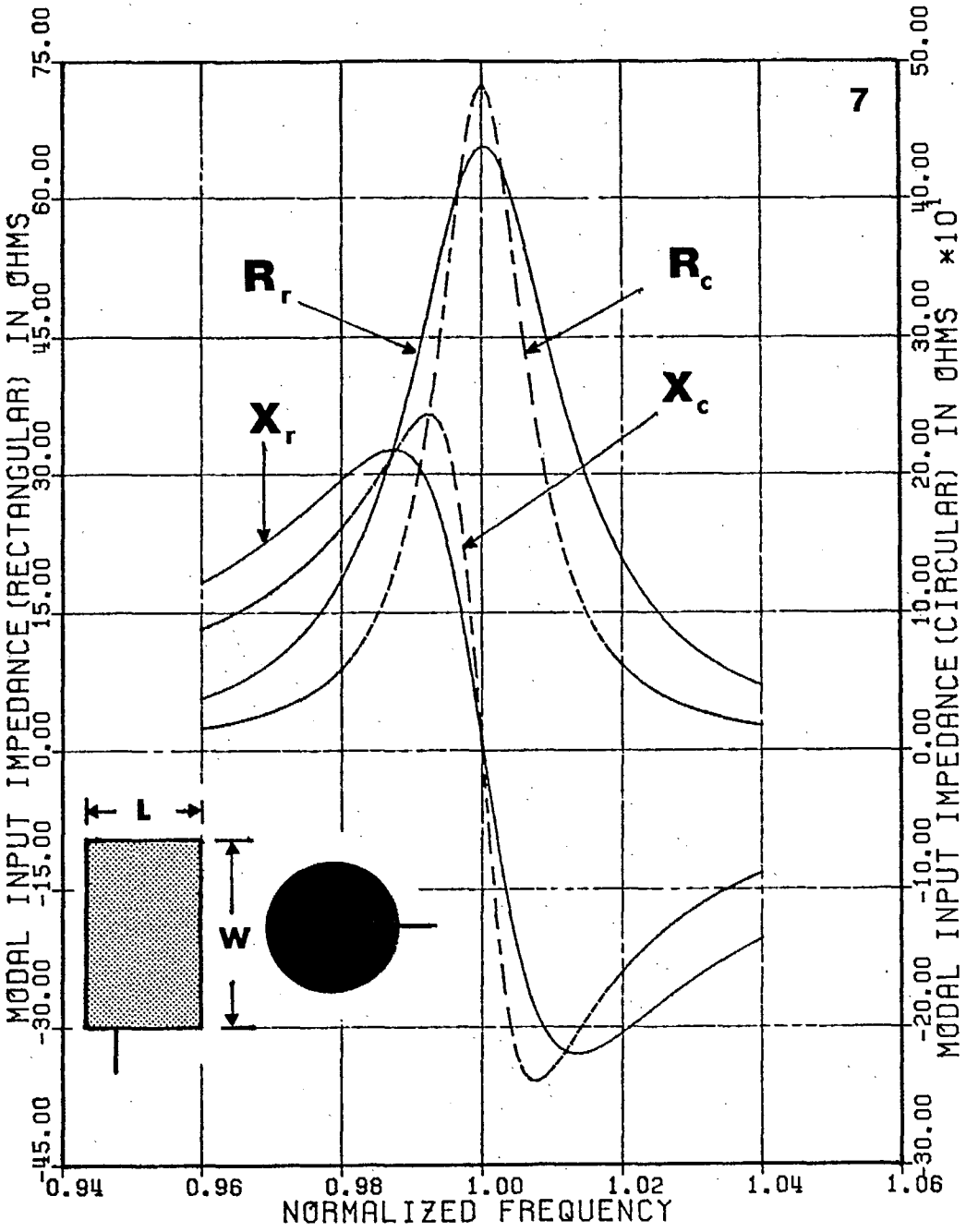
7
$R_r$
$R_c$
$X_r$
$X_c$
L
W
MODAL INPUT IMPEDANCE (RECTANGULAR) IN OHMS
MODAL INPUT IMPEDANCE (CIRCULAR) IN OHMS *10
NORMALIZED FREQUENCY
75.00
60.00
45.00
30.00
15.00
0.00
-15.00
-30.00
-45.00
50.00
40.00
30.00
20.00
10.00
0.00
-10.00
-20.00
-30.00
0.94
0.96
0.98
1.00
1.02
1.04
1.06

Fig. 7

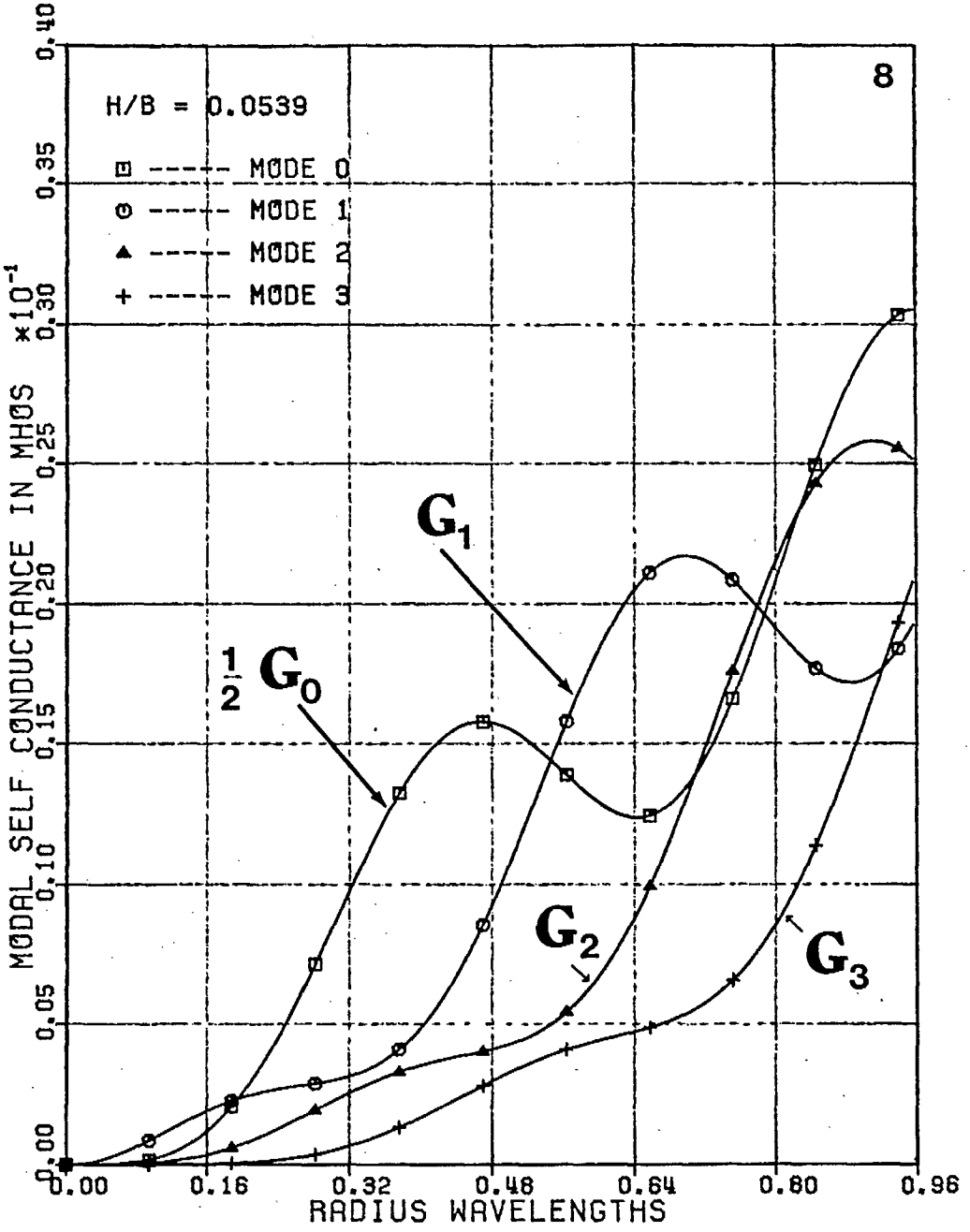
8
H/B = 0.0539
MODE 0
MODE 1
MODE 2
MODE 3
$G_1$
$\frac{1}{2} G_0$
$G_2$
$G_3$
MODAL SELF CONDUCTANCE IN MHOS $\times 10^{-1}$
0.00
0.05
0.10
0.15
0.20
0.25
0.30
0.35
0.40
0.00
0.16
0.32
0.48
0.64
0.80
0.96
RADIUS WAVELENGTHS

Fig. 8

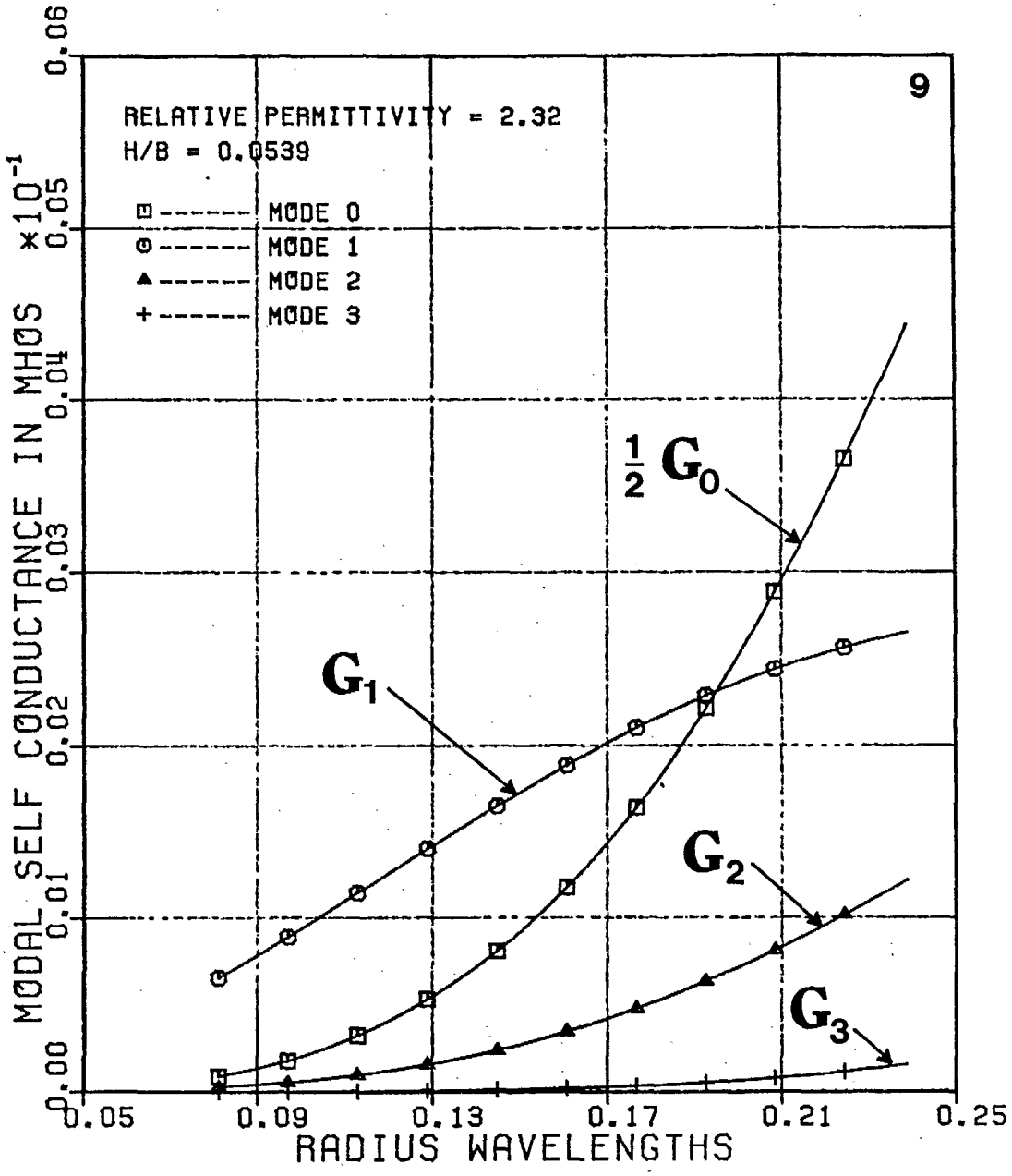
9
RELATIVE PERMITTIVITY = 2.32
H/B = 0.0539
MODE 0
MODE 1
MODE 2
MODE 3
MODAL SELF CONDUCTANCE IN MHOS ×10⁻¹
0.00
0.01
0.02
0.03
0.04
0.05
0.06
0.05
0.09
0.13
0.17
0.21
0.25
RADIUS WAVELENGTHS
½ G0
G1
G2
G3

Fig. 9

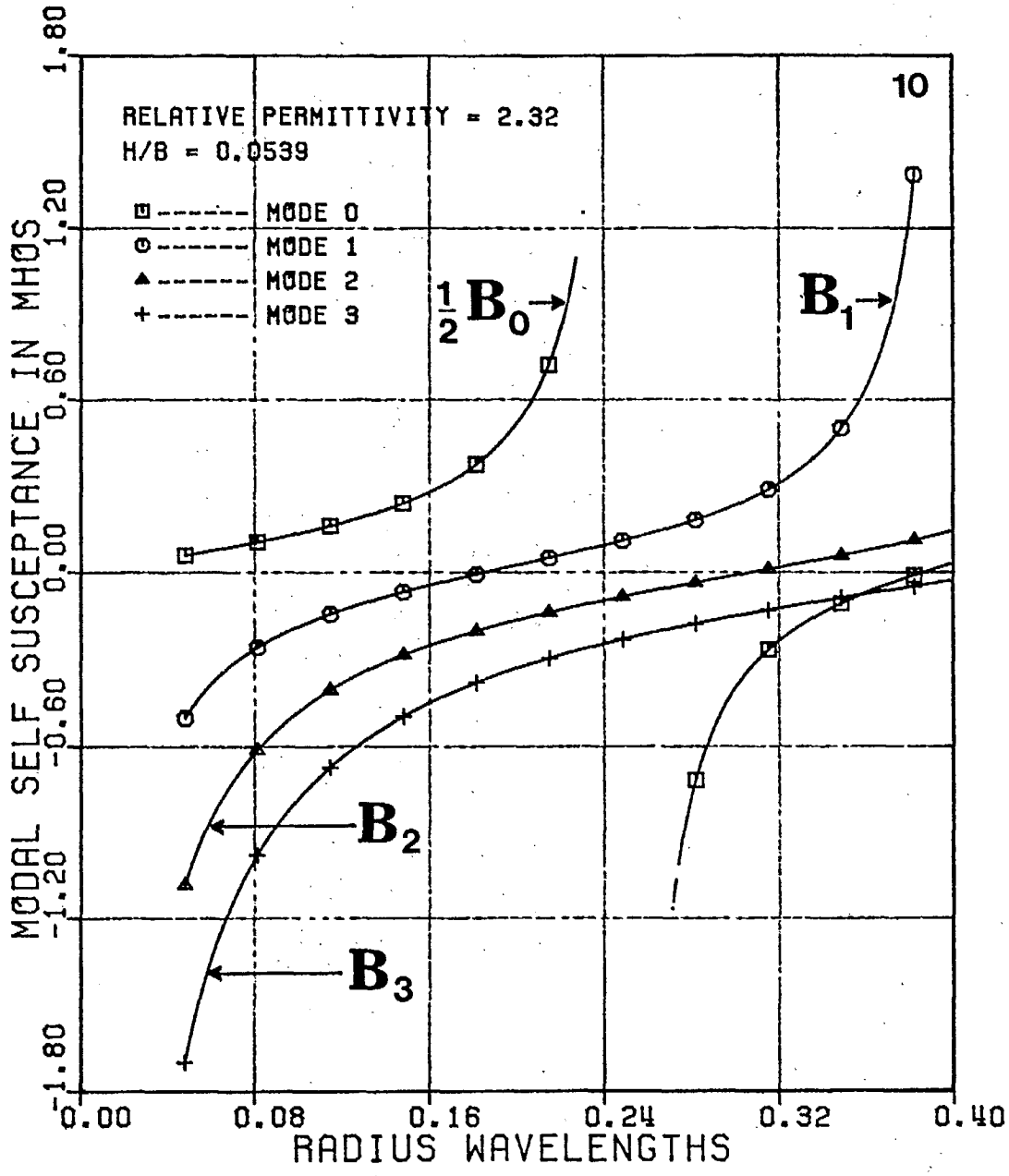
10
RELATIVE PERMITTIVITY = 2.32
H/B = 0.0539
MODE 0
MODE 1
MODE 2
MODE 3
$\frac{1}{2}B_0$
$B_1$
$B_2$
$B_3$
MODAL SELF SUSCEPTANCE IN MHOS
1.80
1.20
0.60
0.00
-0.60
-1.20
-1.80
0.00
0.08
0.16
0.24
0.32
0.40
RADIUS WAVELENGTHS

Fig. 10

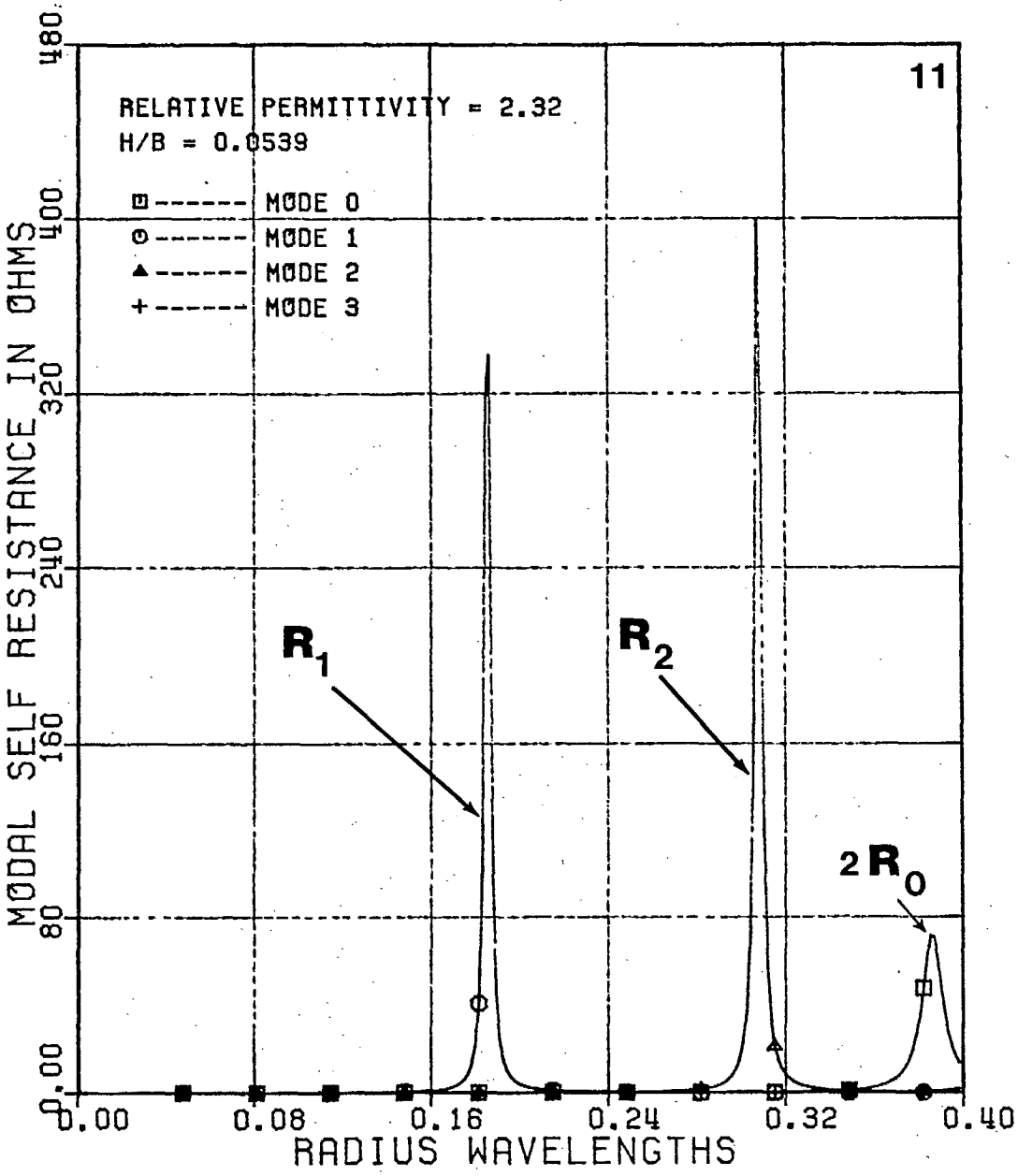
11
RELATIVE PERMITTIVITY = 2.32
H/B = 0.0539
MODE 0
MODE 1
MODE 2
MODE 3
MODAL SELF RESISTANCE IN OHMS
480
400
320
240
160
80
0.00
0.00
0.08
0.16
0.24
0.32
0.40
RADIUS WAVELENGTHS
R1
R2
2R0

Fig.II

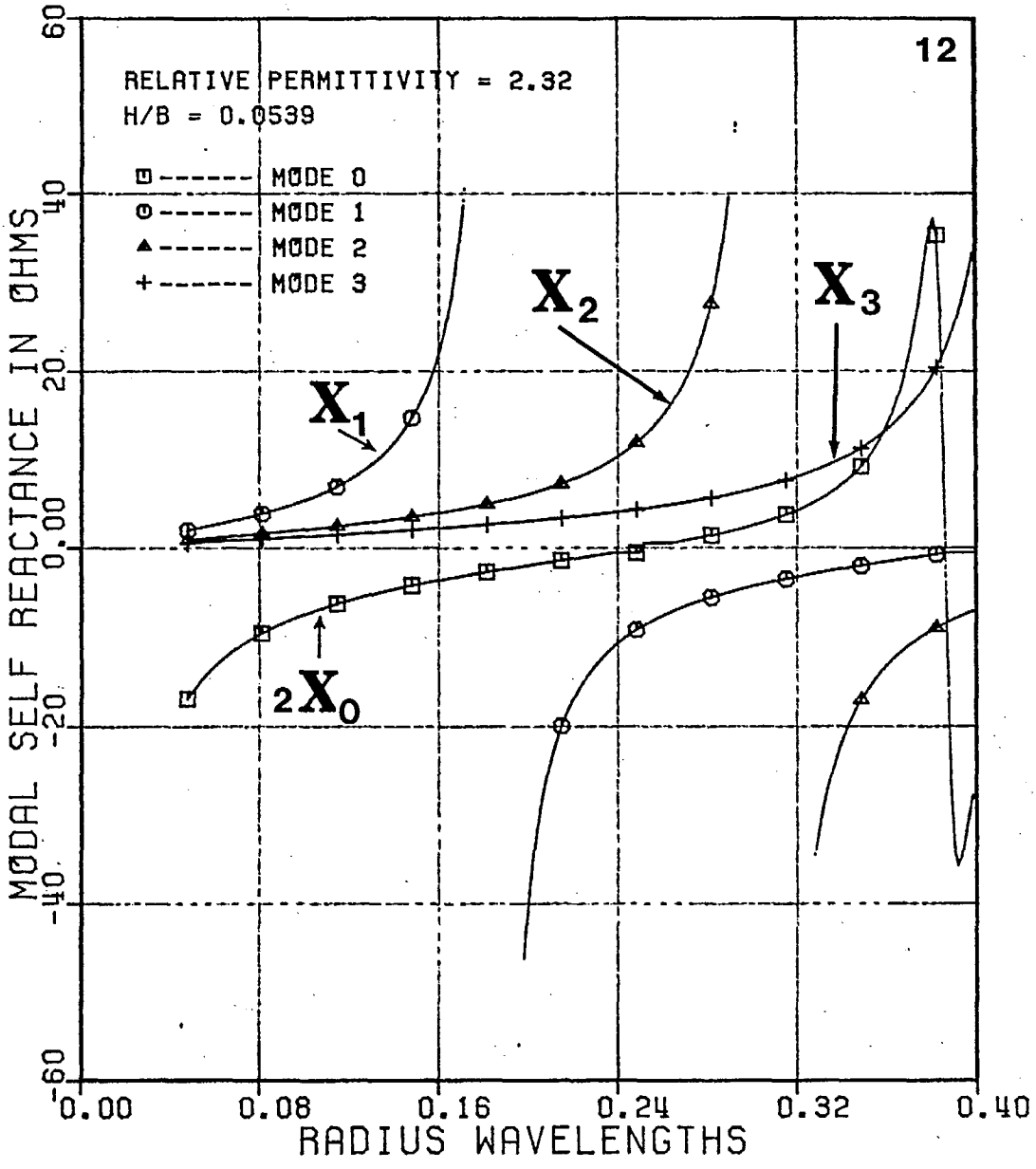
12
RELATIVE PERMITTIVITY = 2.32
H/B = 0.0539
MODE 0
MODE 1
MODE 2
MODE 3
$X_1$
$X_2$
$X_3$
$2X_0$
MODAL SELF REACTANCE IN OHMS
60
40
20
0.00
-20
-40
-60
0.00
0.08
0.16
0.24
0.32
0.40
RADIUS WAVELENGTHS

Fig. 12

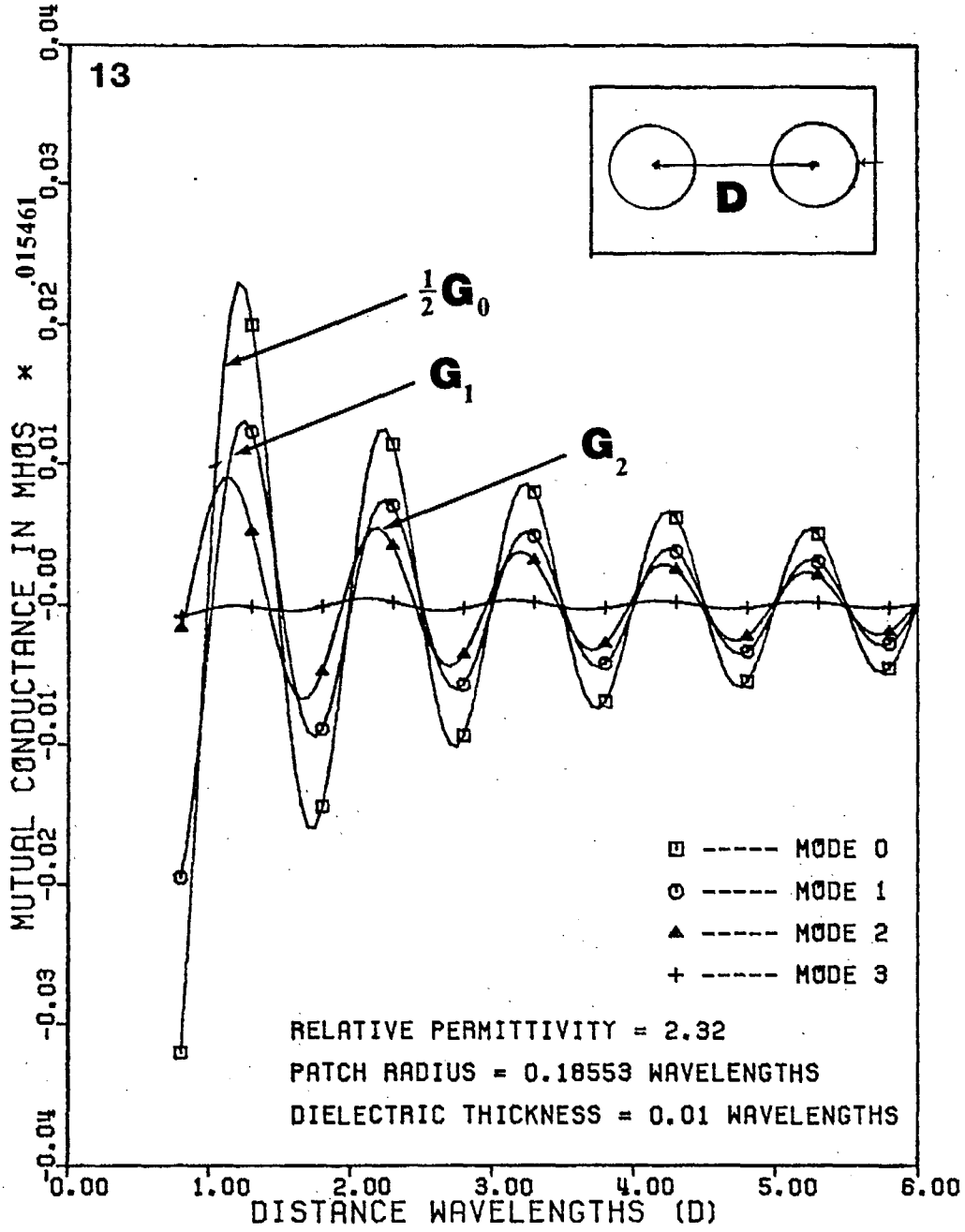
13
D
$\frac{1}{2}G_0$
$G_1$
$G_2$
MUTUAL CONDUCTANCE IN MHOS * .015461
0.04
0.03
0.02
0.01
-0.00
-0.01
-0.02
-0.03
-0.04
0.00
1.00
2.00
3.00
4.00
5.00
6.00
DISTANCE WAVELENGTHS (D)
----- MODE 0
----- MODE 1
----- MODE 2
----- MODE 3
RELATIVE PERMITTIVITY = 2.32
PATCH RADIUS = 0.18553 WAVELENGTHS
DIELECTRIC THICKNESS = 0.01 WAVELENGTHS

Fig. 13

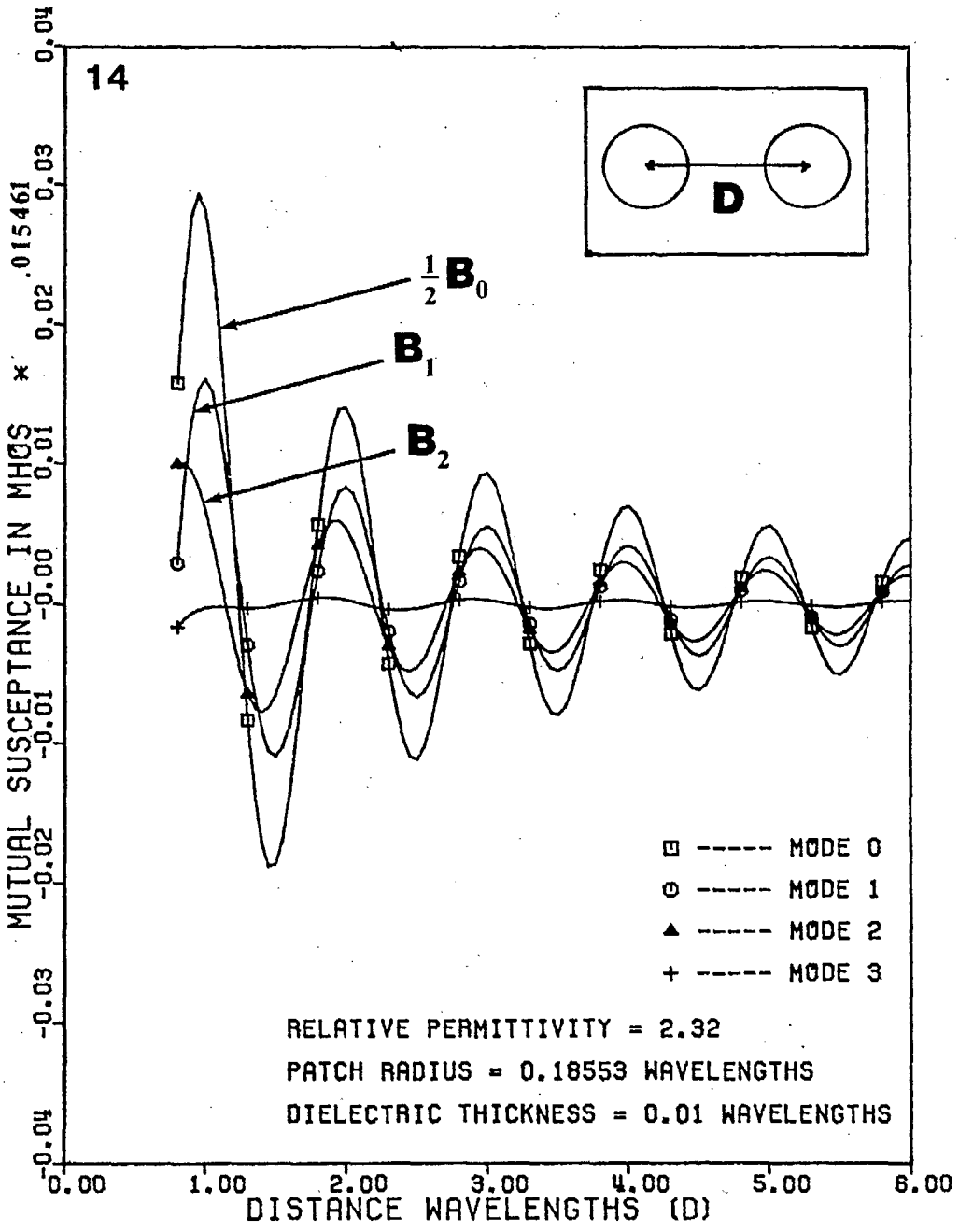
14
D
$\frac{1}{2}B_0$
$B_1$
$B_2$
MUTUAL SUSCEPTANCE IN MHOS * .015461
0.04
0.03
0.02
0.01
0.00
-0.01
-0.02
-0.03
-0.04
0.00
1.00
2.00
3.00
4.00
5.00
6.00
DISTANCE WAVELENGTHS (D)
MODE 0
MODE 1
MODE 2
MODE 3
RELATIVE PERMITTIVITY = 2.32
PATCH RADIUS = 0.18553 WAVELENGTHS
DIELECTRIC THICKNESS = 0.01 WAVELENGTHS

Fig. 14

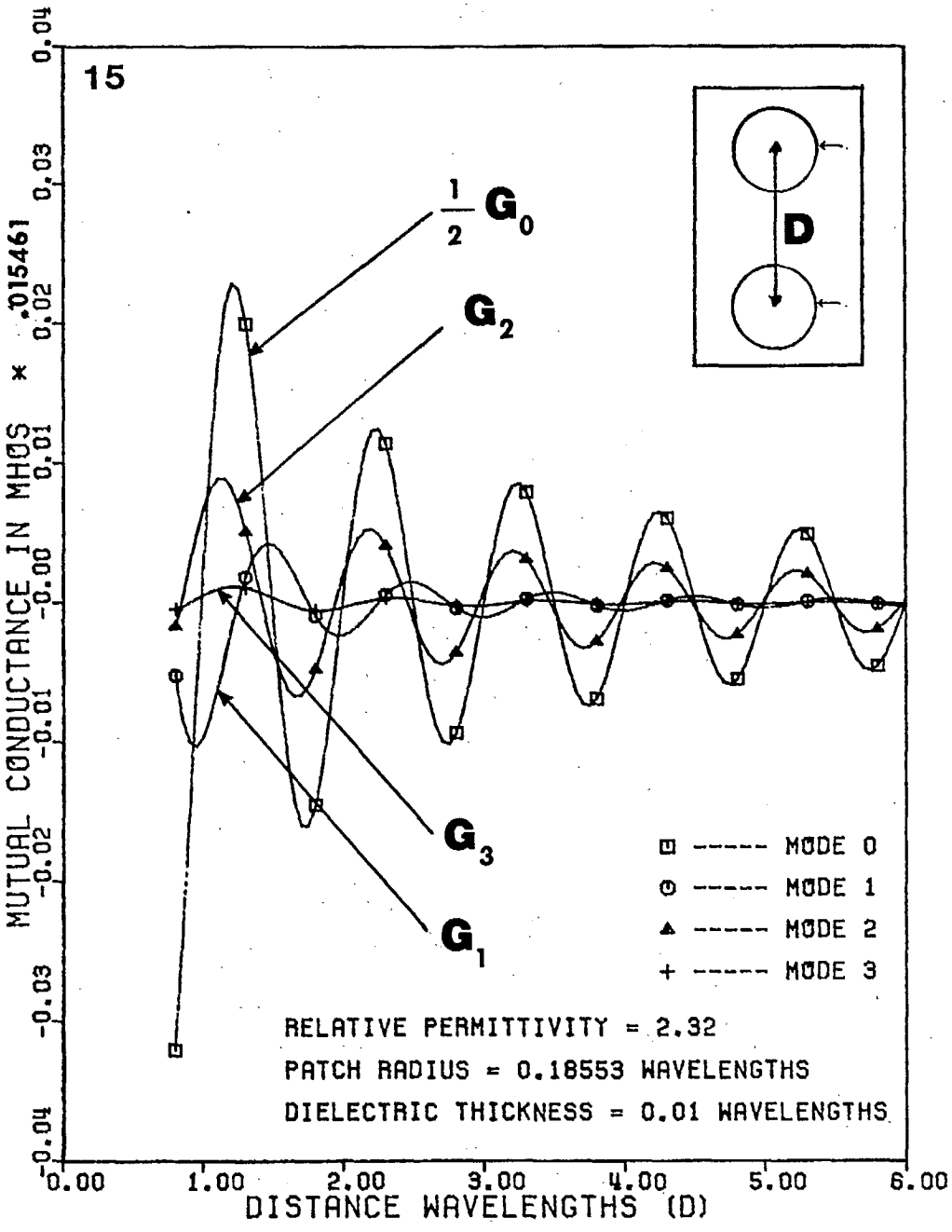
15
D
$\frac{1}{2}G_0$
$G_2$
$G_3$
$G_1$
MODE 0
MODE 1
MODE 2
MODE 3
RELATIVE PERMITTIVITY = 2.32
PATCH RADIUS = 0.18553 WAVELENGTHS
DIELECTRIC THICKNESS = 0.01 WAVELENGTHS
MUTUAL CONDUCTANCE IN MHOS × .015461
0.04
0.03
0.02
0.01
0.00
-0.01
-0.02
-0.03
-0.04
0.00
1.00
2.00
3.00
4.00
5.00
6.00
DISTANCE WAVELENGTHS (D)

Fig. 15

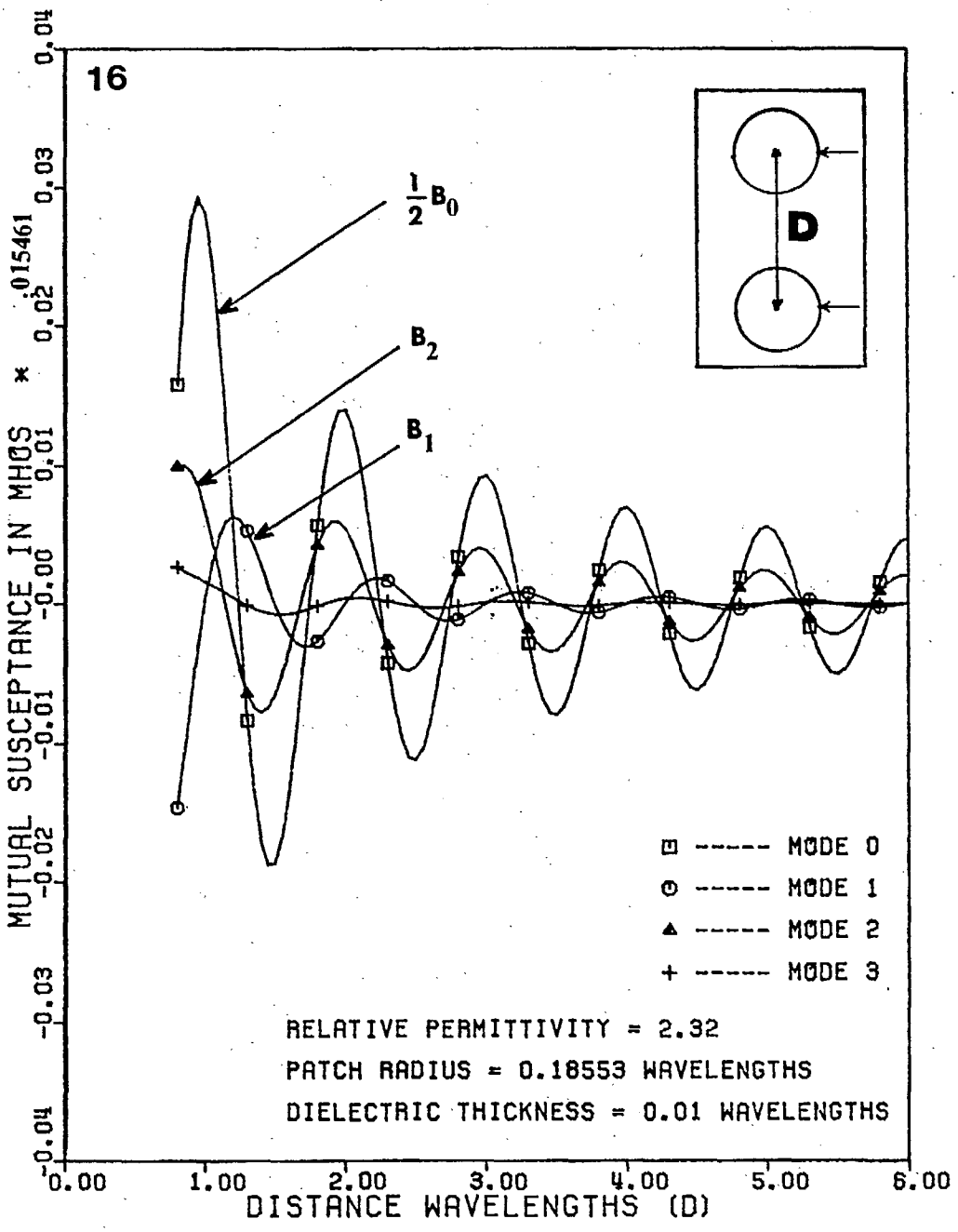
16
D
$\frac{1}{2}B_0$
$B_2$
$B_1$
MUTUAL SUSCEPTANCE IN MHOS * .015461
0.04
0.03
0.02
0.01
-0.00
-0.01
-0.02
-0.03
-0.04
0.00
1.00
2.00
3.00
4.00
5.00
6.00
DISTANCE WAVELENGTHS (D)
MODE 0
MODE 1
MODE 2
MODE 3
RELATIVE PERMITTIVITY = 2.32
PATCH RADIUS = 0.18553 WAVELENGTHS
DIELECTRIC THICKNESS = 0.01 WAVELENGTHS

Fig. 16

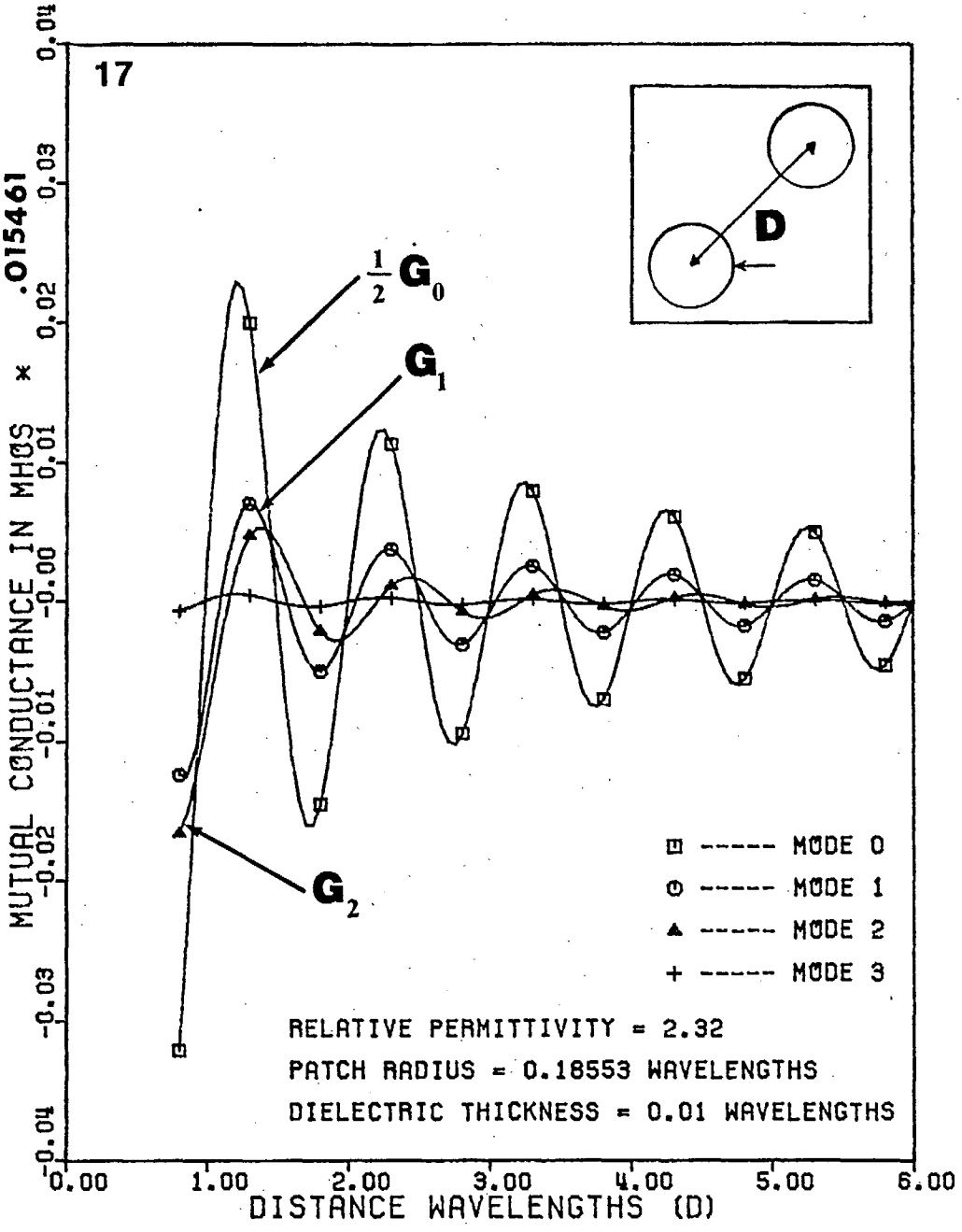
17
D
$\frac{1}{2}G_0$
$G_1$
$G_2$
MUTUAL CONDUCTANCE IN MHOS × .015461
0.04
0.03
0.02
0.01
-0.00
-0.01
-0.02
-0.03
-0.04
0.00
1.00
2.00
3.00
4.00
5.00
6.00
DISTANCE WAVELENGTHS (D)
MODE 0
MODE 1
MODE 2
MODE 3
RELATIVE PERMITTIVITY = 2.32
PATCH RADIUS = 0.18553 WAVELENGTHS
DIELECTRIC THICKNESS = 0.01 WAVELENGTHS

Fig. 17

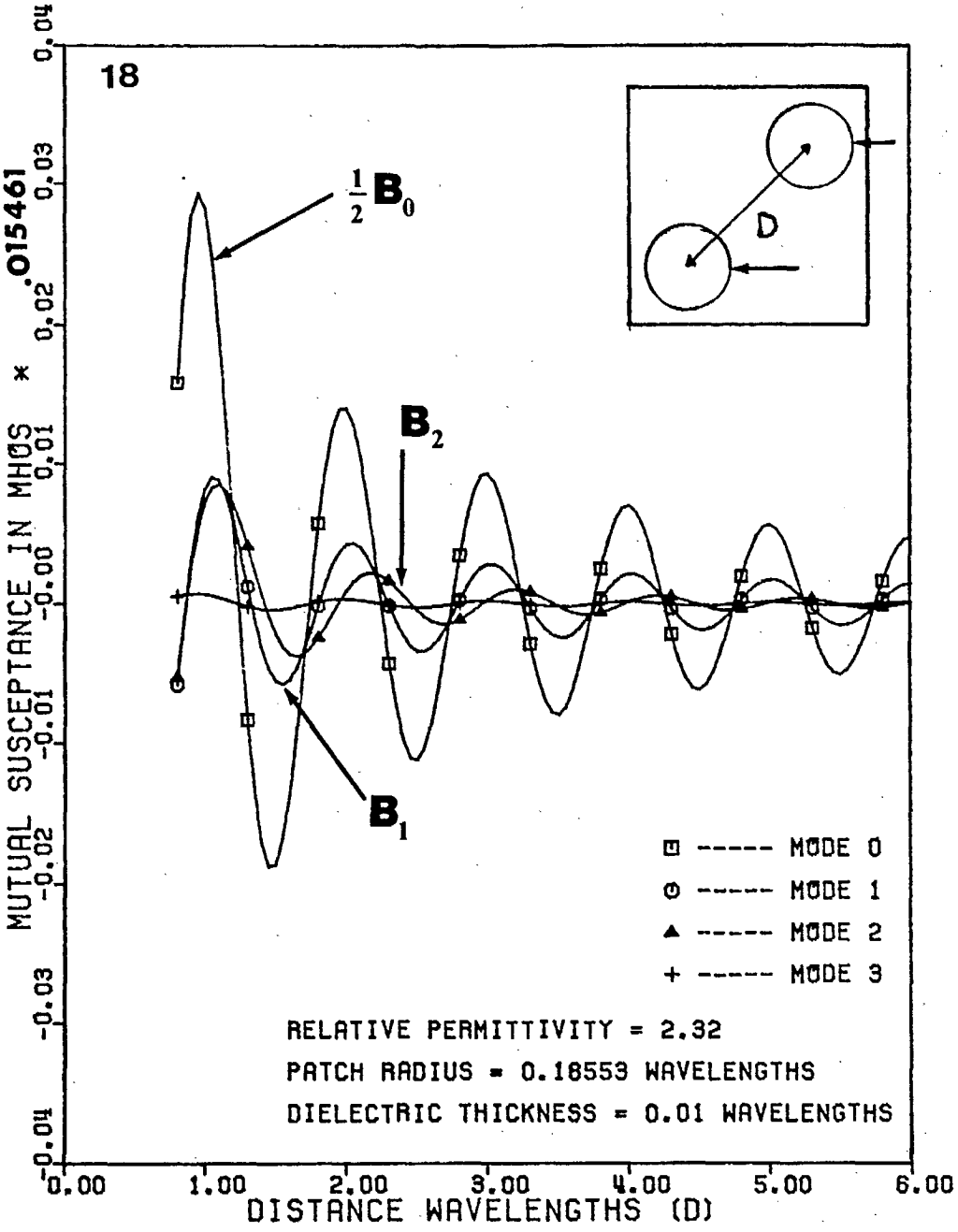
18
$\frac{1}{2}B_0$
$B_2$
$B_1$
D
MUTUAL SUSCEPTANCE IN MHOS * .015461
0.04
0.03
0.02
0.01
-0.00
-0.01
-0.02
-0.03
-0.04
0.00
1.00
2.00
3.00
4.00
5.00
6.00
DISTANCE WAVELENGTHS (D)
MODE 0
MODE 1
MODE 2
MODE 3
RELATIVE PERMITTIVITY = 2.32
PATCH RADIUS = 0.16553 WAVELENGTHS
DIELECTRIC THICKNESS = 0.01 WAVELENGTHS

Fig. 18

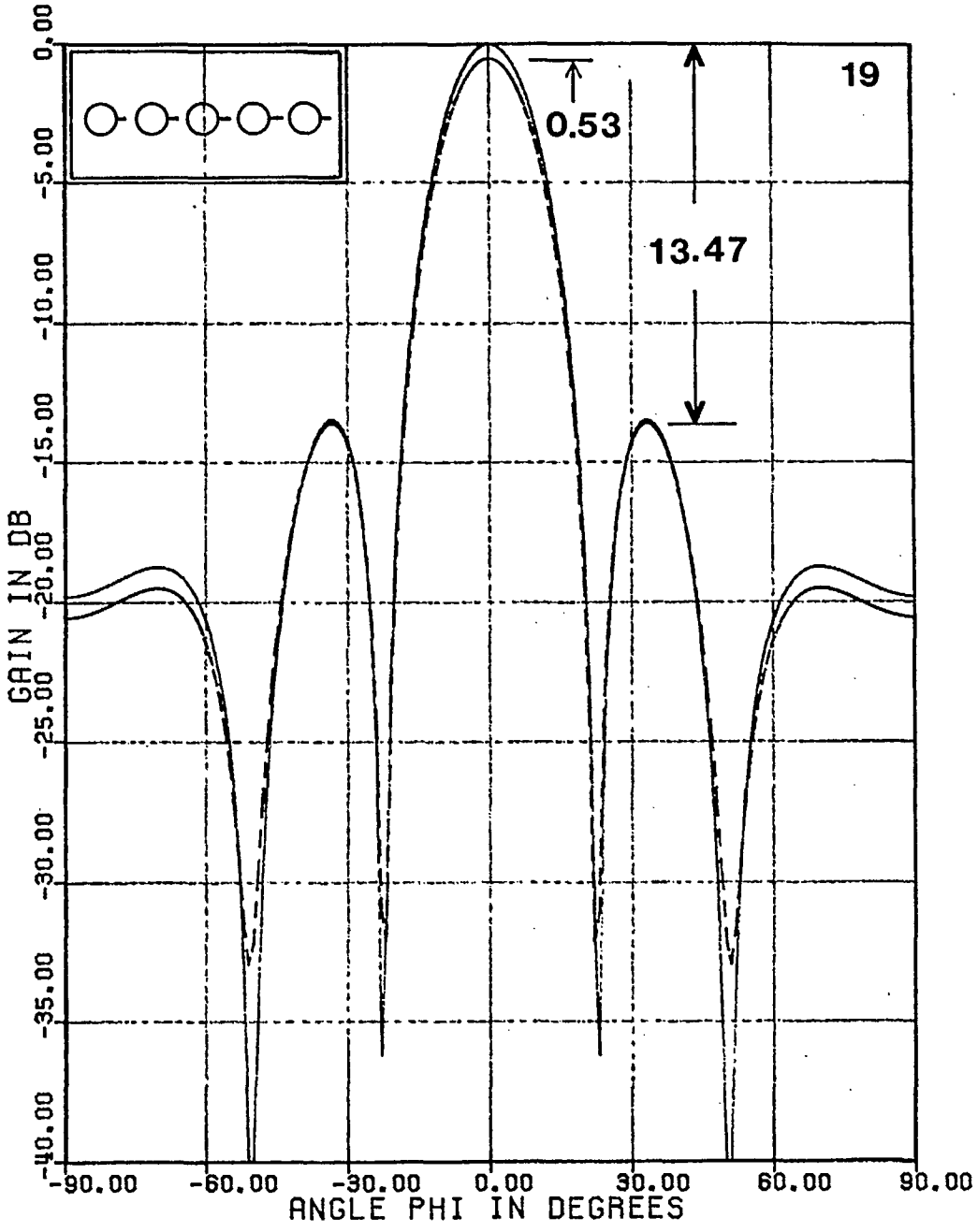


A 5 CIRCULAR PATCH ARRAY
PATCHES ARE 0.52λ APART ON X-AXIS
E-PLANE RADIATION PATTERN

Fig. 19

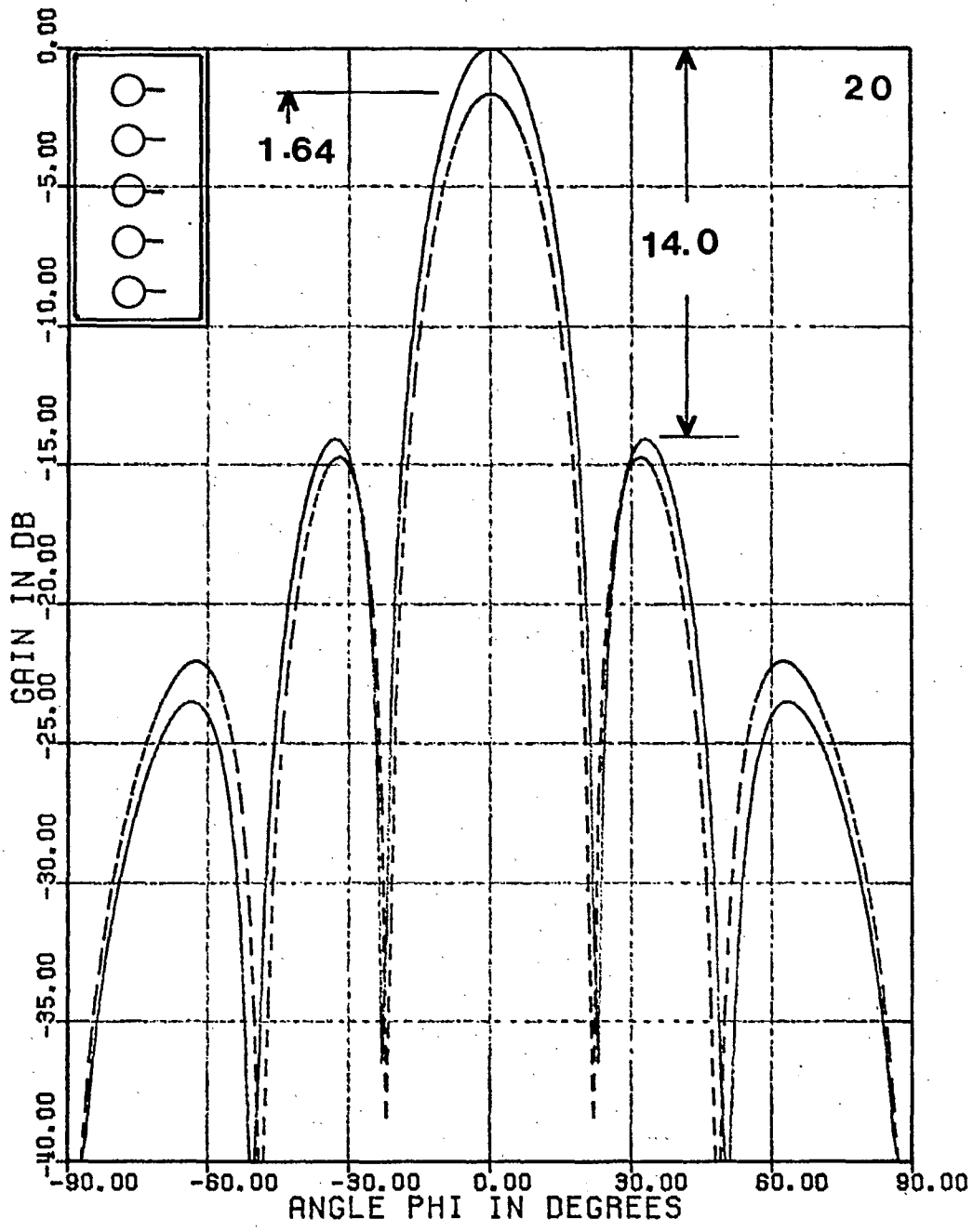


A 5 CIRCULAR PATCH ARRAY
PATCHES ARE 0.52λ APART ON Y-AXIS
H-PLANE RADIATION PATTERN

Fig. 20

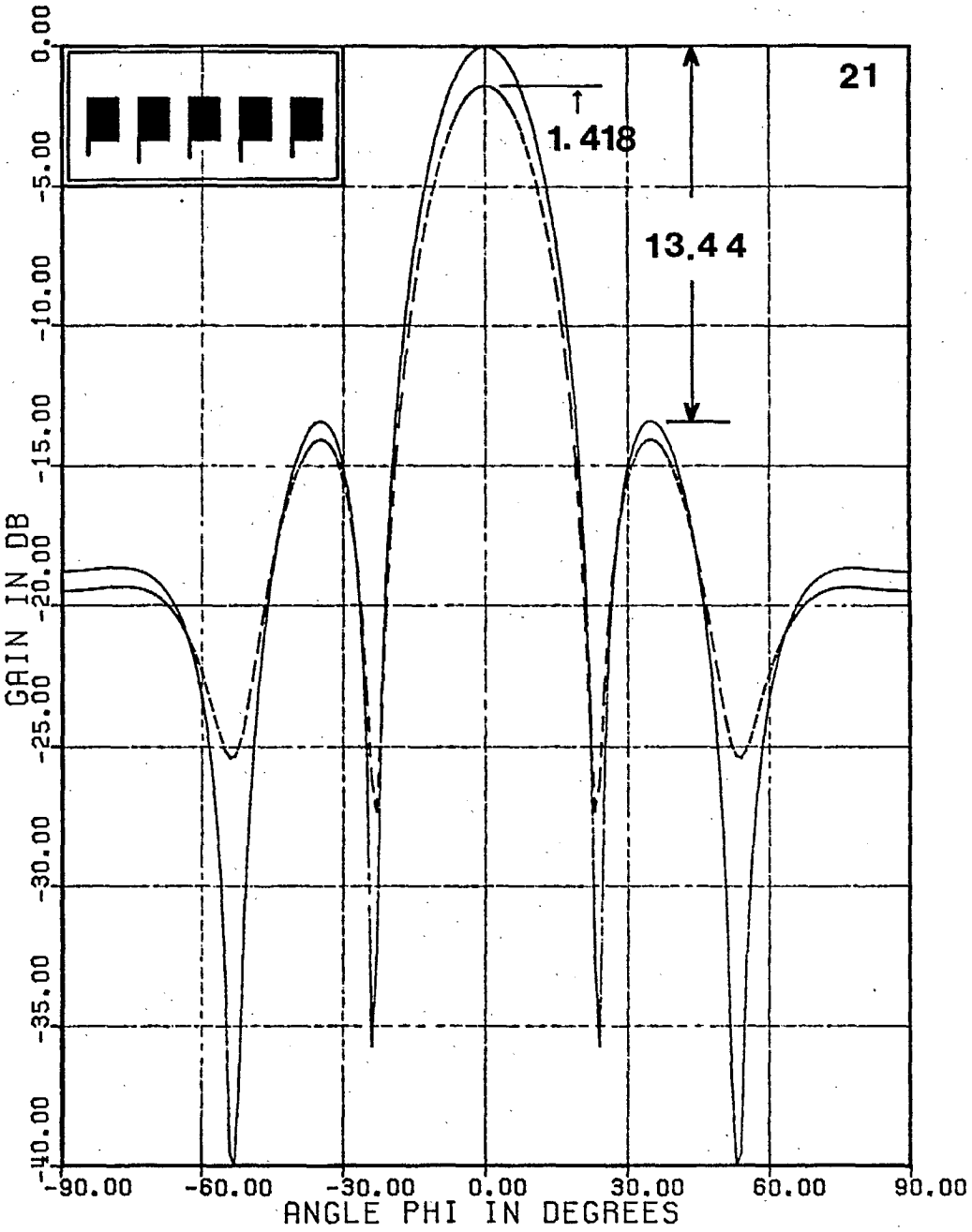


A 5 RECTANGULAR PATCH ARRAY
PATCHES ARE 0.5λ APART ON X-AXIS
E-PLANE RADIATION PATTERN

Fig. 21

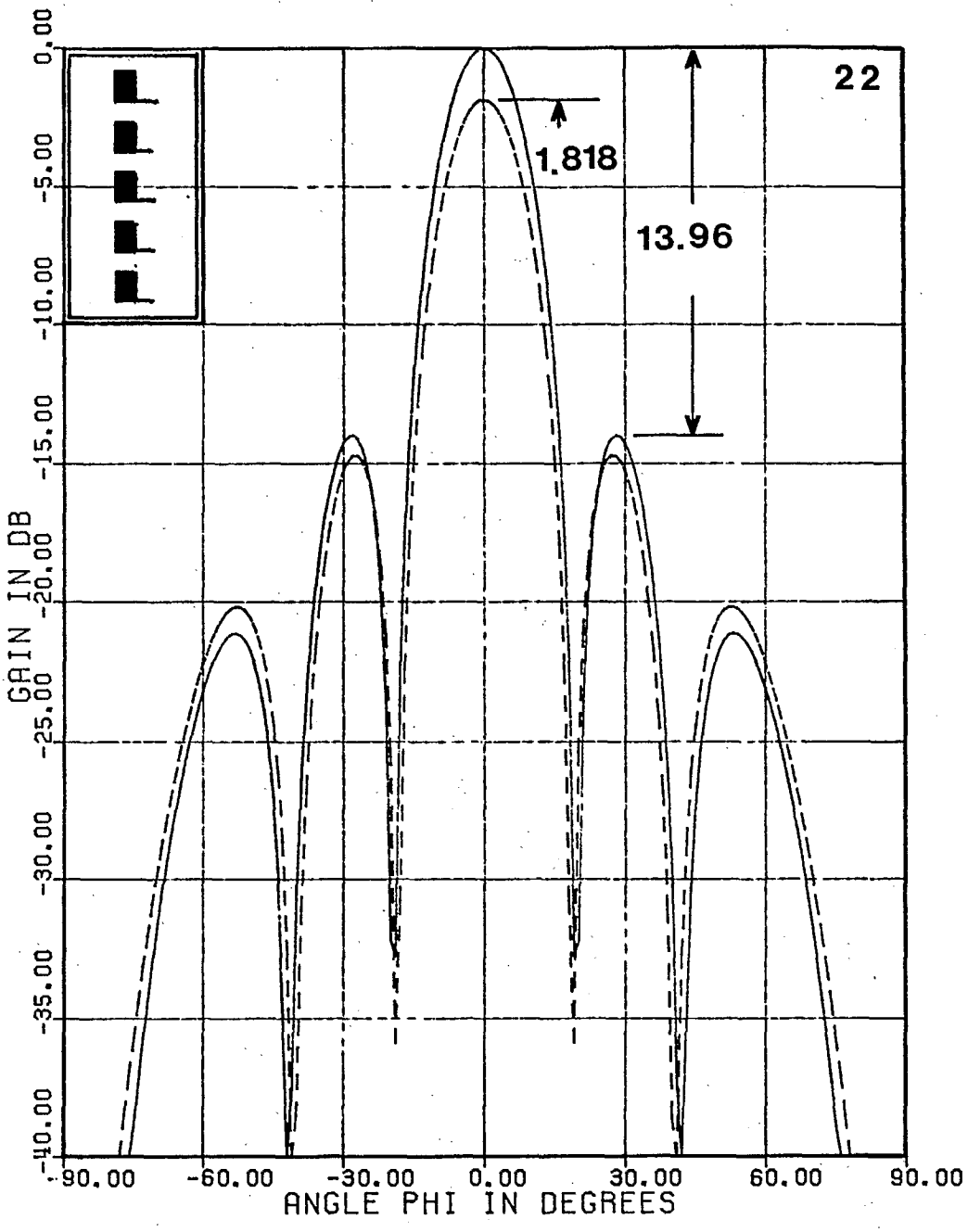


A 5 RECTANGULAR PATCH ARRAY
PATCHES ARE 0.6λ APART ON Y-AXIS
H-PLANE RADIATION PATTERN

Fig. 22

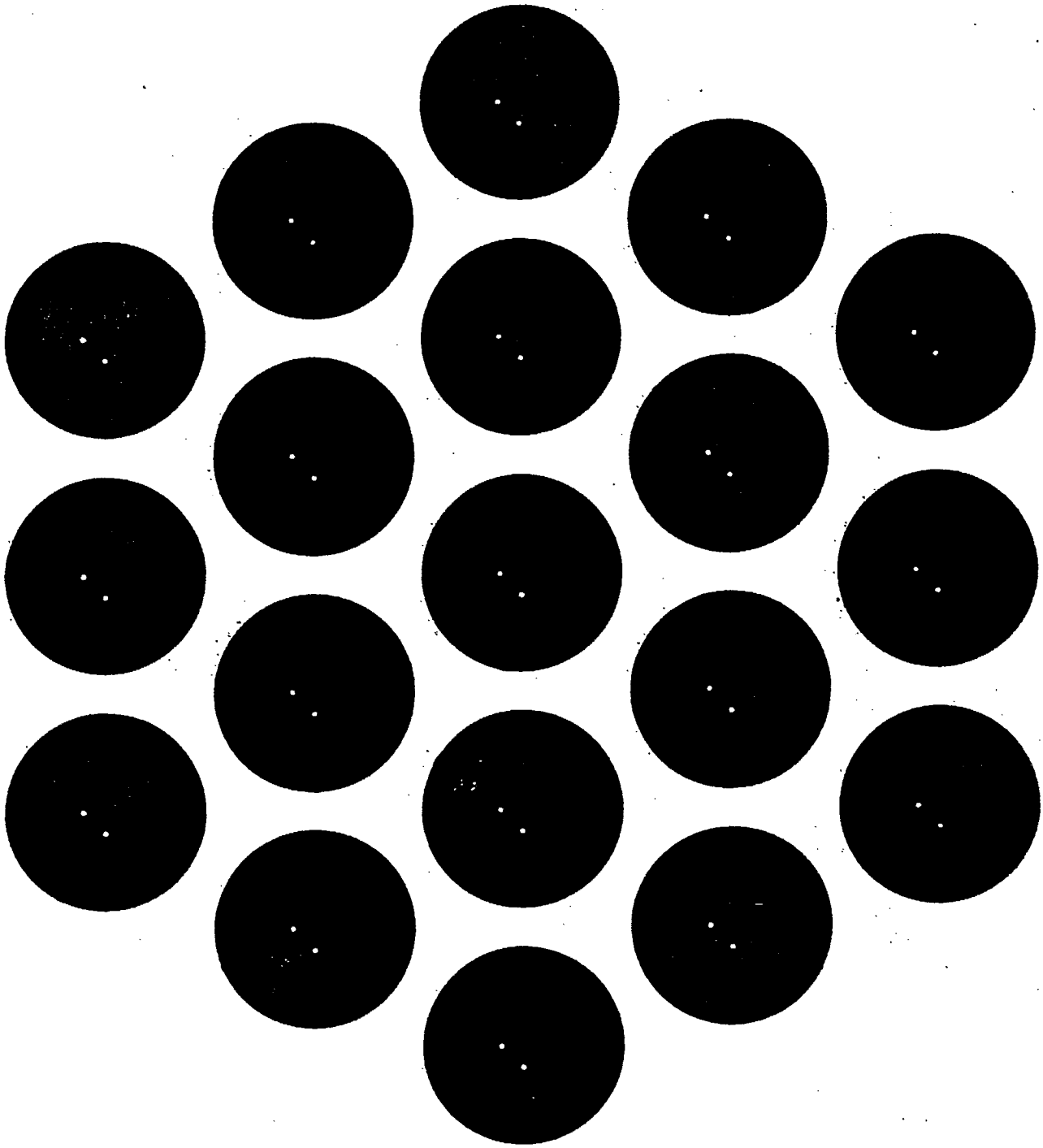

Fig. 23. Geometry of a 19-element circular patch array

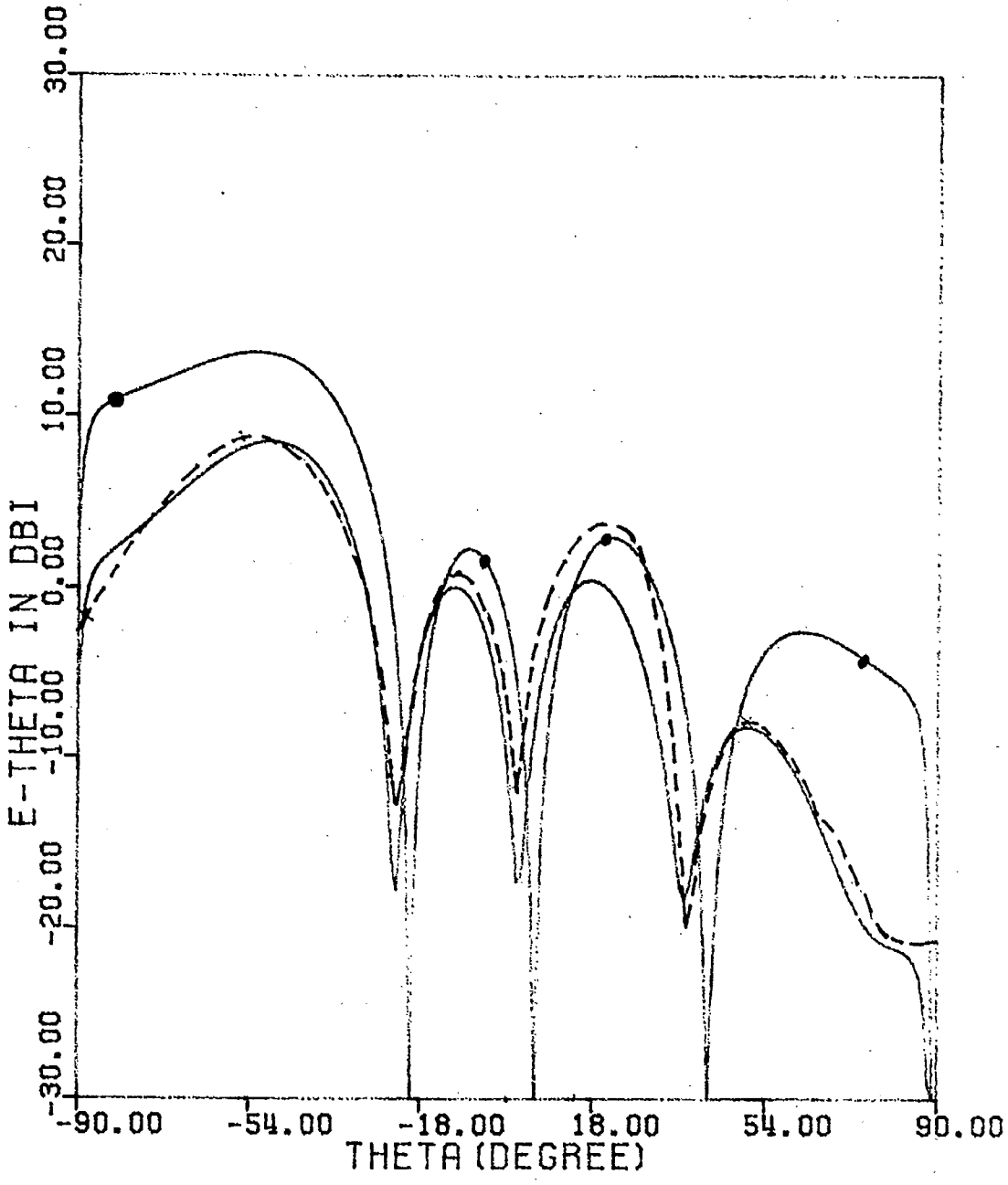


Fig. 24. Measured and computed patterns of the array in Fig. 23.
_____ measured, —●— computed no coupling
----- computed with coupling

# APPENDIX A

# RADIATION PATTERN OUTPUTS

TABULATION OF THE RADIATION PATTERN
A PLANAR ARRAY OF RECTANGULAR PATCHES

| PHI *** | E-PLANE ******* | | H-PLANE ******* | |
|---|---|---|---|---|
| IN | FIELD IN DB | | FIELD IN DB | |
| DEGREES | COUPLED | UNCOUPLED | COUPLED | UNCOUPLED |
| -90.000 | -19.486 | -18.791 | -40.000 | -40.000 |
| -89.000 | -19.484 | -18.789 | -40.000 | -38.887 |
| -88.000 | -19.479 | -18.784 | -34.282 | -32.864 |
| -87.000 | -19.470 | -18.775 | -30.756 | -29.338 |
| -86.000 | -19.459 | -18.763 | -28.251 | -26.833 |
| -85.000 | -19.444 | -18.749 | -26.306 | -24.888 |
| -84.000 | -19.428 | -18.734 | -24.714 | -23.295 |
| -83.000 | -19.411 | -18.717 | -23.364 | -21.946 |
| -82.000 | -19.393 | -18.701 | -22.193 | -20.775 |
| -81.000 | -19.375 | -18.685 | -21.156 | -19.738 |
| -80.000 | -19.360 | -18.673 | -20.226 | -18.808 |
| -79.000 | -19.347 | -18.664 | -19.382 | -17.964 |
| -78.000 | -19.338 | -18.661 | -18.609 | -17.191 |
| -77.000 | -19.335 | -18.665 | -17.895 | -16.477 |
| -76.000 | -19.339 | -18.678 | -17.231 | -15.813 |
| -75.000 | -19.353 | -18.702 | -16.610 | -15.192 |
| -74.000 | -19.377 | -18.741 | -16.027 | -14.609 |
| -73.000 | -19.415 | -18.796 | -15.477 | -14.059 |
| -72.000 | -19.468 | -18.870 | -14.956 | -13.538 |
| -71.000 | -19.539 | -18.967 | -14.461 | -13.042 |
| -70.000 | -19.630 | -19.091 | -13.988 | -12.570 |
| -69.000 | -19.745 | -19.245 | -13.537 | -12.119 |
| -68.000 | -19.887 | -19.436 | -13.105 | -11.687 |
| -67.000 | -20.058 | -19.667 | -12.690 | -11.271 |
| -66.000 | -20.263 | -19.947 | -12.290 | -10.872 |
| -65.000 | -20.506 | -20.284 | -11.906 | -10.487 |
| -64.000 | -20.790 | -20.687 | -11.534 | -10.116 |
| -63.000 | -21.121 | -21.170 | -11.175 | -9.757 |
| -62.000 | -21.500 | -21.750 | -10.828 | -9.410 |
| -61.000 | -21.933 | -22.449 | -10.491 | -9.073 |
| -60.000 | -22.419 | -23.299 | -10.165 | -8.747 |
| -59.000 | -22.956 | -24.344 | -9.848 | -8.430 |
| -58.000 | -23.532 | -25.657 | -9.541 | -8.123 |
| -57.000 | -24.123 | -27.356 | -9.242 | -7.824 |
| -56.000 | -24.682 | -29.668 | -8.951 | -7.533 |
| -55.000 | -25.135 | -33.119 | -8.668 | -7.250 |
| -54.000 | -25.382 | -39.511 | -8.392 | -6.974 |
| -53.000 | -25.329 | -40.000 | -8.124 | -6.705 |
| -52.000 | -24.936 | -36.780 | -7.862 | -6.444 |
| -51.000 | -24.243 | -31.074 | -7.607 | -6.189 |
| -50.000 | -23.347 | -27.550 | -7.358 | -5.940 |

TABULATION OF THE RADIATION PATTERN
A PLANAR ARRAY OF RECTANGULAR PATCHES

| PHI | E-PLANE | | H-PLANE | |
|---|---|---|---|---|
| *** | ******* | | ******* | |
| IN | FIELD IN DB | | FIELD IN DB | |
| DEGREES | COUPLED | UNCOUPLED | COUPLED | UNCOUPLED |
| -49.000 | -22.348 | -24.983 | -7.116 | -5.698 |
| -48.000 | -21.326 | -22.965 | -6.879 | -5.461 |
| -47.000 | -20.330 | -21.308 | -6.649 | -5.231 |
| -46.000 | -19.389 | -19.912 | -6.424 | -5.006 |
| -45.000 | -18.516 | -18.718 | -6.205 | -4.787 |
| -44.000 | -17.718 | -17.687 | -5.992 | -4.573 |
| -43.000 | -16.997 | -16.794 | -5.783 | -4.365 |
| -42.000 | -16.354 | -16.022 | -5.580 | -4.162 |
| -41.000 | -15.789 | -15.359 | -5.383 | -3.965 |
| -40.000 | -15.302 | -14.798 | -5.190 | -3.772 |
| -39.000 | -14.893 | -14.333 | -5.003 | -3.585 |
| -38.000 | -14.564 | -13.964 | -4.820 | -3.402 |
| -37.000 | -14.317 | -13.690 | -4.643 | -3.225 |
| -36.000 | -14.156 | -13.512 | -4.470 | -3.052 |
| -35.000 | -14.086 | -13.437 | -4.303 | -2.885 |
| -34.000 | -14.114 | -13.471 | -4.140 | -2.722 |
| -33.000 | -14.251 | -13.626 | -3.982 | -2.564 |
| -32.000 | -14.510 | -13.918 | -3.829 | -2.411 |
| -31.000 | -14.910 | -14.370 | -3.681 | -2.262 |
| -30.000 | -15.477 | -15.017 | -3.537 | -2.119 |
| -29.000 | -16.250 | -15.911 | -3.398 | -1.980 |
| -28.000 | -17.284 | -17.139 | -3.264 | -1.846 |
| -27.000 | -18.667 | -18.856 | -3.135 | -1.717 |
| -26.000 | -20.536 | -21.381 | -3.010 | -1.592 |
| -25.000 | -23.079 | -25.560 | -2.890 | -1.472 |
| -24.000 | -26.213 | -35.699 | -2.775 | -1.357 |
| -23.000 | -27.332 | -32.575 | -2.664 | -1.246 |
| -22.000 | -24.074 | -23.499 | -2.559 | -1.140 |
| -21.000 | -20.358 | -18.912 | -2.457 | -1.039 |
| -20.000 | -17.370 | -15.770 | -2.361 | -0.943 |
| -19.000 | -14.978 | -13.365 | -2.269 | -0.851 |
| -18.000 | -13.008 | -11.415 | -2.182 | -0.764 |
| -17.000 | -11.346 | -9.778 | -2.100 | -0.681 |
| -16.000 | -9.918 | -8.374 | -2.022 | -0.604 |
| -15.000 | -8.675 | -7.152 | -1.949 | -0.531 |
| -14.000 | -7.584 | -6.080 | -1.880 | -0.462 |
| -13.000 | -6.622 | -5.133 | -1.817 | -0.399 |
| -12.000 | -5.770 | -4.294 | -1.758 | -0.340 |
| -11.000 | -5.016 | -3.551 | -1.704 | -0.286 |
| -10.000 | -4.350 | -2.895 | -1.654 | -0.236 |
| -9.000 | -3.764 | -2.317 | -1.609 | -0.191 |

TABULATION OF THE RADIATION PATTERN
A PLANAR ARRAY OF RECTANGULAR PATCHES

| PHI *** IN DEGREES | E-PLANE ******* FIELD IN DB COUPLED | E-PLANE ******* FIELD IN DB UNCOUPLED | H-PLANE ******* FIELD IN DB COUPLED | H-PLANE ******* FIELD IN DB UNCOUPLED |
|---|---|---|---|---|
| -8.000 | -3.252 | -1.812 | -1.569 | -0.151 |
| -7.000 | -2.810 | -1.375 | -1.534 | -0.116 |
| -6.000 | -2.433 | -1.003 | -1.503 | -0.085 |
| -5.000 | -2.118 | -0.692 | -1.477 | -0.059 |
| -4.000 | -1.864 | -0.441 | -1.456 | -0.038 |
| -3.000 | -1.668 | -0.247 | -1.439 | -0.021 |
| -2.000 | -1.529 | -0.109 | -1.428 | -0.009 |
| -1.000 | -1.446 | -0.027 | -1.420 | -0.002 |
| 0.000 | -1.418 | 0.000 | -1.418 | 0.000 |
| 1.000 | -1.446 | -0.027 | -1.420 | -0.002 |
| 2.000 | -1.529 | -0.110 | -1.428 | -0.009 |
| 3.000 | -1.668 | -0.247 | -1.439 | -0.021 |
| 4.000 | -1.864 | -0.441 | -1.456 | -0.038 |
| 5.000 | -2.119 | -0.693 | -1.477 | -0.059 |
| 6.000 | -2.433 | -1.004 | -1.503 | -0.085 |
| 7.000 | -2.810 | -1.376 | -1.534 | -0.116 |
| 8.000 | -3.253 | -1.813 | -1.569 | -0.151 |
| 9.000 | -3.765 | -2.318 | -1.609 | -0.191 |
| 10.000 | -4.351 | -2.896 | -1.654 | -0.236 |
| 11.000 | -5.017 | -3.553 | -1.704 | -0.286 |
| 12.000 | -5.771 | -4.296 | -1.758 | -0.340 |
| 13.000 | -6.622 | -5.135 | -1.817 | -0.399 |
| 14.000 | -7.585 | -6.082 | -1.880 | -0.462 |
| 15.000 | -8.676 | -7.154 | -1.949 | -0.531 |
| 16.000 | -9.919 | -8.376 | -2.022 | -0.604 |
| 17.000 | -11.347 | -9.780 | -2.100 | -0.681 |
| 18.000 | -13.009 | -11.417 | -2.182 | -0.764 |
| 19.000 | -14.978 | -13.368 | -2.269 | -0.851 |
| 20.000 | -17.370 | -15.773 | -2.361 | -0.943 |
| 21.000 | -20.357 | -18.915 | -2.457 | -1.039 |
| 22.000 | -24.072 | -23.502 | -2.559 | -1.140 |
| 23.000 | -27.331 | -32.579 | -2.664 | -1.246 |
| 24.000 | -26.215 | -35.702 | -2.775 | -1.357 |
| 25.000 | -23.083 | -25.564 | -2.890 | -1.472 |
| 26.000 | -20.539 | -21.384 | -3.010 | -1.592 |
| 27.000 | -18.670 | -18.860 | -3.135 | -1.717 |
| 28.000 | -17.287 | -17.143 | -3.264 | -1.846 |
| 29.000 | -16.253 | -15.915 | -3.398 | -1.980 |
| 30.000 | -15.480 | -15.021 | -3.537 | -2.119 |
| 31.000 | -14.913 | -14.374 | -3.681 | -2.262 |
| 32.000 | -14.513 | -13.923 | -3.829 | -2.411 |

TABULATION OF THE RADIATION PATTERN
A PLANAR ARRAY OF RECTANGULAR PATCHES

| PHI *** IN DEGREES | E-PLANE ******* FIELD IN DB ----- -- -- COUPLED | UNCOUPLED | H-PLANE ******* FIELD IN DB ----- -- -- COUPLED | UNCOUPLED |
|---|---|---|---|---|
| 33.000 | -14.254 | -13.631 | -3.982 | -2.564 |
| 34.000 | -14.117 | -13.476 | -4.140 | -2.722 |
| 35.000 | -14.089 | -13.442 | -4.303 | -2.885 |
| 36.000 | -14.158 | -13.518 | -4.470 | -3.052 |
| 37.000 | -14.319 | -13.695 | -4.643 | -3.225 |
| 38.000 | -14.566 | -13.970 | -4.820 | -3.402 |
| 39.000 | -14.895 | -14.339 | -5.003 | -3.585 |
| 40.000 | -15.304 | -14.803 | -5.190 | -3.772 |
| 41.000 | -15.791 | -15.365 | -5.383 | -3.965 |
| 42.000 | -16.356 | -16.028 | -5.580 | -4.162 |
| 43.000 | -16.998 | -16.800 | -5.783 | -4.365 |
| 44.000 | -17.718 | -17.693 | -5.992 | -4.573 |
| 45.000 | -18.516 | -18.724 | -6.205 | -4.787 |
| 46.000 | -19.388 | -19.919 | -6.424 | -5.006 |
| 47.000 | -20.328 | -21.315 | -6.649 | -5.231 |
| 48.000 | -21.323 | -22.972 | -6.879 | -5.461 |
| 49.000 | -22.344 | -24.991 | -7.116 | -5.698 |
| 50.000 | -23.342 | -27.557 | -7.358 | -5.940 |
| 51.000 | -24.238 | -31.081 | -7.607 | -6.189 |
| 52.000 | -24.932 | -36.788 | -7.862 | -6.444 |
| 53.000 | -25.326 | -40.000 | -8.124 | -6.705 |
| 54.000 | -25.382 | -39.519 | -8.392 | -6.974 |
| 55.000 | -25.138 | -33.127 | -8.668 | -7.250 |
| 56.000 | -24.687 | -29.676 | -8.951 | -7.533 |
| 57.000 | -24.130 | -27.364 | -9.242 | -7.824 |
| 58.000 | -23.541 | -25.665 | -9.541 | -8.123 |
| 59.000 | -22.966 | -24.353 | -9.848 | -8.430 |
| 60.000 | -22.430 | -23.308 | -10.165 | -8.747 |
| 61.000 | -21.944 | -22.458 | -10.491 | -9.073 |
| 62.000 | -21.512 | -21.759 | -10.828 | -9.410 |
| 63.000 | -21.132 | -21.180 | -11.175 | -9.757 |
| 64.000 | -20.802 | -20.696 | -11.534 | -10.116 |
| 65.000 | -20.518 | -20.293 | -11.906 | -10.487 |
| 66.000 | -20.276 | -19.957 | -12.290 | -10.872 |
| 67.000 | -20.071 | -19.677 | -12.690 | -11.271 |
| 68.000 | -19.899 | -19.446 | -13.105 | -11.687 |
| 69.000 | -19.758 | -19.256 | -13.537 | -12.119 |
| 70.000 | -19.643 | -19.101 | -13.988 | -12.570 |
| 71.000 | -19.552 | -18.978 | -14.461 | -13.042 |
| 72.000 | -19.481 | -18.881 | -14.956 | -13.538 |
| 73.000 | -19.428 | -18.807 | -15.477 | -14.059 |

TABULATION OF THE RADIATION PATTERN
A PLANAR ARRAY OF RECTANGULAR PATCHES

| PHI | E-PLANE | | H-PLANE | |
|---|---|---|---|---|
| *** | ******* | | ******* | |
| IN | FIELD IN DB | | FIELD IN DB | |
| DEGREES | COUPLED | UNCOUPLED | COUPLED | UNCOUPLED |
| 74.000 | -19.390 | -18.752 | -16.027 | -14.609 |
| 75.000 | -19.366 | -18.713 | -16.610 | -15.192 |
| 76.000 | -19.352 | -18.689 | -17.231 | -15.813 |
| 77.000 | -19.348 | -18.676 | -17.895 | -16.477 |
| 78.000 | -19.351 | -18.672 | -18.609 | -17.191 |
| 79.000 | -19.360 | -18.675 | -19.382 | -17.964 |
| 80.000 | -19.372 | -18.684 | -20.226 | -18.808 |
| 81.000 | -19.388 | -18.697 | -21.156 | -19.738 |
| 82.000 | -19.406 | -18.712 | -22.193 | -20.775 |
| 83.000 | -19.424 | -18.729 | -23.364 | -21.946 |
| 84.000 | -19.441 | -18.745 | -24.714 | -23.295 |
| 85.000 | -19.457 | -18.761 | -26.306 | -24.888 |
| 86.000 | -19.472 | -18.775 | -28.251 | -26.833 |
| 87.000 | -19.483 | -18.786 | -30.756 | -29.338 |
| 88.000 | -19.492 | -18.795 | -34.282 | -32.864 |
| 89.000 | -19.497 | -18.800 | -40.000 | -38.887 |
| 90.000 | -19.499 | -18.802 | -40.000 | -40.000 |

**** TABULATION COMPLETED ****

TABULATION OF THE RADIATION PATTERN
A PLANAR ARRAY OF RECTANGULAR PATCHES

| PHI *** | E-PLANE ******* | | H-PLANE ******* | |
|---|---|---|---|---|
| IN | FIELD IN DB | | FIELD IN DB | |
| DEGREES | COUPLED | UNCOUPLED | COUPLED | UNCOUPLED |
| -90.000 | -6.628 | -4.811 | -40.000 | -40.000 |
| -89.000 | -6.626 | -4.809 | -40.000 | -40.000 |
| -88.000 | -6.621 | -4.804 | -40.000 | -40.000 |
| -87.000 | -6.612 | -4.795 | -40.000 | -40.000 |
| -86.000 | -6.599 | -4.782 | -40.000 | -40.000 |
| -85.000 | -6.583 | -4.766 | -40.000 | -40.000 |
| -84.000 | -6.563 | -4.747 | -40.000 | -40.000 |
| -83.000 | -6.540 | -4.724 | -40.000 | -40.000 |
| -82.000 | -6.514 | -4.697 | -40.000 | -40.000 |
| -81.000 | -6.484 | -4.667 | -40.000 | -40.000 |
| -80.000 | -6.450 | -4.634 | -40.000 | -40.000 |
| -79.000 | -6.414 | -4.597 | -40.000 | -40.000 |
| -78.000 | -6.374 | -4.558 | -39.959 | -40.000 |
| -77.000 | -6.332 | -4.515 | -38.478 | -40.000 |
| -76.000 | -6.286 | -4.469 | -37.065 | -40.000 |
| -75.000 | -6.237 | -4.421 | -35.717 | -38.913 |
| -74.000 | -6.186 | -4.369 | -34.431 | -37.279 |
| -73.000 | -6.132 | -4.315 | -33.206 | -35.756 |
| -72.000 | -6.075 | -4.258 | -32.039 | -34.332 |
| -71.000 | -6.016 | -4.199 | -30.929 | -33.001 |
| -70.000 | -5.954 | -4.138 | -29.873 | -31.754 |
| -69.000 | -5.891 | -4.074 | -28.871 | -30.586 |
| -68.000 | -5.825 | -4.008 | -27.922 | -29.492 |
| -67.000 | -5.757 | -3.940 | -27.024 | -28.469 |
| -66.000 | -5.687 | -3.870 | -26.178 | -27.514 |
| -65.000 | -5.615 | -3.798 | -25.383 | -26.625 |
| -64.000 | -5.541 | -3.724 | -24.638 | -25.799 |
| -63.000 | -5.466 | -3.649 | -23.946 | -25.037 |
| -62.000 | -5.390 | -3.573 | -23.305 | -24.338 |
| -61.000 | -5.312 | -3.495 | -22.717 | -23.701 |
| -60.000 | -5.233 | -3.416 | -22.183 | -23.129 |
| -59.000 | -5.153 | -3.336 | -21.706 | -22.622 |
| -58.000 | -5.072 | -3.255 | -21.286 | -22.183 |
| -57.000 | -4.991 | -3.174 | -20.928 | -21.814 |
| -56.000 | -4.908 | -3.091 | -20.634 | -21.519 |
| -55.000 | -4.825 | -3.008 | -20.408 | -21.304 |
| -54.000 | -4.741 | -2.924 | -20.257 | -21.174 |
| -53.000 | -4.658 | -2.840 | -20.185 | -21.139 |
| -52.000 | -4.573 | -2.756 | -20.203 | -21.209 |
| -51.000 | -4.489 | -2.672 | -20.319 | -21.399 |
| -50.000 | -4.405 | -2.588 | -20.548 | -21.728 |

TABULATION OF THE RADIATION PATTERN
A PLANAR ARRAY OF RECTANGULAR PATCHES

| PHI | E-PLANE | | H-PLANE | |
|---|---|---|---|---|
| *** | ******* | | ******* | |
| IN | FIELD IN DB | | FIELD IN DB | |
| DEGREES | COUPLED | UNCOUPLED | COUPLED | UNCOUPLED |
| -49.000 | -4.320 | -2.503 | -20.909 | -22.223 |
| -48.000 | -4.236 | -2.419 | -21.425 | -22.924 |
| -47.000 | -4.153 | -2.335 | -22.133 | -23.892 |
| -46.000 | -4.069 | -2.252 | -23.087 | -25.226 |
| -45.000 | -3.986 | -2.169 | -24.370 | -27.108 |
| -44.000 | -3.904 | -2.086 | -26.131 | -29.928 |
| -43.000 | -3.822 | -2.005 | -28.663 | -34.819 |
| -42.000 | -3.741 | -1.924 | -32.671 | -40.000 |
| -41.000 | -3.661 | -1.843 | -40.000 | -37.466 |
| -40.000 | -3.581 | -1.764 | -38.521 | -30.206 |
| -39.000 | -3.503 | -1.686 | -31.113 | -26.155 |
| -38.000 | -3.426 | -1.608 | -26.839 | -23.328 |
| -37.000 | -3.350 | -1.532 | -23.907 | -21.173 |
| -36.000 | -3.275 | -1.457 | -21.703 | -19.456 |
| -35.000 | -3.201 | -1.384 | -19.968 | -18.059 |
| -34.000 | -3.129 | -1.312 | -18.572 | -16.914 |
| -33.000 | -3.058 | -1.241 | -17.440 | -15.981 |
| -32.000 | -2.989 | -1.171 | -16.529 | -15.235 |
| -31.000 | -2.921 | -1.103 | -15.811 | -14.662 |
| -30.000 | -2.855 | -1.037 | -15.272 | -14.257 |
| -29.000 | -2.790 | -0.973 | -14.906 | -14.022 |
| -28.000 | -2.727 | -0.910 | -14.714 | -13.963 |
| -27.000 | -2.666 | -0.849 | -14.704 | -14.099 |
| -26.000 | -2.607 | -0.790 | -14.896 | -14.458 |
| -25.000 | -2.550 | -0.732 | -15.318 | -15.087 |
| -24.000 | -2.494 | -0.677 | -16.023 | -16.065 |
| -23.000 | -2.441 | -0.623 | -17.096 | -17.534 |
| -22.000 | -2.389 | -0.571 | -18.695 | -19.785 |
| -21.000 | -2.340 | -0.522 | -21.151 | -23.565 |
| -20.000 | -2.292 | -0.474 | -25.358 | -32.246 |
| -19.000 | -2.247 | -0.429 | -35.873 | -32.756 |
| -18.000 | -2.204 | -0.386 | -30.798 | -22.425 |
| -17.000 | -2.163 | -0.345 | -22.388 | -17.525 |
| -16.000 | -2.124 | -0.306 | -17.919 | -14.226 |
| -15.000 | -2.087 | -0.269 | -14.830 | -11.725 |
| -14.000 | -2.053 | -0.235 | -12.466 | -9.715 |
| -13.000 | -2.021 | -0.203 | -10.561 | -8.046 |
| -12.000 | -1.991 | -0.173 | -8.980 | -6.633 |
| -11.000 | -1.963 | -0.145 | -7.644 | -5.422 |
| -10.000 | -1.938 | -0.120 | -6.505 | -4.378 |
| -9.000 | -1.915 | -0.098 | -5.530 | -3.477 |

TABULATION OF THE RADIATION PATTERN
A PLANAR ARRAY OF RECTANGULAR PATCHES

| PHI *** | E-PLANE ******* | | H-PLANE ******* | |
|---|---|---|---|---|
| IN | FIELD IN DB | | FIELD IN DB | |
| DEGREES | COUPLED | UNCOUPLED | COUPLED | UNCOUPLED |
| -8.000 | -1.895 | -0.077 | -4.696 | -2.703 |
| -7.000 | -1.877 | -0.059 | -3.987 | -2.041 |
| -6.000 | -1.861 | -0.043 | -3.391 | -1.482 |
| -5.000 | -1.848 | -0.030 | -2.899 | -1.020 |
| -4.000 | -1.837 | -0.019 | -2.504 | -0.648 |
| -3.000 | -1.829 | -0.011 | -2.201 | -0.362 |
| -2.000 | -1.823 | -0.005 | -1.988 | -0.160 |
| -1.000 | -1.819 | -0.001 | -1.860 | -0.040 |
| 0.000 | -1.818 | 0.000 | -1.818 | 0.000 |
| 1.000 | -1.819 | -0.001 | -1.860 | -0.040 |
| 2.000 | -1.823 | -0.005 | -1.988 | -0.160 |
| 3.000 | -1.829 | -0.011 | -2.201 | -0.362 |
| 4.000 | -1.838 | -0.020 | -2.504 | -0.648 |
| 5.000 | -1.849 | -0.031 | -2.899 | -1.020 |
| 6.000 | -1.862 | -0.044 | -3.391 | -1.482 |
| 7.000 | -1.878 | -0.060 | -3.987 | -2.041 |
| 8.000 | -1.896 | -0.078 | -4.696 | -2.703 |
| 9.000 | -1.917 | -0.099 | -5.530 | -3.477 |
| 10.000 | -1.940 | -0.122 | -6.505 | -4.378 |
| 11.000 | -1.965 | -0.147 | -7.644 | -5.422 |
| 12.000 | -1.993 | -0.175 | -8.980 | -6.633 |
| 13.000 | -2.023 | -0.205 | -10.561 | -8.046 |
| 14.000 | -2.055 | -0.237 | -12.466 | -9.715 |
| 15.000 | -2.090 | -0.271 | -14.830 | -11.725 |
| 16.000 | -2.127 | -0.308 | -17.919 | -14.226 |
| 17.000 | -2.166 | -0.347 | -22.388 | -17.525 |
| 18.000 | -2.207 | -0.388 | -30.798 | -22.425 |
| 19.000 | -2.250 | -0.432 | -35.873 | -32.756 |
| 20.000 | -2.296 | -0.477 | -25.358 | -32.246 |
| 21.000 | -2.343 | -0.525 | -21.151 | -23.565 |
| 22.000 | -2.393 | -0.575 | -18.695 | -19.785 |
| 23.000 | -2.445 | -0.626 | -17.096 | -17.534 |
| 24.000 | -2.498 | -0.680 | -16.023 | -16.065 |
| 25.000 | -2.554 | -0.736 | -15.318 | -15.087 |
| 26.000 | -2.612 | -0.793 | -14.896 | -14.458 |
| 27.000 | -2.671 | -0.853 | -14.704 | -14.099 |
| 28.000 | -2.732 | -0.914 | -14.714 | -13.963 |
| 29.000 | -2.795 | -0.977 | -14.906 | -14.022 |
| 30.000 | -2.860 | -1.042 | -15.272 | -14.257 |
| 31.000 | -2.926 | -1.108 | -15.811 | -14.662 |
| 32.000 | -2.994 | -1.176 | -16.529 | -15.235 |

TABULATION OF THE RADIATION PATTERN
A PLANAR ARRAY OF RECTANGULAR PATCHES

| PHI | E-PLANE | | H-PLANE | |
|---|---|---|---|---|
| *** | ******* | | ******* | |
| IN | FIELD IN DB | | FIELD IN DB | |
| DEGREES | COUPLED | UNCOUPLED | COUPLED | UNCOUPLED |
| 33.000 | -3.064 | -1.245 | -17.440 | -15.981 |
| 34.000 | -3.135 | -1.316 | -18.572 | -16.914 |
| 35.000 | -3.207 | -1.389 | -19.968 | -18.059 |
| 36.000 | -3.281 | -1.463 | -21.703 | -19.456 |
| 37.000 | -3.356 | -1.538 | -23.907 | -21.173 |
| 38.000 | -3.433 | -1.614 | -26.839 | -23.328 |
| 39.000 | -3.510 | -1.691 | -31.113 | -26.155 |
| 40.000 | -3.589 | -1.770 | -38.521 | -30.206 |
| 41.000 | -3.668 | -1.849 | -40.000 | -37.466 |
| 42.000 | -3.748 | -1.930 | -32.671 | -40.000 |
| 43.000 | -3.830 | -2.011 | -28.663 | -34.819 |
| 44.000 | -3.912 | -2.093 | -26.131 | -29.928 |
| 45.000 | -3.994 | -2.175 | -24.370 | -27.108 |
| 46.000 | -4.077 | -2.259 | -23.087 | -25.226 |
| 47.000 | -4.161 | -2.342 | -22.133 | -23.892 |
| 48.000 | -4.245 | -2.426 | -21.425 | -22.924 |
| 49.000 | -4.329 | -2.510 | -20.909 | -22.223 |
| 50.000 | -4.414 | -2.595 | -20.548 | -21.728 |
| 51.000 | -4.498 | -2.679 | -20.319 | -21.399 |
| 52.000 | -4.583 | -2.764 | -20.203 | -21.209 |
| 53.000 | -4.667 | -2.848 | -20.185 | -21.139 |
| 54.000 | -4.751 | -2.932 | -20.257 | -21.174 |
| 55.000 | -4.835 | -3.016 | -20.408 | -21.304 |
| 56.000 | -4.918 | -3.099 | -20.634 | -21.519 |
| 57.000 | -5.001 | -3.182 | -20.928 | -21.814 |
| 58.000 | -5.083 | -3.264 | -21.286 | -22.183 |
| 59.000 | -5.164 | -3.345 | -21.706 | -22.622 |
| 60.000 | -5.244 | -3.425 | -22.183 | -23.129 |
| 61.000 | -5.323 | -3.504 | -22.717 | -23.701 |
| 62.000 | -5.401 | -3.582 | -23.305 | -24.338 |
| 63.000 | -5.478 | -3.659 | -23.946 | -25.037 |
| 64.000 | -5.553 | -3.734 | -24.638 | -25.799 |
| 65.000 | -5.627 | -3.808 | -25.383 | -26.625 |
| 66.000 | -5.699 | -3.879 | -26.178 | -27.514 |
| 67.000 | -5.769 | -3.950 | -27.024 | -28.469 |
| 68.000 | -5.837 | -4.018 | -27.922 | -29.492 |
| 69.000 | -5.903 | -4.084 | -28.871 | -30.586 |
| 70.000 | -5.967 | -4.148 | -29.873 | -31.754 |
| 71.000 | -6.029 | -4.210 | -30.929 | -33.001 |
| 72.000 | -6.088 | -4.269 | -32.039 | -34.332 |
| 73.000 | -6.145 | -4.326 | -33.206 | -35.756 |

TABULATION OF THE RADIATION PATTERN
A PLANAR ARRAY OF RECTANGULAR PATCHES

| PHI *** | E-PLANE ******* | | H-PLANE ******* | |
|---|---|---|---|---|
| IN -- | FIELD IN DB ----- -- -- | | FIELD IN DB ----- -- -- | |
| DEGREES | COUPLED | UNCOUPLED | COUPLED | UNCOUPLED |
| 74.000 | -6.199 | -4.380 | -34.431 | -37.279 |
| 75.000 | -6.251 | -4.432 | -35.717 | -38.913 |
| 76.000 | -6.300 | -4.480 | -37.065 | -40.000 |
| 77.000 | -6.345 | -4.526 | -38.478 | -40.000 |
| 78.000 | -6.388 | -4.569 | -39.959 | -40.000 |
| 79.000 | -6.428 | -4.609 | -40.000 | -40.000 |
| 80.000 | -6.464 | -4.645 | -40.000 | -40.000 |
| 81.000 | -6.498 | -4.678 | -40.000 | -40.000 |
| 82.000 | -6.528 | -4.708 | -40.000 | -40.000 |
| 83.000 | -6.554 | -4.735 | -40.000 | -40.000 |
| 84.000 | -6.578 | -4.758 | -40.000 | -40.000 |
| 85.000 | -6.597 | -4.778 | -40.000 | -40.000 |
| 86.000 | -6.613 | -4.794 | -40.000 | -40.000 |
| 87.000 | -6.626 | -4.807 | -40.000 | -40.000 |
| 88.000 | -6.635 | -4.816 | -40.000 | -40.000 |
| 89.000 | -6.641 | -4.821 | -40.000 | -40.000 |
| 90.000 | -6.642 | -4.823 | -40.000 | -40.000 |

**** TABULATION COMPLETED ****

TABULATION OF THE RADIATION PATTERN
A PLANAR ARRAY OF CIRCULAR PATCHES

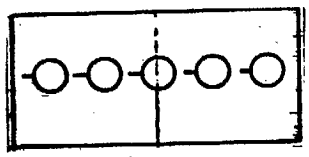

| PHI *** | E-PLANE ******* | | H-PLANE ******* | |
|---|---|---|---|---|
| IN | FIELD IN DB | | FIELD IN DB | |
| DEGREES | COUPLED | UNCOUPLED | COUPLED | UNCOUPLED |
| -90.000 | -20.558 | -19.805 | -40.000 | -40.000 |
| -89.000 | -20.552 | -19.799 | -37.213 | -36.682 |
| -88.000 | -20.536 | -19.783 | -31.193 | -30.661 |
| -87.000 | -20.509 | -19.756 | -27.671 | -27.139 |
| -86.000 | -20.472 | -19.719 | -25.172 | -24.640 |
| -85.000 | -20.425 | -19.673 | -23.233 | -22.702 |
| -84.000 | -20.370 | -19.618 | -21.649 | -21.118 |
| -83.000 | -20.307 | -19.556 | -20.310 | -19.779 |
| -82.000 | -20.237 | -19.487 | -19.149 | -18.618 |
| -81.000 | -20.162 | -19.413 | -18.126 | -17.595 |
| -80.000 | -20.084 | -19.335 | -17.210 | -16.679 |
| -79.000 | -20.003 | -19.254 | -16.382 | -15.851 |
| -78.000 | -19.921 | -19.173 | -15.626 | -15.095 |
| -77.000 | -19.841 | -19.093 | -14.930 | -14.399 |
| -76.000 | -19.764 | -19.017 | -14.286 | -13.755 |
| -75.000 | -19.692 | -18.945 | -13.686 | -13.155 |
| -74.000 | -19.628 | -18.882 | -13.125 | -12.594 |
| -73.000 | -19.574 | -18.828 | -12.599 | -12.067 |
| -72.000 | -19.533 | -18.786 | -12.102 | -11.571 |
| -71.000 | -19.507 | -18.760 | -11.633 | -11.101 |
| -70.000 | -19.500 | -18.752 | -11.187 | -10.656 |
| -69.000 | -19.515 | -18.765 | -10.764 | -10.233 |
| -68.000 | -19.555 | -18.803 | -10.360 | -9.829 |
| -67.000 | -19.625 | -18.871 | -9.975 | -9.444 |
| -66.000 | -19.729 | -18.972 | -9.607 | -9.076 |
| -65.000 | -19.873 | -19.113 | -9.254 | -8.722 |
| -64.000 | -20.062 | -19.298 | -8.915 | -8.384 |
| -63.000 | -20.303 | -19.536 | -8.589 | -8.058 |
| -62.000 | -20.606 | -19.834 | -8.276 | -7.745 |
| -61.000 | -20.981 | -20.204 | -7.974 | -7.443 |
| -60.000 | -21.440 | -20.660 | -7.683 | -7.152 |
| -59.000 | -22.000 | -21.218 | -7.402 | -6.871 |
| -58.000 | -22.682 | -21.902 | -7.131 | -6.599 |
| -57.000 | -23.515 | -22.747 | -6.868 | -6.337 |
| -56.000 | -24.536 | -23.799 | -6.615 | -6.083 |
| -55.000 | -25.796 | -25.137 | -6.369 | -5.838 |
| -54.000 | -27.360 | -26.890 | -6.131 | -5.600 |
| -53.000 | -29.278 | -29.313 | -5.901 | -5.369 |
| -52.000 | -31.433 | -33.021 | -5.677 | -5.146 |
| -51.000 | -32.944 | -40.000 | -5.461 | -4.929 |
| -50.000 | -32.189 | -40.000 | -5.250 | -4.719 |

TABULATION OF THE RADIATION PATTERN
A PLANAR ARRAY OF CIRCULAR PATCHES

| PHI *** IN -- DEGREES ------- | E-PLANE ******* FIELD IN DB ----- -- -- COUPLED ------- | UNCOUPLED --------- | H-PLANE ******* FIELD IN DB ----- -- -- COUPLED ------- | UNCOUPLED --------- |
|---|---|---|---|---|
| -49.000 | -29.734 | -34.805 | -5.047 | -4.516 |
| -48.000 | -27.135 | -29.609 | -4.849 | -4.318 |
| -47.000 | -24.870 | -26.284 | -4.657 | -4.126 |
| -46.000 | -22.956 | -23.831 | -4.471 | -3.940 |
| -45.000 | -21.332 | -21.893 | -4.290 | -3.759 |
| -44.000 | -19.941 | -20.302 | -4.114 | -3.583 |
| -43.000 | -18.742 | -18.966 | -3.944 | -3.413 |
| -42.000 | -17.704 | -17.831 | -3.779 | -3.248 |
| -41.000 | -16.805 | -16.861 | -3.619 | -3.087 |
| -40.000 | -16.030 | -16.032 | -3.463 | -2.932 |
| -39.000 | -15.369 | -15.331 | -3.312 | -2.781 |
| -38.000 | -14.815 | -14.746 | -3.166 | -2.635 |
| -37.000 | -14.364 | -14.271 | -3.024 | -2.493 |
| -36.000 | -14.015 | -13.905 | -2.887 | -2.356 |
| -35.000 | -13.769 | -13.648 | -2.754 | -2.223 |
| -34.000 | -13.629 | -13.501 | -2.625 | -2.094 |
| -33.000 | -13.603 | -13.473 | -2.501 | -1.970 |
| -32.000 | -13.699 | -13.573 | -2.380 | -1.849 |
| -31.000 | -13.933 | -13.817 | -2.264 | -1.733 |
| -30.000 | -14.326 | -14.229 | -2.152 | -1.621 |
| -29.000 | -14.910 | -14.841 | -2.044 | -1.513 |
| -28.000 | -15.732 | -15.709 | -1.940 | -1.409 |
| -27.000 | -16.871 | -16.920 | -1.839 | -1.308 |
| -26.000 | -18.460 | -18.632 | -1.743 | -1.212 |
| -25.000 | -20.759 | -21.176 | -1.650 | -1.119 |
| -24.000 | -24.380 | -25.441 | -1.562 | -1.031 |
| -23.000 | -31.085 | -36.207 | -1.477 | -0.946 |
| -22.000 | -32.077 | -31.560 | -1.396 | -0.865 |
| -21.000 | -23.946 | -22.850 | -1.318 | -0.787 |
| -20.000 | -19.257 | -18.341 | -1.245 | -0.713 |
| -19.000 | -16.035 | -15.232 | -1.175 | -0.643 |
| -18.000 | -13.576 | -12.846 | -1.108 | -0.577 |
| -17.000 | -11.591 | -10.909 | -1.046 | -0.515 |
| -16.000 | -9.931 | -9.284 | -0.987 | -0.456 |
| -15.000 | -8.514 | -7.892 | -0.931 | -0.400 |
| -14.000 | -7.287 | -6.684 | -0.880 | -0.348 |
| -13.000 | -6.214 | -5.626 | -0.831 | -0.300 |
| -12.000 | -5.272 | -4.696 | -0.787 | -0.256 |
| -11.000 | -4.442 | -3.876 | -0.746 | -0.215 |
| -10.000 | -3.713 | -3.154 | -0.709 | -0.177 |
| -9.000 | -3.074 | -2.521 | -0.675 | -0.144 |

TABULATION OF THE RADIATION PATTERN
A PLANAR ARRAY OF CIRCULAR PATCHES

| PHI *** IN DEGREES | E-PLANE ******* FIELD IN DB ----- -- -- COUPLED | UNCOUPLED | H-PLANE ******* FIELD IN DB ----- -- -- COUPLED | UNCOUPLED |
|---|---|---|---|---|
| -8.000 | -2.517 | -1.970 | -0.645 | -0.114 |
| -7.000 | -2.036 | -1.494 | -0.618 | -0.087 |
| -6.000 | -1.628 | -1.088 | -0.595 | -0.064 |
| -5.000 | -1.288 | -0.751 | -0.575 | -0.044 |
| -4.000 | -1.013 | -0.478 | -0.560 | -0.028 |
| -3.000 | -0.801 | -0.268 | -0.547 | -0.016 |
| -2.000 | -0.651 | -0.119 | -0.538 | -0.007 |
| -1.000 | -0.561 | -0.030 | -0.533 | -0.002 |
| 0.000 | -0.531 | 0.000 | -0.531 | 0.000 |
| 1.000 | -0.561 | -0.030 | -0.533 | -0.002 |
| 2.000 | -0.651 | -0.119 | -0.538 | -0.007 |
| 3.000 | -0.801 | -0.268 | -0.547 | -0.016 |
| 4.000 | -1.013 | -0.478 | -0.560 | -0.028 |
| 5.000 | -1.288 | -0.751 | -0.575 | -0.044 |
| 6.000 | -1.628 | -1.088 | -0.595 | -0.064 |
| 7.000 | -2.036 | -1.494 | -0.618 | -0.087 |
| 8.000 | -2.517 | -1.970 | -0.645 | -0.114 |
| 9.000 | -3.074 | -2.521 | -0.675 | -0.144 |
| 10.000 | -3.713 | -3.154 | -0.709 | -0.177 |
| 11.000 | -4.442 | -3.876 | -0.746 | -0.215 |
| 12.000 | -5.272 | -4.696 | -0.787 | -0.256 |
| 13.000 | -6.214 | -5.626 | -0.831 | -0.300 |
| 14.000 | -7.287 | -6.684 | -0.880 | -0.348 |
| 15.000 | -8.514 | -7.892 | -0.931 | -0.400 |
| 16.000 | -9.931 | -9.284 | -0.987 | -0.456 |
| 17.000 | -11.591 | -10.909 | -1.046 | -0.515 |
| 18.000 | -13.576 | -12.846 | -1.108 | -0.577 |
| 19.000 | -16.035 | -15.232 | -1.175 | -0.643 |
| 20.000 | -19.257 | -18.341 | -1.245 | -0.713 |
| 21.000 | -23.946 | -22.850 | -1.318 | -0.787 |
| 22.000 | -32.077 | -31.560 | -1.396 | -0.865 |
| 23.000 | -31.085 | -36.207 | -1.477 | -0.946 |
| 24.000 | -24.380 | -25.441 | -1.562 | -1.031 |
| 25.000 | -20.759 | -21.176 | -1.650 | -1.119 |
| 26.000 | -18.460 | -18.632 | -1.743 | -1.212 |
| 27.000 | -16.871 | -16.920 | -1.839 | -1.308 |
| 28.000 | -15.732 | -15.709 | -1.940 | -1.409 |
| 29.000 | -14.910 | -14.841 | -2.044 | -1.513 |
| 30.000 | -14.326 | -14.229 | -2.152 | -1.621 |
| 31.000 | -13.933 | -13.817 | -2.264 | -1.733 |
| 32.000 | -13.699 | -13.573 | -2.380 | -1.849 |

TABULATION OF THE RADIATION PATTERN
A PLANAR ARRAY OF CIRCULAR PATCHES

| PHI | E-PLANE | | H-PLANE | |
|---|---|---|---|---|
| *** | ******* | | ******* | |
| IN | FIELD IN DB | | FIELD IN DB | |
| DEGREES | COUPLED | UNCOUPLED | COUPLED | UNCOUPLED |
| 33.000 | -13.603 | -13.473 | -2.501 | -1.970 |
| 34.000 | -13.629 | -13.501 | -2.625 | -2.094 |
| 35.000 | -13.769 | -13.648 | -2.754 | -2.223 |
| 36.000 | -14.015 | -13.905 | -2.887 | -2.356 |
| 37.000 | -14.364 | -14.271 | -3.024 | -2.493 |
| 38.000 | -14.815 | -14.746 | -3.166 | -2.635 |
| 39.000 | -15.369 | -15.331 | -3.312 | -2.781 |
| 40.000 | -16.030 | -16.032 | -3.463 | -2.932 |
| 41.000 | -16.805 | -16.861 | -3.619 | -3.087 |
| 42.000 | -17.704 | -17.831 | -3.779 | -3.248 |
| 43.000 | -18.742 | -18.966 | -3.944 | -3.413 |
| 44.000 | -19.941 | -20.302 | -4.114 | -3.583 |
| 45.000 | -21.332 | -21.893 | -4.290 | -3.759 |
| 46.000 | -22.956 | -23.831 | -4.471 | -3.940 |
| 47.000 | -24.870 | -26.284 | -4.657 | -4.126 |
| 48.000 | -27.135 | -29.609 | -4.849 | -4.318 |
| 49.000 | -29.734 | -34.805 | -5.047 | -4.516 |
| 50.000 | -32.189 | -40.000 | -5.250 | -4.719 |
| 51.000 | -32.944 | -40.000 | -5.461 | -4.929 |
| 52.000 | -31.433 | -33.021 | -5.677 | -5.146 |
| 53.000 | -29.278 | -29.313 | -5.901 | -5.369 |
| 54.000 | -27.360 | -26.890 | -6.131 | -5.600 |
| 55.000 | -25.796 | -25.137 | -6.369 | -5.838 |
| 56.000 | -24.536 | -23.799 | -6.615 | -6.083 |
| 57.000 | -23.515 | -22.747 | -6.868 | -6.337 |
| 58.000 | -22.682 | -21.902 | -7.131 | -6.599 |
| 59.000 | -22.000 | -21.218 | -7.402 | -6.871 |
| 60.000 | -21.440 | -20.660 | -7.683 | -7.152 |
| 61.000 | -20.981 | -20.204 | -7.974 | -7.443 |
| 62.000 | -20.606 | -19.834 | -8.276 | -7.745 |
| 63.000 | -20.303 | -19.536 | -8.589 | -8.058 |
| 64.000 | -20.062 | -19.298 | -8.915 | -8.384 |
| 65.000 | -19.873 | -19.113 | -9.254 | -8.722 |
| 66.000 | -19.729 | -18.972 | -9.607 | -9.076 |
| 67.000 | -19.625 | -18.871 | -9.975 | -9.444 |
| 68.000 | -19.555 | -18.803 | -10.360 | -9.829 |
| 69.000 | -19.515 | -18.765 | -10.764 | -10.233 |
| 70.000 | -19.500 | -18.752 | -11.187 | -10.656 |
| 71.000 | -19.507 | -18.760 | -11.633 | -11.101 |
| 72.000 | -19.533 | -18.786 | -12.102 | -11.571 |
| 73.000 | -19.574 | -18.828 | -12.599 | -12.067 |

TABULATION OF THE RADIATION PATTERN
A PLANAR ARRAY OF CIRCULAR PATCHES

| PHI *** | E-PLANE ******* | | H-PLANE ******* | |
|---|---|---|---|---|
| IN | FIELD IN DB | | FIELD IN DB | |
| DEGREES | COUPLED | UNCOUPLED | COUPLED | UNCOUPLED |
| 74.000 | -19.628 | -18.882 | -13.125 | -12.594 |
| 75.000 | -19.692 | -18.945 | -13.686 | -13.155 |
| 76.000 | -19.764 | -19.017 | -14.286 | -13.755 |
| 77.000 | -19.841 | -19.093 | -14.930 | -14.399 |
| 78.000 | -19.921 | -19.173 | -15.626 | -15.095 |
| 79.000 | -20.003 | -19.254 | -16.382 | -15.851 |
| 80.000 | -20.084 | -19.335 | -17.210 | -16.679 |
| 81.000 | -20.162 | -19.413 | -18.126 | -17.595 |
| 82.000 | -20.237 | -19.487 | -19.149 | -18.618 |
| 83.000 | -20.307 | -19.556 | -20.310 | -19.779 |
| 84.000 | -20.370 | -19.618 | -21.649 | -21.118 |
| 85.000 | -20.425 | -19.673 | -23.233 | -22.702 |
| 86.000 | -20.472 | -19.719 | -25.172 | -24.640 |
| 87.000 | -20.509 | -19.756 | -27.671 | -27.139 |
| 88.000 | -20.536 | -19.783 | -31.193 | -30.661 |
| 89.000 | -20.552 | -19.799 | -37.213 | -36.682 |
| 90.000 | -20.558 | -19.805 | -40.000 | -40.000 |

**** TABULATION COMPLETED ****

TABULATION OF THE RADIATION PATTERN
A PLANAR ARRAY OF CIRCULAR PATCHES

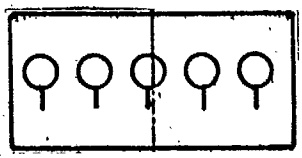

| PHI *** | E-PLANE ******* | | H-PLANE ******* | |
|---|---|---|---|---|
| IN | FIELD IN DB | | FIELD IN DB | |
| DEGREES | COUPLED | UNCOUPLED | COUPLED | UNCOUPLED |
| -90.000 | -7.048 | -5.406 | -40.000 | -40.000 |
| -89.000 | -7.046 | -5.404 | -40.000 | -40.000 |
| -88.000 | -7.040 | -5.398 | -40.000 | -40.000 |
| -87.000 | -7.029 | -5.388 | -40.000 | -40.000 |
| -86.000 | -7.015 | -5.373 | -37.740 | -38.986 |
| -85.000 | -6.997 | -5.355 | -35.779 | -37.020 |
| -84.000 | -6.974 | -5.333 | -34.168 | -35.404 |
| -83.000 | -6.948 | -5.306 | -32.798 | -34.028 |
| -82.000 | -6.917 | -5.276 | -31.606 | -32.829 |
| -81.000 | -6.883 | -5.242 | -30.549 | -31.766 |
| -80.000 | -6.845 | -5.204 | -29.600 | -30.810 |
| -79.000 | -6.804 | -5.162 | -28.739 | -29.943 |
| -78.000 | -6.758 | -5.117 | -27.953 | -29.151 |
| -77.000 | -6.710 | -5.068 | -27.231 | -28.424 |
| -76.000 | -6.658 | -5.016 | -26.567 | -27.755 |
| -75.000 | -6.602 | -4.961 | -25.954 | -27.140 |
| -74.000 | -6.544 | -4.902 | -25.388 | -26.574 |
| -73.000 | -6.482 | -4.841 | -24.868 | -26.054 |
| -72.000 | -6.417 | -4.776 | -24.391 | -25.581 |
| -71.000 | -6.350 | -4.709 | -23.955 | -25.152 |
| -70.000 | -6.280 | -4.639 | -23.562 | -24.769 |
| -69.000 | -6.208 | -4.566 | -23.210 | -24.432 |
| -68.000 | -6.133 | -4.491 | -22.901 | -24.142 |
| -67.000 | -6.055 | -4.414 | -22.636 | -23.901 |
| -66.000 | -5.976 | -4.334 | -22.417 | -23.714 |
| -65.000 | -5.895 | -4.253 | -22.247 | -23.582 |
| -64.000 | -5.811 | -4.170 | -22.129 | -23.512 |
| -63.000 | -5.726 | -4.085 | -22.066 | -23.509 |
| -62.000 | -5.640 | -3.999 | -22.065 | -23.580 |
| -61.000 | -5.552 | -3.911 | -22.131 | -23.737 |
| -60.000 | -5.463 | -3.821 | -22.273 | -23.990 |
| -59.000 | -5.372 | -3.731 | -22.500 | -24.358 |
| -58.000 | -5.281 | -3.640 | -22.825 | -24.862 |
| -57.000 | -5.189 | -3.547 | -23.267 | -25.537 |
| -56.000 | -5.096 | -3.454 | -23.849 | -26.428 |
| -55.000 | -5.002 | -3.361 | -24.604 | -27.614 |
| -54.000 | -4.908 | -3.267 | -25.582 | -29.223 |
| -53.000 | -4.814 | -3.172 | -26.862 | -31.510 |
| -52.000 | -4.719 | -3.077 | -28.575 | -35.089 |
| -51.000 | -4.624 | -2.983 | -30.975 | -40.000 |
| -50.000 | -4.529 | -2.888 | -34.622 | -40.000 |

TABULATION OF THE RADIATION PATTERN
A PLANAR ARRAY OF CIRCULAR PATCHES

| PHI *** IN -- DEGREES ------- | E-PLANE ******* FIELD IN DB ----- -- -- COUPLED ------- | UNCOUPLED --------- | H-PLANE ******* FIELD IN DB ----- -- -- COUPLED ------- | UNCOUPLED --------- |
|---|---|---|---|---|
| -49.000 | -4.435 | -2.793 | -40.000 | -36.527 |
| -48.000 | -4.340 | -2.699 | -40.000 | -31.227 |
| -47.000 | -4.246 | -2.605 | -34.319 | -27.805 |
| -46.000 | -4.153 | -2.511 | -29.889 | -25.259 |
| -45.000 | -4.060 | -2.418 | -26.814 | -23.234 |
| -44.000 | -3.967 | -2.326 | -24.474 | -21.559 |
| -43.000 | -3.876 | -2.234 | -22.600 | -20.145 |
| -42.000 | -3.785 | -2.144 | -21.052 | -18.935 |
| -41.000 | -3.695 | -2.054 | -19.750 | -17.894 |
| -40.000 | -3.607 | -1.965 | -18.645 | -16.999 |
| -39.000 | -3.519 | -1.878 | -17.706 | -16.234 |
| -38.000 | -3.433 | -1.791 | -16.911 | -15.589 |
| -37.000 | -3.348 | -1.706 | -16.248 | -15.058 |
| -36.000 | -3.264 | -1.623 | -15.708 | -14.638 |
| -35.000 | -3.182 | -1.540 | -15.285 | -14.330 |
| -34.000 | -3.101 | -1.460 | -14.980 | -14.136 |
| -33.000 | -3.022 | -1.381 | -14.795 | -14.062 |
| -32.000 | -2.945 | -1.303 | -14.734 | -14.119 |
| -31.000 | -2.869 | -1.228 | -14.809 | -14.323 |
| -30.000 | -2.796 | -1.154 | -15.034 | -14.695 |
| -29.000 | -2.724 | -1.082 | -15.433 | -15.272 |
| -28.000 | -2.654 | -1.012 | -16.042 | -16.105 |
| -27.000 | -2.586 | -0.944 | -16.915 | -17.284 |
| -26.000 | -2.520 | -0.878 | -18.143 | -18.966 |
| -25.000 | -2.456 | -0.814 | -19.894 | -21.481 |
| -24.000 | -2.394 | -0.753 | -22.516 | -25.719 |
| -23.000 | -2.334 | -0.693 | -26.972 | -36.460 |
| -22.000 | -2.277 | -0.636 | -38.386 | -31.789 |
| -21.000 | -2.222 | -0.581 | -31.292 | -23.057 |
| -20.000 | -2.169 | -0.528 | -23.423 | -18.526 |
| -19.000 | -2.119 | -0.477 | -19.109 | -15.398 |
| -18.000 | -2.071 | -0.429 | -16.092 | -12.994 |
| -17.000 | -2.025 | -0.384 | -13.764 | -11.040 |
| -16.000 | -1.982 | -0.340 | -11.871 | -9.399 |
| -15.000 | -1.941 | -0.300 | -10.283 | -7.992 |
| -14.000 | -1.903 | -0.262 | -8.925 | -6.771 |
| -13.000 | -1.867 | -0.226 | -7.749 | -5.701 |
| -12.000 | -1.834 | -0.193 | -6.724 | -4.759 |
| -11.000 | -1.804 | -0.162 | -5.826 | -3.929 |
| -10.000 | -1.776 | -0.134 | -5.040 | -3.198 |
| -9.000 | -1.750 | -0.109 | -4.354 | -2.556 |

TABULATION OF THE RADIATION PATTERN
A PLANAR ARRAY OF CIRCULAR PATCHES

| PHI *** | E-PLANE ******* | | H-PLANE ******* | |
|---|---|---|---|---|
| IN | FIELD IN DB | | FIELD IN DB | |
| DEGREES | COUPLED | UNCOUPLED | COUPLED | UNCOUPLED |
| -8.000 | -1.727 | -0.086 | -3.757 | -1.997 |
| -7.000 | -1.707 | -0.066 | -3.244 | -1.515 |
| -6.000 | -1.690 | -0.048 | -2.808 | -1.104 |
| -5.000 | -1.675 | -0.034 | -2.446 | -0.761 |
| -4.000 | -1.663 | -0.022 | -2.153 | -0.485 |
| -3.000 | -1.654 | -0.012 | -1.928 | -0.272 |
| -2.000 | -1.647 | -0.005 | -1.768 | -0.120 |
| -1.000 | -1.643 | -0.001 | -1.673 | -0.030 |
| 0.000 | -1.641 | 0.000 | -1.641 | 0.000 |
| 1.000 | -1.643 | -0.001 | -1.673 | -0.030 |
| 2.000 | -1.647 | -0.005 | -1.768 | -0.120 |
| 3.000 | -1.654 | -0.012 | -1.928 | -0.272 |
| 4.000 | -1.663 | -0.022 | -2.153 | -0.485 |
| 5.000 | -1.675 | -0.034 | -2.446 | -0.761 |
| 6.000 | -1.690 | -0.048 | -2.808 | -1.104 |
| 7.000 | -1.707 | -0.066 | -3.244 | -1.515 |
| 8.000 | -1.727 | -0.086 | -3.757 | -1.997 |
| 9.000 | -1.750 | -0.109 | -4.354 | -2.556 |
| 10.000 | -1.776 | -0.134 | -5.040 | -3.198 |
| 11.000 | -1.804 | -0.162 | -5.826 | -3.929 |
| 12.000 | -1.834 | -0.193 | -6.724 | -4.759 |
| 13.000 | -1.867 | -0.226 | -7.749 | -5.701 |
| 14.000 | -1.903 | -0.262 | -8.925 | -6.771 |
| 15.000 | -1.941 | -0.300 | -10.283 | -7.992 |
| 16.000 | -1.982 | -0.340 | -11.871 | -9.399 |
| 17.000 | -2.025 | -0.384 | -13.764 | -11.040 |
| 18.000 | -2.071 | -0.429 | -16.092 | -12.994 |
| 19.000 | -2.119 | -0.477 | -19.109 | -15.398 |
| 20.000 | -2.169 | -0.528 | -23.423 | -18.526 |
| 21.000 | -2.222 | -0.581 | -31.292 | -23.057 |
| 22.000 | -2.277 | -0.636 | -38.386 | -31.789 |
| 23.000 | -2.334 | -0.693 | -26.972 | -36.460 |
| 24.000 | -2.394 | -0.753 | -22.516 | -25.719 |
| 25.000 | -2.456 | -0.814 | -19.894 | -21.481 |
| 26.000 | -2.520 | -0.878 | -18.143 | -18.966 |
| 27.000 | -2.586 | -0.944 | -16.915 | -17.284 |
| 28.000 | -2.654 | -1.012 | -16.042 | -16.105 |
| 29.000 | -2.724 | -1.082 | -15.433 | -15.272 |
| 30.000 | -2.796 | -1.154 | -15.034 | -14.695 |
| 31.000 | -2.869 | -1.228 | -14.809 | -14.323 |
| 32.000 | -2.945 | -1.303 | -14.734 | -14.119 |

TABULATION OF THE RADIATION PATTERN
A PLANAR ARRAY OF CIRCULAR PATCHES

| PHI *** IN DEGREES | E-PLANE ******* FIELD IN DB COUPLED | E-PLANE ******* FIELD IN DB UNCOUPLED | H-PLANE ******* FIELD IN DB COUPLED | H-PLANE ******* FIELD IN DB UNCOUPLED |
|---|---|---|---|---|
| 33.000 | -3.022 | -1.381 | -14.795 | -14.062 |
| 34.000 | -3.101 | -1.460 | -14.980 | -14.136 |
| 35.000 | -3.182 | -1.540 | -15.285 | -14.330 |
| 36.000 | -3.264 | -1.623 | -15.708 | -14.638 |
| 37.000 | -3.348 | -1.706 | -16.248 | -15.058 |
| 38.000 | -3.433 | -1.791 | -16.911 | -15.589 |
| 39.000 | -3.519 | -1.878 | -17.706 | -16.234 |
| 40.000 | -3.607 | -1.965 | -18.645 | -16.999 |
| 41.000 | -3.695 | -2.054 | -19.750 | -17.894 |
| 42.000 | -3.785 | -2.144 | -21.052 | -18.935 |
| 43.000 | -3.876 | -2.234 | -22.600 | -20.145 |
| 44.000 | -3.967 | -2.326 | -24.474 | -21.559 |
| 45.000 | -4.060 | -2.418 | -26.814 | -23.234 |
| 46.000 | -4.153 | -2.511 | -29.889 | -25.259 |
| 47.000 | -4.246 | -2.605 | -34.319 | -27.805 |
| 48.000 | -4.340 | -2.699 | -40.000 | -31.227 |
| 49.000 | -4.435 | -2.793 | -40.000 | -36.527 |
| 50.000 | -4.529 | -2.888 | -34.622 | -40.000 |
| 51.000 | -4.624 | -2.983 | -30.975 | -40.000 |
| 52.000 | -4.719 | -3.077 | -28.575 | -35.089 |
| 53.000 | -4.814 | -3.172 | -26.862 | -31.510 |
| 54.000 | -4.908 | -3.267 | -25.582 | -29.223 |
| 55.000 | -5.002 | -3.361 | -24.604 | -27.614 |
| 56.000 | -5.096 | -3.454 | -23.849 | -26.428 |
| 57.000 | -5.189 | -3.547 | -23.267 | -25.537 |
| 58.000 | -5.281 | -3.640 | -22.825 | -24.862 |
| 59.000 | -5.372 | -3.731 | -22.500 | -24.358 |
| 60.000 | -5.463 | -3.821 | -22.273 | -23.990 |
| 61.000 | -5.552 | -3.911 | -22.131 | -23.737 |
| 62.000 | -5.640 | -3.999 | -22.065 | -23.580 |
| 63.000 | -5.726 | -4.085 | -22.066 | -23.509 |
| 64.000 | -5.811 | -4.170 | -22.129 | -23.512 |
| 65.000 | -5.895 | -4.253 | -22.247 | -23.582 |
| 66.000 | -5.976 | -4.334 | -22.417 | -23.714 |
| 67.000 | -6.055 | -4.414 | -22.636 | -23.901 |
| 68.000 | -6.133 | -4.491 | -22.901 | -24.142 |
| 69.000 | -6.208 | -4.566 | -23.210 | -24.432 |
| 70.000 | -6.280 | -4.639 | -23.562 | -24.769 |
| 71.000 | -6.350 | -4.709 | -23.955 | -25.152 |
| 72.000 | -6.417 | -4.776 | -24.391 | -25.581 |
| 73.000 | -6.482 | -4.841 | -24.868 | -26.054 |

TABULATION OF THE RADIATION PATTERN
A PLANAR ARRAY OF CIRCULAR PATCHES

| PHI | E-PLANE | | H-PLANE | |
|---|---|---|---|---|
| *** | ******* | | ******* | |
| IN | FIELD IN DB | | FIELD IN DB | |
| -- | ----- -- -- | | ----- -- -- | |
| DEGREES | COUPLED | UNCOUPLED | COUPLED | UNCOUPLED |
| ------- | ------- | --------- | ------- | --------- |
| 74.000 | -6.544 | -4.902 | -25.388 | -26.574 |
| 75.000 | -6.602 | -4.961 | -25.954 | -27.140 |
| 76.000 | -6.658 | -5.016 | -26.567 | -27.755 |
| 77.000 | -6.710 | -5.068 | -27.231 | -28.424 |
| 78.000 | -6.758 | -5.117 | -27.953 | -29.151 |
| 79.000 | -6.804 | -5.162 | -28.739 | -29.943 |
| 80.000 | -6.845 | -5.204 | -29.600 | -30.810 |
| 81.000 | -6.883 | -5.242 | -30.549 | -31.766 |
| 82.000 | -6.917 | -5.276 | -31.606 | -32.829 |
| 83.000 | -6.948 | -5.306 | -32.798 | -34.028 |
| 84.000 | -6.974 | -5.333 | -34.168 | -35.404 |
| 85.000 | -6.997 | -5.355 | -35.779 | -37.020 |
| 86.000 | -7.015 | -5.373 | -37.740 | -38.986 |
| 87.000 | -7.029 | -5.388 | -40.000 | -40.000 |
| 88.000 | -7.040 | -5.398 | -40.000 | -40.000 |
| 89.000 | -7.046 | -5.404 | -40.000 | -40.000 |
| 90.000 | -7.048 | -5.406 | -40.000 | -40.000 |

**** TABULATION COMPLETED ****

# APPENDIX B

# COMPUTER PROGRAM LISTING

```
100. //RZIN JOB ',,T=10,I=5','LAI'
101. //  EXEC WATFIV,P=D
102. /*ROUTE PRINT SELF
103. //FT08F001 DD DSN=LLAI.RZIN,DISP=OLD
104. //SYSIN DD *
105. $JOB  WATFIV   LAI,NOEXT
106. C ************************************************************
107. C * INPUT IMPEDANCE OF AN ISOLATED RECTANGULAR(SQUARE) PATCH. *
108. C ************************************************************
109.       IMPLICIT REAL*8(A-B,D-H,O-Z),COMPLEX*16(C),INTEGER(I-N)
110.       REAL*8 L,LN,LPOS,LNEG
111.       REAL Z0,Z1,Z2
112.       PI=3.14159265D0
113.       L=0.3036D0*1.001
114.       LPOS=0.22909D0*1.001
115.       LNEG=0.07451D0*1.001
116.       W=0.50292D0
117.       H=0.01166D0
118.       CJ=(0.D0,1.D0)
119.       FACT=376.73D0*H/W
120.       EPSR=2.62
121.       EPSE=(EPSR-1)/DSQRT(1.+12.*H/W)
122.       EPSE=EPSR+1.+EPSE
123.       EPSE=0.5*EPSE
124.       FN=0.96D0
125.       WHILE (FN.LE.1.04D0) DO
126.       HN=H*FN
127.       WN=W*FN
128.       LN=L*FN
129.       ARG=DSQRT(EPSE)*2.*PI*FN
130.       SNPT=DSIN(ARG*LPOS)
131.       SNMT=DSIN(ARG*LNEG)
132.       BOTT=DSIN(ARG*L)
133.       SNP=SNPT/BOTT
134.       SNM=SNMT/BOTT
135.       CALL PSLFR(LN,WN,HN,EPSR,GII,BII)
136.       CP=DCMPLX(GII,BII)
137.       CALL QSLFR(LN,WN,HN,EPSR,QSR,QSI)
138.       CQ=DCMPLX(QSR,QSI)
139.       CZ1=(SNP**2+SNM**2)*CP
140.       CZ2=2.*SNP*SNM*CQ
141.       CZ=(CZ1-CZ2)/(CP**2-CQ**2)+SNP*SNM*BOTT*CJ/DSQRT(EPSE)
142.       CZ=FACT*CZ
143.       Z0=FN
144.       Z1=DREAL(CZ)
145.       Z2=DAIMAG(CZ)
146.       WRITE(8,*)Z0,Z1,Z2
147.       FN=FN+0.001D0
148.       END WHILE
149.       STOP
150.       END
151. C ************************************************************
152. C * SUBROUTINE OF SELF APERTURE NORMALIZED ADMITTANCE.        *
153. C ************************************************************
154.       SUBROUTINE PSLFR(LN,WN,HN,EPSR,GII,BII)
155.       IMPLICIT REAL*8(A-B,D-H,O-Z),COMPLEX*16(C),INTEGER(I-N)
156.       REAL*8 LN,LPOS,LNEG
157.       TOPI=2.*3.14159265D0
158.       WK0=TOPI*WN
159.       X2=WK0**2
160.       GII=0.D0
161.       K=1
162.       DO 1 I=1,26
163.       K=-K
```

```
      J=26-I
      M=2*J+1
      MM=(M+1)*(M+2)
1     GII=(GII+K/M)*X2/MM
      GII=(4/TOPI)*(HN/WN)*GII
      EPSE=(EPSR-1)/DSQRT(1.+12.*HN/WN)
      EPSE=EPSE+EPSR+1.
      EPSE=0.5*EPSE
      EP=DSQRT(EPSE)
      F1=(EPSE+.3)*(.264+WN/HN)
      F2=(EPSE-.258)*(.8+WN/HN)
      F3=.412*F1/F2
      BII=TOPI*HN*F3*EPSE
      BII=BII-EP*DCOTAN(TOPI*LN*EP)
      RETURN
      END
C ***************************************************************
C * SUBROUTINE OF THE MUTUAL ADMITTANCE BETWEEN TWO APERTURES *
C * OF THE SAME PATCH.                                          *
C ***************************************************************
      SUBROUTINE QSLFR(LN,WN,HN,EPSR,QSR,QSI)
      IMPLICIT REAL*8(A-B,D-H,O-Z),COMPLEX*16(C),INTEGER(I-N)
      REAL*8 LN,LPOS,LNEG,LN2
      N=30
      TOPI=2.*3.14159265D0
      R11=LN
      LN2=LN*LN
      R12=DSQRT(LN2+WN**2)
      X11=TOPI*R11
      X12=TOPI*R12
      QSR=2.*(DSIN(X12)/X12-DSIN(X11)/X11)
      QSI=2.*(DCOS(X12)/X12-DCOS(X11)/X11)
      SUM1=0.D0
      SUM2=0.D0
      DO 1 I=1,N
      DO 1 J=1,N
      RIJ=DSQRT(LN2+((J-I)*WN/N)**2)
      XIJ=TOPI*RIJ
      SUM1=SUM1+DSIN(XIJ)/XIJ
1     SUM2=SUM2+DCOS(XIJ)/XIJ
      DEL2=(TOPI*WN/N)**2
      SUM1=SUM1*DEL2
      SUM2=SUM2*DEL2
      QSR=-(HN/WN)*(QSR+SUM1)/TOPI
      QSI=-(HN/WN)*(QSI+SUM2)/TOPI
      EPSE=(EPSR-1.)/DSQRT(1.+12.*HN/WN)
      EPSE=EPSE+EPSR+1.
      EPSE=0.5*EPSE
      EP=DSQRT(EPSE)
      QSI=QSI+EP/DSIN(TOPI*LN*EP)
      RETURN
      END
$ENTRY
```

## User Guide to the Numerical Programming

Program function: Radiation pattern of a microstrip planar array.
Patch shape: Rectangular(square) elements of identical dimensions.

(1) User must fill in the array dimensions(line 117) with the exact number of radiating patches because of the library subroutine LEQT1C.

(2) Output data are written into a dataset(allocated by the user, line 103 and 334)from the radiation pattern program. The data are then read by a plot-program from the dataset for plotting.

(3) Due to different array shape, three cases are introduced to the user for time saving purpose.
Case A: A planar array with arbitrary patch locations.
Case B: A rectangular array shape with a fixed horizontal and vertical separations between adjacent patches.
Case C: An array of Case B above with missing patch(patches).

(4) Starting from the bottom row, the patches are numbered from left to right.

(5) Input data in the dimension of length are normalized to the wavelength of the corresponding operating frequency.

(6) Input data are in double precision and are supplied in free format as follows:

Case A:

```
N,0,0,0
LN,WN,HN,EPSR
XCR(I),YCR(I),CI(I),SNP(I),SNM(I)
  .      .      .      .      .
  .      .      .      .      .
XCR(N),YCR(N),CI(N),SNP(N),SNM(N)
NPDG
```

Case B:

```
0,NX,NY,0
LN,WN,HN,EPSR
HDN,VDN
CI(1),SNP(1),SNM(1)
  .      .      .
  .      .      .
CI(K),SNP(K),SNM(K)
NPDG
```

Case C:

```
0,NX,NY,M
LN,WN,HN,EPSR
HDN,VDN
CI(1),SNP(1),SNM(1)
  .      .      .
  .      .      .
CI(K),SNP(K),SNM(K)
MCEL(1),...,MCEL(M)
NPDG
```

## Variable Dictionary

| | |
|---|---|
| N | - integer, total number of radiating elements not in rectangular array form. |
| NX,NY | - integer, number of radiating elements on the x-, and y-axis which are in a rectangular array form. |
| LN,WN | - real, normalized length and width of the patch. |
| HN | - real, normalized depth of the substrate. |
| EPSR | - real, relative permittivity of the substrate. |
| XCR(I),YCR(I) | - real, normalized x and y coordinates of the Ith radiating element. |
| CI(I) | - complex, normalized feeding current of the Ith cell. |
| SNP(I),SNM(I) | - real, the mathematical expression $\sin(KL^{+})/\sin(KL)$ and $\sin(KL^{-})/\sin(KL)$ respectively. |
| K | - integer, product of NX and NY. |
| HDN,VDN | - real, normalized horizontal and vertical distance between any two adjacent patches. |
| MCEL(I) | - integer, position number of the Ith missing patch in ascending order. |
| NPDG | - integer, number of points per degree for the radiation pattern plot. |

Remark: Subroutine LEQT1C of the program is the IMSL (International Mathematical and Statistical Library) routine for complex matrix equation solution.

```
100. //RARRAY JOB ',,T=2,I=5,F=BDK1','LAI'
101. //  EXEC WATFIV,SIZE=1024K,P=D
102. /*ROUTE PRINT LOCAL
103. //FT08F001 DD DSN=LLAI.DATA,DISP=OLD
104. //SYSIN DD *
105. $JOB  WATFIV   LAI,NOEXT
106. C ************************************************************
107. C * A PROGRAM OF FINDING THE RADIATION PATTERN OF A SQUARE OR *
108. C * RECTANGULAR MICROSTRIP PLANAR ARRAY. CASES A,B,AND C ARE  *
109. C * INTRODUCED DUE TO DIFFERENT ARRAY SHAPE IN ORDER TO       *
110. C * REDUCE THE COMPUTING TIME.                                *
111. C ************************************************************
112.       IMPLICIT REAL*8(A-B,D-H,O-Z),COMPLEX*16(C),INTEGER(I-N)
113. C ************************************************************
114. C * USER MUST USE A DECLARED DUMMY ARRAYS WITH EXACT NUMBER   *
115. C * OF RADIATING PATCHES BECAUSE OF THE SUBROUTINE LEQT1C.    *
116. C ************************************************************
117.       COMPLEX*16 CRPL( , ),CRM1( , ),CEP( ),CEM( )
118.       COMPLEX*16 CP(100,100),CQ(100,100),CQT(100,100),CI(100)
119.       COMPLEX*16 CE(100),DCMPLX
120.       REAL*8 XCR(100),YCR(100),SNP(100),SNM(100),LN,WA(100)
121.       REAL*8 ANG(500),EC(500),E(500),HC(500),H(500),CDABS
122.       REAL ALOG10,Z0,Z1,Z2,Z3,Z4
123.       INTEGER MCEL(20)
124.       READ,NR,NX,NY,NMIS
125.       READ,LN,WN,HN,EPSR
126.       IF (NR.EQ.0) GOTO 5
127. C ************************************************************
128. C * CASE A                                                    *
129. C * A GENERAL PLANAR ARRAY WITH ARBITRARY PATCH LOCATIONS.    *
130. C ************************************************************
131.       DO 1 I=1,NR
132. 1     READ,XCR(I),YCR(I),CI(I),SNP(I),SNM(I)
133.       CALL PSLFR(LN,WN,HN,EPSR,GII,BII)
134.       CALL QSLFR(LN,WN,HN,EPSR,QSR,QSI)
135.       DO 2 I=1,NR
136.       CE(I)=CI(I)
137.       CP(I,I)=DCMPLX(GII,BII)
138. 2     CQ(I,I)=DCMPLX(QSR,QSI)
139.       L=NR-1
140.       IF (L.GT.0) THEN
141.       DO 3 I=1,L
142.       XI=XCR(I)
143.       YI=YCR(I)
144.       K=I+1
145.       DO 3 J=K,NR
146.       XJ=XCR(J)
147.       YJ=YCR(J)
148.       CALL PMUTR(LN,WN,HN,XI,YI,XJ,YJ,PMR,PMI)
149.       CP(I,J)=DCMPLX(PMR,PMI)
150.       CALL QMUTR(LN,WN,HN,XI,YI,XJ,YJ,QMR,QMI)
151. 3     CQ(I,J)=DCMPLX(QMR,QMI)
152.       DO 4 I=2,NR
153.       XI=XCR(I)
154.       YI=YCR(I)
155.       K=I-1
156.       DO 4 J=1,K
157.       XJ=XCR(J)
158.       YJ=YCR(J)
159.       CP(I,J)=CP(J,I)
160.       CALL QMUTR(LN,WN,HN,XI,YI,XJ,YJ,QMR,QMI)
161. 4     CQ(I,J)=DCMPLX(QMR,QMI)
162.       END IF
163.       NEND=NR
```

```
      GOTO 19
C ************************************************************
C * CASE B                                                   *
C * PLANAR ARRAY IN A RECTANGULAR SHAPE WITH A FIXED VERTICAL *
C * AND HORIZONTAL SEPARATIONS BETWEEN ADJACENT PATCHES.     *
C ************************************************************
5     NCAL=NX*NY
      READ,HDN,VDN
      DO 6 J=1,NY
      DO 6 I=1,NX
      XCR(NX*(J-1)+I)=(I-1)*HDN
6     YCR(NX*(J-1)+I)=(J-1)*VDN
      CALL PSLFR(LN,WN,HN,EPSR,GII,BII)
      CALL QSLFR(LN,WN,HN,EPSR,QSR,QSI)
      DO 7 I=1,NCAL
      CP(I,I)=DCMPLX(GII,BII)
7     CQ(I,I)=DCMPLX(QSR,QSI)
      YI=YCR(1)
      DO 8 J=2,NCAL
      XI=XCR(1)
      XJ=XCR(J)
      YJ=YCR(J)
      CALL PMUTR(LN,WN,HN,XI,YI,XJ,YJ,PMR,PMI)
      CP(1,J)=DCMPLX(PMR,PMI)
      CALL QMUTR(LN,WN,HN,XI,YI,XJ,YJ,QMR,QMI)
      CQ(1,J)=DCMPLX(QMR,QMI)
      XI=XCR(J)
      XJ=XCR(1)
      CALL QMUTR(LN,WN,HN,XI,YI,XJ,YJ,QMR,QMI)
8     CQ(J,1)=DCMPLX(QMR,QMI)
      IF (NX.EQ.1) GOTO 11
      DO 10 I=2,NX
      DO 10 K=1,NY
      MM=(K-1)*NX+I
      NN=K*NX
      IM1=I-1
      DO 9 L=1,IM1
      CQ(I,MM-L)=CQ(MM+L+1-I,1)
9     CP(I,MM-L)=CP(I-L,MM)
      DO 10 J=MM,NN
      CQ(I,J)=CQ(I-1,J-1)
10    CP(I,J)=CP(I-1,J-1)
11    CONTINUE
      IF (NY.EQ.1) GOTO 14
      DO 12 K=2,NY
      I=(K-1)*NX
      DO 12 L=1,NX
      DO 12 J=1,NX
      CQ(I+L,J)=CQ(L,J+I)
12    CP(I+L,J)=CP(J,I+L)
      NXP1=NX+1
      DO 13 I=NXP1,NCAL
      DO 13 J=NXP1,NCAL
      CQ(I,J)=CQ(I-NX,J-NX)
13    CP(I,J)=CP(I-NX,J-NX)
14    DO 15 J=1,NCAL
15    READ,CI(J),SNP(J),SNM(J)
      NEND=NCAL
      IF (NMIS.EQ.0) GOTO 19
C ************************************************************
C * CASE C                                                   *
C * A PLANAR ARRAY OF CASE B WITH MISSING PATCH(PATCHES).    *
C ************************************************************
      READ,(MCEL(I),I=1,NMIS)
```

```
228.          K=1
229.          WHILE (K.LE.NMIS) DO
230.          NREV=NMIS+1-K
231.          NSTRT=MCEL(NREV)
232.          NEND=NCAL-K
233.          IF (NSTRT.GT.NEND) GOTO 18
234.          NNI=NEND+1
235.          DO 16 I=1,NNI
236.          DO 16 J=NSTRT,NEND
237.          CQ(I,J)=CQ(I,J+1)
238. 16       CP(I,J)=CP(I,J+1)
239.          DO 17 I=NSTRT,NEND
240.          CI(I)=CI(I+1)
241.          XCR(I)=XCR(I+1)
242.          YCR(I)=YCR(I+1)
243.          DO 17 J=1,NEND
244.          CQ(I,J)=CQ(I+1,J)
245. 17       CP(I,J)=CP(I+1,J)
246. 18       K=K+1
247.          END WHILE
248. 19       N=NEND
249.          DO 20 I=1,N
250.          DO 20 J=1,N
251.          CQT(I,J)=CQ(J,I)
252.          CRPL(I,J)=CP(I,J)
253. 20       CRM1(I,J)=(0.D0,0.D0)
254.          DO 21 I=1,N
255. 21       CRM1(I,I)=(1.0D0,0.0D0)
256.          CALL LEQT1C(CRPL,N,N,CRM1,N,N,0,WA,IER)
257.          CCP=1./(CP(1,1)+CQ(1,1))
258.          CCN=1./(CP(1,1)-CQ(1,1))
259.          DO 24 I=1,N
260.          CXX1=CYY1=(0.D0,0.D0)
261.          DO 23 J=1,N
262.          CXIJ=CXX=CYY=(0.D0,0.D0)
263.          DO 22 K=1,N
264.          CXX=CXX+CQT(I,K)*CRM1(K,J)
265.          CYY=CYY+CQ(I,K)*CRM1(K,J)
266.          DO 22 L=1,N
267. 22       CXIJ=CXIJ+CQT(I,K)*CRM1(K,L)*CQ(L,J)
268.          CRPL(I,J)=CP(I,J)-CXIJ
269.          CP(I,J)=CRPL(I,J)
270.          CXX1=CXX1+SNP(J)*CI(J)*CXX
271. 23       CYY1=CYY1+SNM(J)*CI(J)*CYY
272.          CEP(I)=SNM(I)*CI(I)-CXX1
273. 24       CEM(I)=SNP(I)*CI(I)-CYY1
274.          CALL LEQT1C(CRPL,N,N,CEP,1,N,0,WA,IER)
275.          DO 25 I=1,N
276.          DO 25 J=1,N
277. 25       CRPL(I,J)=CP(I,J)
278.          CALL LEQT1C(CRPL,N,N,CEM,1,N,0,WA,IER)
279.          PI=3.14159265D0
280.          READ,NPDG
281.          DEL=1./NPDG
282.          CJ=(0.0D0,1.0D0)
283.          THETA=-90.D0
284.          K=1
285.          EMAX=HMAX=0.D0
286.          WHILE (THETA.LE.90.D0) DO
287.          RAD=PI*THETA/180.D0
288.          SKL=PI*LN*DSIN(RAD)
289.          SKW=PI*WN*DSIN(RAD)
290.          CKL=SKL*CJ
291.          IF (DABS(SKW).LE.1.D-6) FACT=1.D0
```

```
      IF (DABS(SKW).GT.1.D-6) FACT=DCOS(RAD)*DSIN(SKW)/SKW
      CEIX=CIIX=CEIY=CIIY=(0.D0,0.D0)
      DO 26 I=1,N
      SNA=SNP(I)+SNM(I)
      SND=SNP(I)-SNM(I)
      CPOS=CI(I)*CCP
      CNEG=CI(I)*CCN
      CKXI=2.*PI*XCR(I)*DSIN(RAD)*CJ
      CKYI=2.*PI*YCR(I)*DSIN(RAD)*CJ
      CEIX=CEIX+(CEP(I)*CDEXP(CKL)-CEM(I)*CDEXP(-CKL))
     *     *CDEXP(CKXI)
      CIIX=CIIX+(-SND*CNEG*DCOS(SKL)+SNA*CPOS*DSIN(SKL)*CJ)
     *     *CDEXP(CKXI)
      CEIY=CEIY+(CEP(I)-CEM(I))*CDEXP(CKYI)
26    CIIY=CIIY+(-SND*CNEG*CDEXP(CKYI))
      ABEC=CDABS(CEIX)
      ABE=CDABS(CIIX)
      ABHC=CDABS(FACT*CEIY)
      ABH=CDABS(FACT*CIIY)
      IF (ABE.GT.EMAX) EMAX=ABE
      IF (ABH.GT.HMAX) HMAX=ABH
      ANG(K)=THETA
      EC(K)=ABEC
      E(K)=ABE
      HC(K)=ABHC
      H(K)=ABH
      THETA=THETA+DEL
      K=K+1
      END WHILE
      J=K-1
      DO 27 K=1,J
      Z0=ANG(K)
      Z1=EC(K)/EMAX
      Z2=E(K)/EMAX
      Z3=HC(K)/HMAX
      Z4=H(K)/HMAX
      IF (Z1.LE.0.01) Z1=0.01
      IF (Z2.LE.0.01) Z2=0.01
      IF (Z3.LE.0.01) Z3=0.01
      IF (Z4.LE.0.01) Z4=0.01
      Z1=20.*ALOG10(Z1)
      Z2=20.*ALOG10(Z2)
      Z3=20.*ALOG10(Z3)
      Z4=20.*ALOG10(Z4)
27    WRITE(8,*)Z0,Z1,Z2,Z3,Z4
      STOP
      END
C ***************************************************************
C * SUBROUTINE OF SELF APERTURE NORMALIZED ADMITTANCE.          *
C ***************************************************************
      SUBROUTINE PSLFR(LN,WN,HN,EPSR,GII,BII)
      IMPLICIT REAL*8(A-B,D-H,O-Z),COMPLEX*16(C),INTEGER(I-N)
      REAL*8 LN
      TOPI=2.*3.14159265D0
      WK0=TOPI*WN
      X2=WK0**2
      GII=0.D0
      K=1
      DO 28 I=1,26
      K=-K
      J=26-I
      M=2*J+1
      MM=(M+1)*(M+2)
28    GII=(GII+K/M)*X2/MM
```

```
      GII=(4/TOPI)*(HN/WN)*GII
      EPSE=(EPSR-1)/DSQRT(1.+12.*HN/WN)
      EPSE=EPSE+EPSR+1
      EPSE=0.5*EPSE
      EP=DSQRT(EPSE)
      F1=(EPSE+.3)*(.264+WN/HN)
      F2=(EPSE-.258)*(.8+WN/HN)
      F3=.412*F1/F2
      BII=TOPI*HN*F3*EPSE
      BII=BII-EP*DCOTAN(TOPI*LN*EP)
      RETURN
      END
C ************************************************************
C * SUBROUTINE OF MUTUAL INTERACTION ADMITTANCE BETWEEN TWO   *
C * APERTURES OF THE SAME POLARITY OF ANY TWO PATCHES.        *
C ************************************************************
      SUBROUTINE PMUTR(LN,WN,HN,XI,YI,XJ,YJ,PMR,PMI)
      IMPLICIT REAL*8(A-B,D-H,O-Z),COMPLEX*16(C),INTEGER(I-N)
      REAL*8 LN
      N=30
      DX=XJ-XI
      DY=YJ-YI
      DX2=DX*DX
      R11=DSQRT(DX2+DY**2)
      R12=DSQRT(DX2+(DY+WN)**2)
      R21=DSQRT(DX2+(DY-WN)**2)
      TOPI=2.*3.14159265D0
      X11=TOPI*R11
      X12=TOPI*R12
      X21=TOPI*R21
      PMR=DSIN(X12)/X12+DSIN(X21)/X21-2.*DSIN(X11)/X11
      PMI=DCOS(X12)/X12+DCOS(X21)/X21-2.*DCOS(X11)/X11
      DEL2=(TOPI*WN/N)**2
      SUM1=0.D0
      SUM2=0.D0
      DO 29 K=1,N
      DO 29 L=1,N
      RKL=DSQRT(DX2+(DY+(L-K)*WN/N)**2)
      RK0=TOPI*RKL
      SUM1=SUM1+DSIN(RK0)/RK0
29    SUM2=SUM2+DCOS(RK0)/RK0
      SUM1=SUM1*DEL2
      SUM2=SUM2*DEL2
      PMR=(PMR+SUM1)*(HN/WN)/TOPI
      PMI=(PMI+SUM2)*(HN/WN)/TOPI
      RETURN
      END
C ************************************************************
C * SUBROUTINE OF THE MUTUAL ADMITTANCE BETWEEN TWO APERTURES *
C * OF THE SAME PATCH.                                        *
C ************************************************************
      SUBROUTINE QSLFR(LN,WN,HN,EPSR,QSR,QSI)
      IMPLICIT REAL*8(A-B,D-H,O-Z),COMPLEX*16(C),INTEGER(I-N)
      REAL*8 LN,LN2
      N=30
      TOPI=2.*3.14159265D0
      R11=LN
      LN2=LN*LN
      R12=DSQRT(LN2+WN**2)
      X11=TOPI*R11
      X12=TOPI*R12
      QSR=2.*(DSIN(X12)/X12-DSIN(X11)/X11)
      QSI=2.*(DCOS(X12)/X12-DCOS(X11)/X11)
      SUM1=0.D0
```

```
      SUM2=0.D0
      DO 30 I=1,N
      DO 30 J=1,N
      RIJ=DSQRT(LN2+((J-I)*WN/N)**2)
      XIJ=TOPI*RIJ
      SUM1=SUM1+DSIN(XIJ)/XIJ
30    SUM2=SUM2+DCOS(XIJ)/XIJ
      DEL2=(TOPI*WN/N)**2
      SUM1=SUM1*DEL2
      SUM2=SUM2*DEL2
      QSR=-(HN/WN)*(QSR+SUM1)/TOPI
      QSI=-(HN/WN)*(QSI+SUM2)/TOPI
      EPSE=(EPSR-1.)/DSQRT(1.+12.*HN/WN)
      EPSE=EPSE+EPSR+1.
      EPSE=0.5*EPSE
      EP=DSQRT(EPSE)
      QSI=QSI+EP/DSIN(TOPI*LN*EP)
      RETURN
      END
C ***************************************************************
C * SUBROUTINE OF THE MUTUAL ADMITTANCE BETWEEN TWO APERTURES *
C * OF DIFFERENT POLARITY OF ANY TWO PATCHES.                  *
C ***************************************************************
      SUBROUTINE QMUTR(LN,WN,HN,XI,YI,XJ,YJ,QMR,QMI)
      IMPLICIT REAL*8(A-B,D-H,O-Z),COMPLEX*16(C),INTEGER(I-N)
      REAL*8 LN
      N=30
      TOPI=2.*3.14159265D0
      DX2=(XJ-XI+LN)**2
      DY=YJ-YI
      R11=DSQRT(DX2+DY**2)
      R12=DSQRT(DX2+(DY+WN)**2)
      R21=DSQRT(DX2+(DY-WN)**2)
      X11=TOPI*R11
      X12=TOPI*R12
      X21=TOPI*R21
      QMR=DSIN(X12)/X12+DSIN(X21)/X21-2.*DSIN(X11)/X11
      QMI=DCOS(X12)/X12+DCOS(X21)/X21-2.*DCOS(X11)/X11
      SUM1=0.D0
      SUM2=0.D0
      DO 31 K=1,N
      DO 31 L=1,N
      RKL=DSQRT(DX2+(DY+(L-K)*WN/N)**2)
      RK0=TOPI*RKL
      SUM1=SUM1+DSIN(RK0)/RK0
31    SUM2=SUM2+DCOS(RK0)/RK0
      DEL2=(TOPI*WN/N)**2
      SUM1=SUM1*DEL2
      SUM2=SUM2*DEL2
      QMR=-(HN/WN)*(QMR+SUM1)/TOPI
      QMI=-(HN/WN)*(QMI+SUM2)/TOPI
      RETURN
      END
$ENTRY
```

```
100. //PLOT JOB ',,T=3','LAI'
101. /*ROUTE PRINT SELF
102. //  EXEC FORTXCG,USERLIB='WAILEE.HPPLOT.LOAD',SIZE=256K
103. //FORT.SYSIN DD *
104. C ***************************************************************
105. C * A PLOT-PROGRAM OF THE RADIATION PATTERN.                     *
106. C ***************************************************************
107.       DIMENSION IBUF(5000),X(183),EC(183),E(183),HC(183),H(183)
108.       CALL PLOTS(IBUF,5000)
109.       CALL FACTOR(0.8)
110.       CALL PLOT(1.4,3.4,-3)
111.       X(182)=-90.0
112.       X(183)=30.0
113.       EC(182)=-40.0
114.       EC(183)=5.0
115.       E(182)=-40.0
116.       E(183)=5.0
117.       HC(182)=-40.0
118.       HC(183)=5.0
119.       H(182)=-40.0
120.       H(183)=5.0
121.       CALL AXIS(0.0,0.0,'ANGLE PHI IN DEGREES',-20,6.0,0.0,X(182),
122.      *          X(183))
123.       CALL AXIS(0.0,0.0,'GAIN IN DB',10,8.0,90.0,EC(182),EC(183))
124.       CALL LLGRID(0.0,0.0,6.0,8.0,'LIN','LIN',6,8)
125.       READ(8,*)(X(I),EC(I),E(I),HC(I),H(I),I=1,181)
126.       CALL DASHL(X,EC,181,1,5)
127.       CALL LINE(X,E,181,1,0,0)
128.       CALL PLOT(12.0,0.0,999)
129.       CALL PLOT(12.0,0.0,9999)
130.       STOP
131.       END
132. //GO.FT08F001 DD DSN=LLAI.DATA,DISP=SHR
133. //GO.FT01F001 DD DSN=LLAI.ZPLOT,DISP=OLD
134. //GO.SYSIN DD DUMMY
135. /*
```

```
100. //CZIN JOB ',,T=1,L=50,R=128K,I=5','LAI'
101. // EXEC WATFIV,SIZE=256K
102. /*ROUTE PRINT SELF
103. //FT09F001 DD DSN=LLAI.CZIN,DISP=OLD
104. //SYSIN DD *
105. $JOB  WATFIV   LAI,NOEXT
106. C ************************************************************
107. C * INPUT IMPEDANCE OF AN ISOLATED CIRCULAR PATCH.            *
108. C ************************************************************
109.       IMPLICIT REAL*8(A-B,D-H,O-Z),COMPLEX*16(C),INTEGER(I-N)
110.       REAL Z0,Z1,Z2
111.       NPHI=1
112.       B=0.17419D0
113.       H=0.01166D0
114.       EPSR=2.62D0
115.       FN=0.96D0
116.       WHILE (FN.LE.1.04D0) DO
117.       BN=B*FN
118.       HN=H*FN
119.       CALL PSLFC (NPHI,BN,HN,EPSR,GIIN,BIIN)
120.       CP=DCMPLX(GIIN,BIIN)
121.       CZ=120.*(H/B)/CP
122.       X1=DREAL(CZ)
123.       X2=DAIMAG(CZ)
124.       Z0=FN
125.       Z1=X1
126.       Z2=X2
127.       WRITE(9,*)Z0,Z1,Z2
128.       FN=FN+0.001D0
129.       END WHILE
130.       STOP
131.       END
132. C ************************************************************
133. C * A SUBROUTINE OF FINDING THE SELF WALL ADMITTANCE OF A     *
134. C * SINGLE CIRCULAR PATCH.                                    *
135. C ************************************************************
136.       SUBROUTINE PSLFC(NPHI,BN,HN,EPSR,GIIN,BIIN)
137.       IMPLICIT REAL*8(A-B,D-H,O-Z),INTEGER(I-N)
138.       REAL*8 B1(50),B2(50)
139.       PI=3.14159265D0
140.       HB=HN/BN
141.       BKO=2.0D0*PI*BN
142.       BK=BKO*DSQRT(EPSR)
143.       BEK=BK*DSQRT(1.0D0+2.*HB/(PI*EPSR)*(DLOG(PI/2.0D0/HB)+1.7726))
144.       JACK=NPHI+1
145.       GIIN=0.0D0
146.       X2=BKO**2
147.       K=-1
148.       M=30
149.       IF (NPHI.EQ.0) THEN
150.       WHILE(M.GE.2)DO
151.       K=-K
152.       B=K*M*(M-1.0D0)/(2.0D0*M-1.0D0)
153.       GIIN=(GIIN+B)*X2/M**2
154.       M=M-1
155.       END WHILE
156.       GIIN=HB*GIIN*X2
157.       CALL BJY(BK,1,B1,B2)
158.       B1L1=B1(1)
159.       B2L1=B2(1)
160.       CALL BJY(BEK,2,B1,B2)
161.       B1L2=B1(2)
162.       B2L2=B2(2)
163.       BUP=-2.0D0*B1L2/(PI*BKO*B1L1**2)
```

```
      BDI=B2L2-B2L1*B1L2/B1L1
      BIIN=BUP/BDI
      ELSE
      J=1
      NF=2*NPHI+1
      DO 25 I=1,NF
25    J=J*I
      WHILE (M.GE.2) DO
      K=-K
      TMPN=2.0D0*(M+NPHI)
      B=NPHI+M*(M-1.0)/(TMPN-1.0D0)-NPHI**2/(TMPN+1.0D0)
      GIIN=(GIIN+K*B)*X2/(M*(M+2.0D0*NPHI))
      M=M-1
      END WHILE
      GIIN=GIIN*X2/J
      GIIN=HB*(GIIN-X2*NPHI*(NPHI+3.0D0)/((2.0D0*NPHI+3.0D0)*J)+
     *     NPHI*(NPHI+1.0D0)/J)*X2**NPHI
      CALL BJY(BK,JACK,B1,B2)
      B1L0=B1(JACK)
      B2L0=B2(JACK)
      L1=JACK-1
      L2=JACK+1
      CALL BJY(BEK,L1,B1,B2)
      B1L1=B1(L1)
      B2L1=B2(L1)
      B1L2=B1(L2)
      B2L2=B2(L2)
      BUP=-2.0D0*(B1L1-B1L2)/(PI*BKO*B1L0**2)
      BDI=B2L1-B2L2-B2L0*(B1L1-B1L2)/B1L0
      BIIN=BUP/BDI
      END IF
      RETURN
      END
C ***************************************************************
C * BESSEL FUNCTIONS OF THE FIRST AND SECOND KIND ARE           *
C * COMPUTED IN THIS SUBROUTINE BJY.                            *
C ***************************************************************
      SUBROUTINE BJY(X,N,JN,YN)
      REAL*8 JN(50),YN(50),X,ANORM,PI,SUM,DLOG
      INTEGER N,IM,JX,JX1,I,L,AK,K
      IM=N+20
      JN(IM)=0.0D0
      JN(IM-1)=1.0D0
      JX=IM-2
      JX1=JX+1
      DO 27 I=1,JX
      L=JX1-I
      AK=L-1
27    JN(L)=2.0D0*(AK+1.0)/X*JN(L+1)-JN(L+2)
      ANORM=JN(1)
      DO 28 L=3,IM,2
28    ANORM=ANORM+2.0D0*JN(L)
      DO 29 L=1,IM
29    JN(L)=JN(L)/ANORM
      PI=3.14159265D0
      SUM=0.0D0
      DO 30 L=3,IM,2
      K=(L-1)/2
      AK=K
30    SUM=SUM+(-1.0)**K*JN(L)/AK
      YN(1)=2.0D0/PI*(DLOG(X/2.0D0)+0.577215664)*JN(1)-4./PI*SUM
      YN(2)=(JN(2)*YN(1)-2.0D0/(PI*X))/JN(1)
      DO 31 L=3,IM
      AK=L-1
```

```
228. 31     YN(L)=2.0D0*(AK-1.0D0)/X*YN(L-1)-YN(L-2)
229.        RETURN
230.        END
231. $ENTRY
```

## User Guide to the Numerical Programming

Program function: Radiation pattern of a microstrip planar array.
Patch shape: Circular elements of identical dimensions.

(1) User must fill in the array dimensions(line 117) with the exact number of radiating patches because of the library subroutine LEQT1C.

(2) Output data are written into a dataset(allocated by the user, line 103 and 301)from the radiation pattern program. The data are then read by a plot-program from the dataset for plotting.

(3) Due to different array shape, three cases are introduced to the user for time saving purpose.
Case A: A planar array with arbitrary patch locations.
Case B: A rectangular array shape with a fixed horizontal and vertical separations between adjacent patches.
Case C: An array of Case B above with missing patch(patches).

(4) Starting from the bottom row, the patches are numbered from left to right.

(5) Input data in the dimension of length are normalized to the wavelength of the corresponding operating frequency.

(6) Input data are in double precision and are supplied in free format as follows:

Case A:
```
N,0,0,0,NPHI
BN,HN,EPSR
XCR(I),YCR(I),CI(I)
  .      .      .
  .      .      .
XCR(N),YCR(N),CI(N)
NPDG
```

Case B:
```
0,NX,NY,0,NPHI
BN,HN,EPSR
HDN,VDN
CI(1)
  .
  .
CI(K)
NPDG
```

Case C:
```
0,NX,NY,M,NPHI
BN,HN,EPSR
HDN,VDN
CI(1)
  .
  .
CI(K)
MCEL(1),...,MCEL(M)
NPDG
```

## Variable Dictionary

| | |
|---|---|
| N | - integer, total number of radiating elements not in rectangular array form. |
| NX,NY | - integer, number of radiating elements on the x-, and y-axis which are in a rectangular array form. |
| BN | - real, normalized radius of the patch. |
| HN | - real, normalized depth of the substrate. |
| EPSR | - real, relative permittivity of the substrate. |
| XCR(I),YCR(I) | - real, normalized x and y coordinates of the Ith radiating element. |
| CI(I) | - complex, normalized feeding current of the Ith cell. |
| NPHI | - integer, number of phi-variation in the mode. |
| K | - integer, product of NX and NY. |
| HDN,VDN | - real, normalized horizontal and vertical distance between any two adjacent patches. |
| MCEL(I) | - integer, position number of the Ith missing patch in ascending order. |
| NPDG | - integer, number of points per degree for the radiation pattern plot. |

Remark: Subroutine LEQT1C and MMBSJN of the program are the IMSL (International Mathematical and Statistical Library) routines for complex matrix equation solution and Bessel function respectively.

```
100. //CARRAY JOB ',,T=3M,L=50,R=128K,I=5,','LAI'
101. //  EXEC WATFIV,SIZE=512K,P=D
102. /*ROUTE PRINT LOCAL
103. //FT08F001 DD DSN=LLAI.DATA,DISP=OLD
104. //SYSIN DD *
105. $JOB  WATFIV   LAI,NOEXT
106. C ************************************************************
107. C * A PROGRAM OF FINDING THE RADIATION PATTERN OF A CIRCULAR  *
108. C * MICROSTRIP PLANAR ARRAY. CASES A, B, AND C ARE INTRODUCED *
109. C * DUE TO DIFFERENT ARRAY SHAPE IN ORDER TO REDUCE THE       *
110. C * COMPUTING TIME.                                          *
111. C ************************************************************
112.       IMPLICIT REAL*8(A-B,D-H,O-Z),COMPLEX*16(C),INTEGER(I-N)
113. C ************************************************************
114. C * USER MUST USE A DECLARED DUMMY ARRAYS WITH EXACT NUMBER   *
115. C * OF RADIATING PATCHES BECAUSE OF THE SUBROUTINE LEQT1C.    *
116. C ************************************************************
117.       COMPLEX*16 CRP( , ),CRI( ),CRE( )
118.       COMPLEX*16 CP(100,100),CI(100),CE(100),DCMPLX
119.       REAL*8 XCR(100),YCR(100),WA(100),CDABS,B1(50),B2(50)
120.       REAL*8 ANG(500),EC(500),E(500),HC(500),H(500)
121.       REAL ALOG10,Z0,Z1,Z2,Z3,Z4
122.       INTEGER MCEL(20)
123.       READ,NR,NX,NY,NMIS,NPHI
124.       READ,BN,HN,EPSR
125.       IF (NR.EQ.0) GOTO 5
126. C ************************************************************
127. C * CASE A                                                    *
128. C * A GENERAL PLANAR ARRAY WITH ARBITRARY PATCH LOCATIONS.    *
129. C ************************************************************
130.       DO 1 I=1,NR
131. 1     READ,XCR(I),YCR(I),CI(I)
132.       CALL PSLFC(NPHI,BN,HN,EPSR,GIIN,BIIN)
133.       DO 2 I=1,NR
134.       CE(I)=CI(I)
135. 2     CP(I,I)=DCMPLX(GIIN,BIIN)
136.       L=NR-1
137.       IF (L.GT.0) THEN
138.       DO 3 I=1,L
139.       XI=XCR(I)
140.       YI=YCR(I)
141.       K=I+1
142.       DO 3 J=K,NR
143.       XJ=XCR(J)
144.       YJ=YCR(J)
145.       CALL PMUTC(NPHI,BN,HN,EPSR,XI,YI,XJ,YJ,GIJN,BIJN)
146. 3     CP(I,J)=DCMPLX(GIJN,BIJN)
147.       DO 4 I=2,NR
148.       K=I-1
149.       DO 4 J=1,K
150. 4     CP(I,J)=CP(J,I)
151.       END IF
152.       IJOB=0
153.       IA=NR
154.       IB=NR
155.       M=1
156.       N=NR
157.       GOTO 21
158. C ************************************************************
159. C * CASE B                                                    *
160. C * PLANAR ARRAY IN A RECTANGULAR SHAPE WITH A FIXED VERTICAL *
161. C * AND HORIZONTAL SEPARATIONS BETWEEN ADJACENT PATCHES.      *
162. C ************************************************************
163. 5     NCAL=NX*NY
```

```
      READ,HDN,VDN
      DO 6 J=1,NY
      DO 6 I=1,NX
      XCR(NX*(J-1)+I)=(I-1)*HDN
6     YCR(NX*(J-1)+I)=(J-1)*VDN
      CALL PSLFC(NPHI,BN,HN,EPSR,GIIN,BIIN)
      DO 7 I=1,NCAL
7     CP(I,I)=DCMPLX(GIIN,BIIN)
      XI=XCR(1)
      YI=YCR(1)
      DO 8 J=2,NCAL
      XJ=XCR(J)
      YJ=YCR(J)
      CALL PMUTC(NPHI,BN,HN,EPSR,XI,YI,XJ,YJ,GIJN,BIJN)
8     CP(1,J)=DCMPLX(GIJN,BIJN)
      IF (NX.EQ.1) GOTO 11
      DO 10 I=2,NX
      DO 10 K=1,NY
      MM=(K-1)*NX+I
      NN=K*NX
      IM1=I-1
      DO 9 L=1,IM1
9     CP(I,MM-L)=CP(I-L,MM)
      DO 10 J=MM,NN
10    CP(I,J)=CP(I-1,J-1)
11    CONTINUE
      IF (NY.EQ.1) GOTO 14
      NXP1=NX+1
      DO 13 I=NXP1,NCAL
      IM1=I-1
      DO 12 L=1,IM1
12    CP(I,L)=CP(L,I)
      DO 13 J=I,NCAL
13    CP(I,J)=CP(I-NX,J-NX)
14    DO 15 J=1,NCAL
15    READ,CI(J)
      NEND=NCAL
      IF (NMIS.EQ.0) GOTO 19
C ***************************************************************
C * CASE C                                                      *
C * A PLANAR ARRAY OF CASE B WITH MISSING PATCH(PATCHES).       *
C ***************************************************************
      READ,(MCEL(I),I=1,NMIS)
      K=1
      WHILE (K.LE.NMIS) DO
      NREV=NMIS+1-K
      NSTRT=MCEL(NREV)
      NEND=NCAL-K
      IF (NSTRT.GT.NEND) GOTO 18
      NNI=NEND+1
      DO 16 I=1,NNI
      DO 16 J=NSTRT,NEND
16    CP(I,J)=CP(I,J+1)
      DO 17 I=NSTRT,NEND
      CI(I)=CI(I+1)
      XCR(I)=XCR(I+1)
      YCR(I)=YCR(I+1)
      DO 17 J=1,NEND
17    CP(I,J)=CP(I+1,J)
18    K=K+1
      END WHILE
19    IA=NEND
      IB=NEND
      M=1
```

```
      N=NEND
      IJOB=0
      DO 20 I=1,NEND
20    CE(I)=CI(I)
21    CONTINUE
      DO 22 I=1,N
      CRI(I)=CI(I)
      CRE(I)=CE(I)
      DO 22 J=1,N
22    CRP(I,J)=CP(I,J)
      CALL LEQT1C(CRP,N,IA,CRE,M,IB,IJOB,WA,IER)
      PI=3.14159265D0
      BKO=2.0D0*PI*BN
      READ,NPDG
      DEL=1./NPDG
      CJ=(0.0D0,1.0D0)
      THETA=-90.0D0
      NM=NPHI/2
      NM=2*NM
      K=1
      EMAX=HMAX=0.0D0
      WHILE (THETA.LE.90.0D0) DO
      SANG=DSIN(PI*THETA/180.0D0)
      QANG=DCOS(PI*THETA/180.0D0)
      ARG=DABS(BKO*SANG)
      NB=NPHI+2
      CALL MMBSJN(ARG,NB,B1,IER)
      IF (NPHI.EQ.0) THEN
      BNPI=-B1(2)
      ELSE
      BNPI=0.5*(B1(NPHI)-B1(NPHI+2))
      END IF
      BARG=BNPI+B1(NPHI+2)
      CEIX=CIIX=CEIY=CIIY=(0.0D0,0.0D0)
      DO 23 I=1,N
      CXX=2.0D0*PI*XCR(I)*SANG*CJ
      CYY=2.0D0*PI*YCR(I)*SANG*CJ
      CEIX=CEIX+CRE(I)*CDEXP(CXX)
      CIIX=CIIX+CRI(I)*CDEXP(CXX)
      CEIY=CEIY+CRE(I)*CDEXP(CYY)
23    CIIY=CIIY+CRI(I)*CDEXP(CYY)
      ABEC=CDABS(BNPI*CEIX)
      ABE=CDABS(BNPI*CIIX/CP(1,1))
      IF (NM.NE.NPHI) THEN
      ABHC=CDABS(BARG*QANG*CEIY)
      ABH=CDABS(BARG*QANG*CIIY/CP(1,1))
      ELSE
      ABHC=CDABS(BNPI*CEIY)
      ABH=CDABS(BNPI*CIIY/CP(1,1))
      END IF
      IF (ABE.GT.EMAX) EMAX=ABE
      IF (ABH.GT.HMAX) HMAX=ABH
      ANG(K)=THETA
      EC(K)=ABEC
      E(K)=ABE
      HC(K)=ABHC
      H(K)=ABH
      THETA=THETA+DEL
      K=K+1
      END WHILE
      J=K-1
      DO 24 K=1,J
      Z0=ANG(K)
      Z1=EC(K)/EMAX
```

```
      Z2=E(K)/EMAX
      Z3=HC(K)/HMAX
      Z4=H(K)/HMAX
      IF(Z1.LE.0.01) Z1=0.01
      IF(Z2.LE.0.01) Z2=0.01
      IF(Z3.LE.0.01) Z3=0.01
      IF(Z4.LE.0.01) Z4=0.01
      Z1=20.*ALOG10(Z1)
      Z2=20.*ALOG10(Z2)
      Z3=20.*ALOG10(Z3)
      Z4=20.*ALOG10(Z4)
24    WRITE(8,*)Z0,Z1,Z2,Z3,Z4
      STOP
      END
C ***************************************************************
C * A SUBROUTINE OF FINDIND THE SELF WALL ADMITTANCE OF A      *
C * SINGLE CIRCULAR PATCH.                                      *
C ***************************************************************
      SUBROUTINE PSLFC(NPHI,BN,HN,EPSR,GIIN,BIIN)
      IMPLICIT REAL*8(A-B,D-H,O-Z),INTEGER(I-N)
      REAL*8 B1(50),B2(50)
      PI=3.14159265D0
      HB=HN/BN
      BKO=2.0D0*PI*BN
      BK=BKO*DSQRT(EPSR)
      BEK=BK*DSQRT(1.0D0+2.*HB/(PI*EPSR)*(DLOG(PI/2.0D0/HB)+
     *             1.7726))
      JACK=NPHI+1
      GIIN=0.0D0
      X2=BKO**2
      K=-1
      M=30
      IF (NPHI.EQ.0) THEN
      WHILE(M.GE.2)DO
      K=-K
      B=K*M*(M-1.0D0)/(2.0D0*M-1.0D0)
      GIIN=(GIIN+B)*X2/M**2
      M=M-1
      END WHILE
      GIIN=HB*GIIN*X2
      CALL BJY(BK,1,B1,B2)
      B1L1=B1(1)
      B2L1=B2(1)
      CALL BJY(BEK,2,B1,B2)
      B1L2=B1(2)
      B2L2=B2(2)
      BUP=-2.0D0*B1L2/(PI*BKO*B1L1**2)
      BDI=B2L2-B2L1*B1L2/B1L1
      BIIN=BUP/BDI
      ELSE
      J=1
      NF=2*NPHI+1
      DO 25 I=1,NF
25    J=J*I
      WHILE (M.GE.2) DO
      K=-K
      TMPN=2.0D0*(M+NPHI)
      B=NPHI+M*(M-1.0)/(TMPN-1.0D0)-NPHI**2/(TMPN+1.0D0)
      GIIN=(GIIN+K*B)*X2/(M*(M+2.0D0*NPHI))
      M=M-1
      END WHILE
      GIIN=GIIN*X2/J
      GIIN=HB*(GIIN-X2*NPHI*(NPHI+3.0D0)/((2.0D0*NPHI+3.0D0)*
     *     *J)+NPHI*(NPHI+1.0D0)/J)*X2**NPHI
```

```
      CALL BJY(BK,JACK,B1,B2)
      B1L0=B1(JACK)
      B2L0=B2(JACK)
      L1=JACK-1
      L2=JACK+1
      CALL BJY(BEK,L1,B1,B2)
      B1L1=B1(L1)
      B2L1=B2(L1)
      B1L2=B1(L2)
      B2L2=B2(L2)
      BUP=-2.0D0*(B1L1-B1L2)/(PI*BKO*B1L0**2)
      BDI=B2L1-B2L2-B2L0*(B1L1-B1L2)/B1L0
      BIIN=BUP/BDI
      END IF
      RETURN
      END
C ***************************************************************
C * A SUBROUTINE OF FINDING THE MUTUAL WALL ADMITTANCE          *
C * BETWEEN ANY TWO CIRCULAR PATCHES.                           *
C ***************************************************************
      SUBROUTINE PMUTC(NPHI,BN,HN,EPSR,XI,YI,XJ,YJ,GIJN,BIJN)
      IMPLICIT REAL*8(A-B,D-H,O-Z),INTEGER(I-N)
      PI=3.14159265D0
      BKO=2.0D0*PI*BN
      DM=DSQRT((XJ-XI)**2+(YJ-YI)**2)
      IF (XI.EQ.XJ) THEN
      FIM=PI/2.0D0
      ELSE
      FIM=DATAN((YJ-YI)/(XJ-XI))
      END IF
      N=72*(1+NPHI)
      GIJN=BIJN=0.0D0
      FKTR=(HN/BN)*(BKO/N)**2
      IF (NPHI.NE.0) FKTR=2.*FKTR
      DO 26 I=1,N
      FI=(2*I-1)*PI/N
      A1=FI-FIM
      ELI=DSQRT(DM**2+BN**2+2.*DM*BN*DCOS(A1))
      ALFI=DARSIN((BN/ELI)*DSIN(A1))
      WI=DCOS(NPHI*FI)
      DO 26 J=1,N
      FIP=(2*J-1)*PI/N
      A2=FIP-FI
      A3=FIP-ALFI-FIM
      RN=DSQRT(ELI**2+BN**2-2.*ELI*BN*DCOS(A3))
      RKO=2.0D0*PI*RN
      WJ=DCOS(NPHI*FIP)
      BETA=A3+DARSIN(BN/RN*DSIN(A3))
      TRS=DSIN(RKO)
      TRC=DCOS(RKO)
      FG1=(TRS-RKO*TRC)/(RKO**3)
      FG2=TRS/RKO
      FB1=(TRC+RKO*TRS)/(RKO**3)
      FB2=TRC/RKO
      TRG1=2.0D0*DCOS(A2)
      TRG2=DCOS(BETA)*DCOS(BETA-A2)
      FG3=FG1*TRG1+(FG2-3.0D0*FG1)*TRG2
      FB3=FB1*TRG1+(FB2-3.0D0*FB1)*TRG2
      FG3=WI*WJ*FG3
      FB3=WI*WJ*FB3
      GIJN=GIJN+FG3
26    BIJN=BIJN+FB3
      GIJN=FKTR*GIJN
      BIJN=FKTR*BIJN
```

```
      RETURN
      END
C ***************************************************************
C * BESSEL FUNCTIONS OF THE FIRST AND SECOND KIND ARE           *
C * COMPUTED IN THIS SUBROUTINE BJY.                            *
C ***************************************************************
      SUBROUTINE BJY(X,N,JN,YN)
      REAL*8 JN(50),YN(50),X,ANORM,PI,SUM,DLOG
      INTEGER N,IM,JX,JX1,I,L,AK,K
      IM=N+20
      JN(IM)=0.0D0
      JN(IM-1)=1.0D0
      JX=IM-2
      JX1=JX+1
      DO 27 I=1,JX
      L=JX1-I
      AK=L-1
27    JN(L)=2.0D0*(AK+1.0)/X*JN(L+1)-JN(L+2)
      ANORM=JN(1)
      DO 28 L=3,IM,2
28    ANORM=ANORM+2.0D0*JN(L)
      DO 29 L=1,IM
29    JN(L)=JN(L)/ANORM
      PI=3.14159265D0
      SUM=0.0D0
      DO 30 L=3,IM,2
      K=(L-1)/2
      AK=K
30    SUM=SUM+(-1.0)**K*JN(L)/AK
      YN(1)=2.0D0/PI*(DLOG(X/2.0D0)+0.577215664)*JN(1)-4./PI*SUM
      YN(2)=(JN(2)*YN(1)-2.0D0/(PI*X))/JN(1)
      DO 31 L=3,IM
      AK=L-1
31    YN(L)=2.0D0*(AK-1.0D0)/X*YN(L-1)-YN(L-2)
      RETURN
      END
$ENTRY
```

*cover design:* Diane Weselake, Instructional Media Centre